Novel mechanisms of neurogenesis: the role of the new centrosomal protein Akna

Submitted by

Germán Camargo Ortega

September 24, 2018

Acknowledgements

"Here is my secret. It is very simple: It is only with the heart that one can see rightly; what is essential is invisible to the eye."

Antoine de Saint-Exupéry, Le Petit Prince (The Fox and Prince)

Abstract

Understanding the basic cell biology of neural stem and progenitor cells is fundamental, on the one hand, to know how the large and complex brain of humans has evolved and in the other hand, for their successful application in regenerative medicine. While many central features are shared between different types of neural progenitors from diverse sources, there may be possibly an equal number of differences, and therefore it is of paramount importance to compare them. Towards that end, our laboratory identifies and investigates novel genes and molecular mechanisms regulating homeostasis and fate commitment of neural progenitors common to the developing and the adult brain, in mouse and recently, in humans. This line of experimentation has led to the discovery of new factors and biological phenomena essential for both embryonic and adult neurogenesis, and has been critical in pioneering and further developing direct neuronal reprogramming i.e. forced neurogenesis. My PhD work is the functional characterization of one such common candidate genes called Akna, and the investigation of its molecular regulation. I have discovered that this gene, erroneously annotated as an AT-hook transcription factor, is in fact an integral component of interphase centrosomes in the differentiating subtype of neural stem cells - radial glia - and in basal progenitors of the developing forebrain and in neuronal precursors of the adult brain. It localizes predominantly at subdistal appendages of mother centrioles where it regulates the organization and polymerization of microtubules. Gain- and loss-of-function experiments in the murine developing cerebral cortex show that Akna is necessary and sufficient for the delamination of differentiating neural stem cells in the (apical) ventricular zone towards the adjacent (basal) subventricular zone, where it is highest expressed. There, it is required for the retention of basal progenitors. Its subsequent downregulation allows repolarization and migration of young neurons to the cortical plate, where Akna is not detectable. Notably, cells that express Akna have mostly centrosome-based microtubule nucleation, while those without Akna, i.e. neurons, largely nucleate microtubules from

noncentrosomal sources. This is indeed also the case for other cell types including adult brain neural precursors (neuroblasts) and immune cells; both of which have high levels of Akna. Furthermore, Akna's enrichment in the outer subventricular zone of the folded ferret and macaque brains together with manipulation in human induced pluripotent stem cell-derived cerebral organoids suggest a conserved role in brain ontogeny and phylogeny.

The delamination process of epithelial-like neural stem cells is reminiscent of the mesenchymal transition that can occur in true epithelial cells. In fact, many factors and molecular pathways are common to both processes, and so is Akna. We have found that it is up-regulated early in mammary gland epithelial cells undergoing epithelial to mesenchymal transition. In its absence, disassembly of cell-cell junctions is impaired because degradation of epithelial adhesion molecules is delayed and hence, the resulting mesenchymal cell scattering is impaired. This, together with the above-mentioned results, supports a mechanistic model in which Akna's role as microtubule organizer at centrosomes facilitates disassembly of cell-cell contacts and cell polarization in epithelial cells in general.

Altogether, the results of my work uncover previously unconsidered, and therefore not observed, roles of centrosomal microtubule nucleation and highlights the key relevance of centrosome composition.

Contents

Chapter 1

Introduction

The most notorious feature of the primate forebrain is its intricate, yet particularly well-organized architecture. Clearly, growth in size, area and complexity has contributed to the acquisition of evolutionary advantages that ultimately led to superposition of humans at the top of cognitive beings (Fernandez at al., 2016; Klyachko and Stevens, 2003). How the brain gets its final form, and which factors are key in regulating this process during development is certainly one of the most critical, yet poorly understood matters in neurobiology. In this regard, with exception of recent pioneering studies (see for example Florio et al. 2016; Martinez-Martinez., 2016, Tavano et al., 2018), the large number of efforts so far have focused on characterizing the cellular composition of gyrified brains from different species (including humans) as well as on analyzing the behavior of progenitor cells within (Betizeau et al., 2013; Camp et al, 2015; Fietz et al. 2010; Fietz et al., 2012; Florio et al., 2015; Johnson et al, 2015; Pollen et al, 2015; Reillo et al., 2011). Hence, basic cell biological aspects of folded brain development are still largely in the dark. It has been, therefore, necessary to circumvent this obstacle by investigating neurogenesis in other animal models, most prominently in the mouse. This has had two important advantages, namely, the availability of many genetically modified animals and the relative simplicity to generate them, making detailed experimentation feasible, and the fact that even though their brain is smooth (lissencephalic) the elementary pathways driving brain development are in principle conserved. Murine neurogenesis has therefore been an invaluable tool for the investigation of basic mechanisms of neurogenesis.

I will thus start by introducing embryonic dorsal forebrain development in lissencephalic rodents and other gyrencephalic species and explain key cell and molecular biological process regulating the behavior of neural stem cell maintenance versus differentiation, relevant to this work. Thereafter, I will discuss some aspects of adult neurogenesis, including briefly it's ontogenetic origin, to highlight its special needs and emphasize how this is important towards a more complete understanding of general neurogenic mechanisms. Finally, I make a summary explaining the background knowledge about the gene investigated in my doctoral studies and explain the rationale and motivation of my work.

1.1 Neurogenesis in the developing mammalian forebrain

1.1.1 Radial glia and the neuronal lineage

Neural stem cells (NSCs) of the developing mammalian brain are derived from the ectodermal neurepithelium and are radial glial cells (RGCs) (Götz, el al., 2016; Gotz and Huttner, 2005; Kriegstein and Alvarez-Buylla, 2009; Malatesta et al., 2000). RGCs are the source of the vast majority of pyramidal excitatory neurons; inhibitory interneurons and projection in the mammalian dorsal forebrain, as well as nonneuronal astro-, ependymo- and oligodendroglial cells (Eglund et al., 2005; Fuentealba et al., 2015; Götz et al., 2016; Haubensack et al., 2004; Heins et al., 2002; Kowalczyk et al., 2009; Merkle et al., 2004; Sessa et al., 2008) and the future adult NSCs of the adult brain (Falk et al., 2017; Fuentealba et al., 2015; Merkle et al., 2004; Young et al., 2007). In the mouse dorsal forebrain, the future cerebral neocortex, RGCs emerge roughly at embryonic day 12.5 (E12.5) (Figure 1.1) and, although alike to pre-existing neurepithelial cells (NECs, E10.5-E12.5) in morphology and behavior, there are several important ultrastructural, molecular and functional differences. Briefly, common for both types of cell is their ability to self-renew but also their multipotent capacity regarding the type of cells they can generate if put under specific culture conditions. Furthermore, they have highly polarized radial cell somata that span the entire length of the tissue, with apical and basal processes with end-feet facing the ventricle and the pial surface, respectively (Figure 1.2). At the apical site, cells are anchored to each other by cell adhesion complexes such as adherens junctions, and exposed to the cerebrospinal fluid (CSF) of the ventricles. Here, the primary cilium is located and

serves as receptor of morphogenic signals that regulate their maintenance (see for example Falk et al., 2008; Johansson et al., 2013). Furthermore, also common to NECs and RGCs is the apico-basal migration of their nuclei during cell cycle, a process termed interkinetic nuclear migration (IKNM), which confers to the niche a pseudo-stratified (layered) appearance. Moreover, they express common progenitor makers like Nestin, Blbp and Sox2. On the other side, there are two fundamental properties that make NEs and RGCs different. Firstly is obviously the fact that RGCs, but not NEs, have bona fide glial traits; these include expression of the glutamate transporter Slc1a3/Glast, the intermediate filaments Vim and Gfap (late RGC), the calcium binding protein S100b, the extracellular matrix protein Tnc, the Receptor-type tyrosine-protein phosphatase zeta Ptprz1/Phosphacan, the ability to store Glycogen, to contact blood vessels and to form gap-junctions (for excellent review and detailed comparison please see Götz, 2012 and Gotz and Huttner, 2005). The second, and possibly clearest, difference between NECs and RGCs is the natural proclivity to generate neurons *in vivo* in the case of the later (Gotz and Huttner, 2005). While the transition is directed in part by signaling through the Fgf10-Fgfr2 and Notch pathways (Anthony et al., 2005; Sahara and O'Leary, 2009), certainly the capacity to generate neurons is acquired in great part by expression of the transcription factor Pax6, which is an essential and potent neurogenic fate determinant (Götz et al, 1998; Hack et al., 2005; Heins et al., 2002; Ninkovic et al., 2013). This points out that in addition to the above mentioned ultrastructural and cell biological changes, global rearrangements of transcriptional and signaling programs occur and are required during this transition.

At early neurogenesis (E10.5-12.5) NECs and RGCs largely self-new in a symmetric manner giving rise to two new NECs or RGCs, thereby amplifying the NSC pool. In addition, but less frequently, RGCs can divide asymmetrically regarding the fate of one daughter cell, which eventually leaves the RG niche at the germinal ventricular zone (VZ) and differentiate into a neuron at a basally located nongerminal zone (known as pre-plate) (Figure 1.1) (Chenn and McConnell, 1995; Haubensak et al.,2004; Kosodo et al., 2004; Miyata et al., 2004). Later on, roughly between E12.5 to E16.6, the balance between symmetric and asymmetric division inverses, with the latest becoming the dominant type. Here, the daughter cells of RGCs delaminate from the VZ after division and move basally to form a subventricular zone (SVZ), transforming then and there into intermediate basal progenitors (BPs) (Figures 1.1 and 1.2). Because BPs divide at least once (see for instance Haubensak et al., 2004 and Kowalczyk et al., 2009), the SVZ becomes a second clearly distinguishable

4

germinal area in the developing brain.
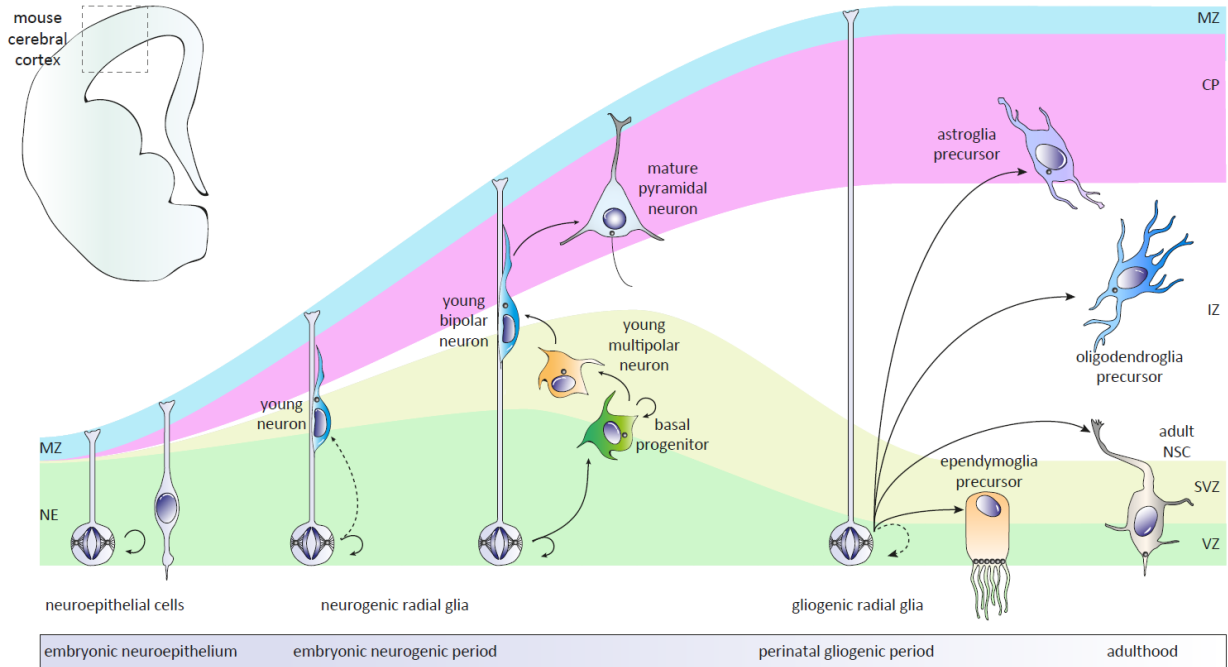
Figure 1.1: **Neural stem and progenitor cells are the source of virtually all neurons and glia in the mammalian forebrain.** NECs at the VZ mostly divide symmetrically to amplify the progenitor pool and subsequently transform into RGCs that both self-renew and generate neurons directly or indirectly via intermediate BPs. The latter further enlarge the neuronal output after additional rounds of cell division, thus forming a secondary germinal layer; the SVZ. This is enlarged in species with folded brains (see below). Gliogenesis starts at perinatal stages; ependymo-, astro- and oligogliogenesis occurs sequentially. A subpopulation of RGCs is separated during neurogenesis, becomes quiescent and transforms later into astrocyte-like cells basally located to ependyma cells. These cells retain neurogenic potential and are therefore considered adult NSCs (see below). CP, cortical plate; IZ, intermediate zone; MZ, marginal zone; NE, neuroepithelium; NSC, neural stem cells; SVZ, subventricular zone; VZ, ventricular zone.

Importantly, in species with gyrified brains, such as primates, carnivores, ungulates and some rodents, the SVZ is dramatically enlarged to the point that it is subdivided in two; an inner and an outer SVZ (iSVZ and oSVZ, respectively) (García-Moreno et al., 2012; Reillo and Borrell, 2012; Smart et al., 2002) (Figure 1.3). The iSVZ is similar to the mouse SVZ in the sense that it is largely populated by intermediate progenitors born in the VZ and they keep some self-renewal capability (Betizeau et al., 2013; Martinez-Martinez et al., 2016). In the oSVZ, however, a major proportion of progenitors is rather made of so-called intermediate or basal radial glia cells (bRGCs) (Dehai et al., 2015; Fernandez et al., 2016; Reillo and Borrell, 2012). Most of these express Pax6, fewer Tbr2, a BP marker

(see below), and have basal processes similar to apical RGC (aRGC) in the VZ but not all of them possess an apical process anchored in apical junctions, so their centrosomes for instance are perinuclear (Betizeau et al., 2013; Fietz et al., 2010; Hansen et al., 2010 Reillo et al., 2011; Reillo and Borrell, 2012) (Figure 1.3). Interestingly, oSVZ RGCs derive originally from VZ aRGCs but later become an independent lineage that can amplify, and thus maintain itself, and can further serve as source for other cells (glia and neurons) (Martinez-Martinez et al., 2016), consequently augmenting in general the size and total surface area of the brain (Figure 1.3).

Murine intermediate BPs originate from so-called differentiating RGCs (see for instance Aprea et al., 2013); also known as nascent BPs (Wilsch-Bräuninger et al., 2012). These are RGCs with decreasing Pax6 expression that up-regulate anti-proliferative genes such as Btg2/Tis21 (Haubensak et al., 2004; Iacopetti et al., 1999), as well as regulators of signaling pathways or transcription factors that promote neuronal differentiation such as Notch ligands Dll1 and Dll3 (Kawaguchi et al., 2008), Wnt (Kuwahara et al., 2010), Neurog1/2 (Britz et al., 2006; Fode et al., 1998; Masserdotti et al., 2015), Insm1 (Tavano et al., 2018, Farkas et al., 2008), NeuroD1 (Guo et al., 2014; Hevner et al., 2006; Pataskar et al., 2016), Eomes/Tbr2 (Arnold et al, 2008; Mihalas et al., 2016; Sessa et al., 2008), members of the Snail family of transcriptional repressors Scrt1 and Scrt2 (Itoh et al., 2013), among others. Correspondingly, the Tis21-negative nonneuronal population is mostly made of proliferating RGCs (Aprea et al., 2013). Hence, the stem cell niche in the developing forebrain (the VZ) is heterogeneous in composition at midneurogenesis, as it encapsulates at least two subtypes or stages of NSCs. Two other type of neural progenitor known as short neural precursor and sub-apical progenitors also co-exist in the VZ, although they represent a smaller fraction of the total of cells within the rodent VZ and they generate neurons directly (Gal et al., 2006; Mizutani et al., 2007; Pilz et al., 2013; Stancik et al., 2010; Taverna et al., 2014). If and how these cells are related to each other awaits further study. By transforming into intermediate BPs, differentiating RGCs retract both end-feet and acquire a characteristic multipolar morphology (Figure 1.2). They also re-position the centrosome and, with that, their microtubule cytoskeleton. This change is necessary to re-orient the cell body as they further differentiate into bipolar neurons that migrate out of the SVZ, passing through the intermediate zone (IZ), towards the cortical plate (CP) (Figure 1.2). It is still not fully understood which mechanisms regulate multipolar to bipolar transition, and most data points towards pathways involving kinases, GTPases

and cell-adhesion molecules, but is it is clear that is indispensable for proper neuronal differentiation (Cappello et al., 2006; Cooper 2014 and refs. therein; Jossin and Cooper, 2011). It is thus reasonable to think that the ultimate goal of a BP is not merely to amplify the neuronal output but also generate a spatiotemporal window to allow major cellular and genetic changes to happen; yet again additional efforts to understand what is actually happening within BPs is may be needed.

1.1.2 Cell biological mechanisms of basal progenitor generation and neuronal migration

As mentioned above, in the mouse developing cerebral cortex, at the peak of neurogenesis, RGCs destined to differentiate into intermediate basal progenitors separate from their layer at the VZ and move basally to form the SVZ, in a bona fide delamination process. This singular event must be correctly orchestrated in order to guarantee that the correct number of neurons of the appropriate fate and position within the brain is generated. It is therefore not surprising, that RGC delamination is subjected to a rigorous and multi-level regulation that includes genetic, epigenetic and cell biological mechanisms (De Juan Romero and Borrell, 2017; Heide et al., 2017). Deregulation of delamination and its concomitant BP generation can, thus, be the origin of developmental neuronal malformations such as periventricular heterotopia (PH) or in the worst cases, lissencephaly or microcephaly (Barkovich et al., 2012; Fernandez et al., 2016). Interestingly, despite being a subject of intense investigation for the mentioned reasons, many important questions remain in ambiguity. For example; what types of processes determine the very first differentiation decisions, and what are their succession, or do they happen in parallel? Can a RGC delaminate and transform into a BP without undergoing a prior cell division? Does the angle of cell division necessarily and always lead to asymmetric fate choices, even if both daughter cells remain anchored apically at the ventricle? Does delamination alone induce neuronal differentiation?

Cell adhesion plays a pivotal role in the regulation of RGC delamination and differentiation (Gotz and Huttner, 2005). As referred before, being epithelial in nature, RGCs are connected to each other at the ventricle by different junctional complexes of the adherens, tight and gap junctions types (Gotz and Huttner, 2005) (Figure 1.2). Adherens junctions (AJs)
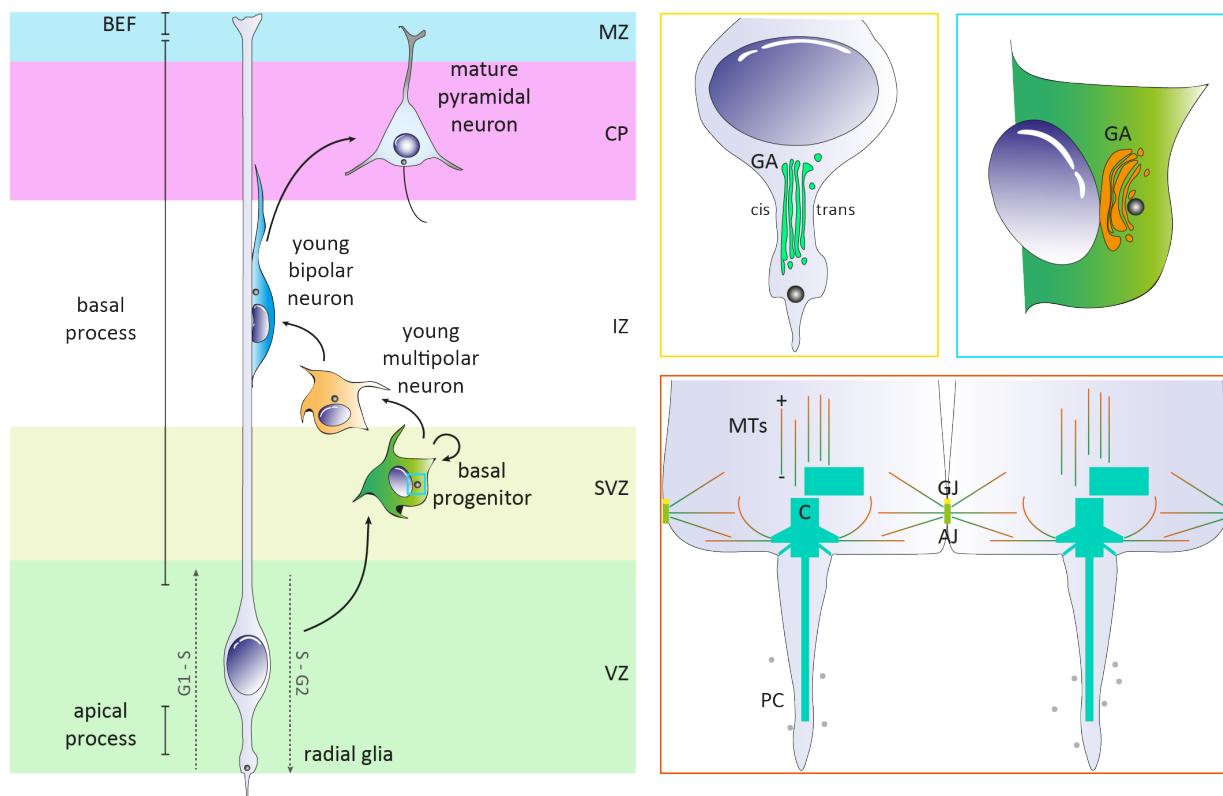
Figure 1.2: **Radial glia cell features and neuronal differentiation.** NECs and RGCs form a pseudostratified epithelium in the developing forebrain. They are attached to each other by adherens and gap junctions at their apical process. Their centrosome is also located here and forms the primary cilium from where cells can sense diverse signaling molecules (small gray spheres) such as morphogens. Most, but not all, MTs have therefore an apico-basal growth direction (minus to plus), as the centrosome is here the main MT organizer. The Golgi apparatus of RGCs is situated between the nucleus and the centrosomes but does not seem to be physically attached to the latter, as is the case in other cells (Taverna et al., 2016). RGCs make a characteristic IKNM i.e. their nucleus moves basally from the ventricular surface during G1-S phase and apically in S-G2 phase, with mitosis occurring at the apical surface. During the neurogenic period, RGCs delaminate from the epithelial layer and transform into multipolar BPs that, as mentioned earlier, divide in the SVZ. BPs subsequently generate and then turn into young neurons that acquire a bi-polar morphology and migrate radially along RGC basal processes towards the CP, where they mature. The centrosome of BPs and bipolar neurons is perinuclear and linked to the Golgi, in contrast to its localization in RGCs. However, the exact timing at which the centrosome re-localizes is not yet clear. AJ, adherens junction; CP, cortical plate; GA, Golgi apparatus; GJ, gap junction; IKNM, interkinetic nuclear migration; IZ, intermediate zone; MT, microtubule; MZ, marginal zone; PC, primary cilium; RGCs, radial glia cells; SVZ, subventricular zone; VZ, ventricular zone.

a Lissencephalic and gyrencephalic species

Basal lamina

Basal lamina

Ventricle

VZ

Ventricle

Early neurogenesis

c Gyrencephalic species

Basal lamina

b Lissencephalic species

Basal lamina

Basal lamina

Ventricle

SVZ

VZ

Ventricle

Basal lamina

Ventricle

OSVZ

ISVZ

VZ

Ventricle

Mid-late neurogenesis

APs

- Apical intermediate progenitor (or short neural precursor)
- Apical radial glia
- Neuroepithelial cell
- Subapical progenitor
- Neuron

BPs

- Transit amplifying progenitor
- Basal intermediate progenitor
- Basal radial glia basal process
- Basal radial glia both processes
- Basal radial glia apical process
- Transient basal radial glia

Figure 1.3: **The folded brain requires additional progenitors and germinal layers.** As introduced earlier, at mid to late neurogenesis, the cerebral cortex of lissencephalic species such as the one of rodents possesses almost exclusively two types of progenitors, namely RGCs and BPs, and they are found only in two distinct germinal areas, the VZ and the SVZ. In gyrencephalic animals (us, for instance), however, the SVZ is enlarged and subdivided into inner and outer SVZ (the goal being to enlarge the number of neuronal and glial progenitor and precursor cells that expand the surface area of the brain). Consequently, the number and diversity of apical and basal progenitors augments (see boxes). Changes in the progenitor composition in different yet ontogenetically conserved, brain regions generate the characteristic gyrus and sulcus. Interestingly, abnormal expansion of murine BPs can induce formation of folds in the otherwise flat murine cerebral cortex (Stahl et al., 2013). AP, apical progenitor; BPs, basal progenitor; ISVZ, inner subventricular zone; OSVZ, outer subventricular zone; RGCs, radial glia cells; SVZ, subventricular zone; VZ, ventricular zone. Adapted by permission from Annual Reviews: Annual review of cell and developmental biology, (Elena Taverna, Magdalena Gotz, Wieland B. Huttner), 4433050878429, (2014), https://doi.org/10.1146/annurev-cellbio-101011-155801

are mainly formed by transmembrane calcium dependent cell adhesion molecules (Cadherins) and cytoplasmic linker proteins of the Catenin superfamily (Meng and Takeichi, 2009). In the developing forebrain Cdh2 (N-cadherin) is the main classical cadherin, while Cdh1 (E-cadherin) expression remains controversial, and Cdh3 (P-cadherin) and Cdh12 (N-cadherin 2) are not or very lowly expressed (see Aprea et al., 2013 for expression levels). There are in addition many other nonclassical Cadherin-like proteins expressed in the developing brain, some of them also playing important roles during neurogenesis (see for example Capello et al., 2013; Stoykova, Götz, et al., 1997), but their description here goes beyond the scope of this work (see nevertheless Meng and Takeichi, 2009; Nishimura and Takeichi, 2009 for outstanding reviews). In the cytoplasm, Alpha- (Ctnna), Beta- (Ctnnb) and Delta-Catenin (Ctnnd/p120) link Cadherins to the actin cytoskeleton and regulate their stability and dynamic (Meng and Takeichi, 2009). Ctnnd in addition also regulates MT organization together with Plekha7, the MT minus-end binding proteins Camsap2 and Camsap3 and the kinesin-2 family member Kif3c (Meng et al., 2008; Sako-Kubota et al., 2014). Importantly, Ctnnd loss-of-function leads to a destabilization of the whole catenin complex, subsequent internalization of Cadherins and loss of cell-cell attachments (Reynolds 2007, and refs. therein). So, Ctnnd is at the top of the hierarchy of adherens junctions. It has been shown that the levels and stability of many components of AJs are decisive to maintain cells anchored to the belt at the VZ (Asami et al., 2011; Schmid et al., 2014; Tavano et al., 2018). However, mechanistically, how AJ dynamics at the moment of delamination are controlled in the developing forebrain, remains largely unknown. Rousso et al., 2012; Das and Storey, 2014; Kasioulis et al., 2017 have given some insights but in chicken spinal cord, which is partly different (no generation of BPs and few radial migration along radial processes). Here, apical abcision of the membrane of the basal end-food of RGCs, driven by both the microtubule and actin cytoskeleton, in conjunctions with a aparent observed reduction in N-Cadherin levels, triggers the detachment and delamination from the apical surface. If this is, nontheless, the major mode of delamination in the developing cebral cortex remains unclear. What has been shown in several other systems, however, is that centrosomes, in their virtue as MT organizing center (MTOC) can, in some epithelial cell types, fine tune AJ architecture and dynamics by means that include for example the redistribution of components via vesicle transport and motor proteins, interference of GTPase-mediated signaling important to maintain actin-based AJ stability, and sequestration of available pools of Tubulin to reduce nucleation at AJs (Krendel et al., 2002; Meng et al., 2008; Nagae et al., 2013; Sako-kubota et al., 2014). Hence, similar

mechanisms are conceivable in NSC delamination but are yet unexplored.

The centrosome is a membrane-less organelle made of two barrel-like structures made of stable microtubules called centrioles surrounded by pericentriolar material (a protein-rich matrix) from where microtubules are nucleated (Figure 1.4) (Nigg and Stearns, 2011). Most animal cells possess one centrosome, except at least for female gametes (egg cells) and syncytial skeletal muscles cells, which are devoid of them (Bornens, 2012; Borrego-Pinto et al., 2016; Bury et al., 2017; Coelho et al., 2013; Pimenta-Marquez et al., 2016). Both centrioles are kept together during interphase by a proteinaceous linker attached at the proximal ends (PEs) of the centrioles (Bornens et al., 2002). One centriole is older than its partner and therefore called mother centriole (the other being therefore the daughter centriole). Centriole maturation is identified by the acquisition of blade-shaped ultra-structural modifications called appendages at the distal and subdistal parts of the older centriole and happens during and after mitosis (i.e. G1) (Nigg and Stearn, 2011; Tanos et al., 2013). Distal appendages (DAs) are necessary to couple the mother centriole to the cell membrane, making it capable to form a primary cilium (or similar structures like immune synapses in lymphocytes) (Sorokin, 1962; Nigg and Stearns, 2011; Stinchcombe et al., 2015; Stinchcombe and Griffiths, 2014). Subdistal appendages (SDAs) are the anchoring place of some, but not all, centrosomal-born microtubules, as many of them can be severed and then transported to different cellular compartments (Dong et al., 2017; Mogensen et al., 2000; Rios, 2014; Sanchez and Feldman, 2017; Wu and Akhmanova, 2017). Anchoring of MTs at SDA can be interpreted as a way to keep them stably bound to the centrosome and thereby facilitate the centrosome-directed movement of MT-associated organelles such as the nucleus and the Golgi apparatus (Hung et al., 2016; Hurtado et al., 2011; Tanaka et al., 2004). In fact, LOF of SDAs associated proteins causes disorganization of MT at centrosomes (Casenghi et al., 2003; Delgehyr et al., 2005; Guarguaglini et al., 2005; Huang et al., 2017; Ibi et al., 2011; Ishikawa et al., 2005; Kodani et al., 2013; Lüders et al., 2006; Mazo et al., 2016). A second (nonexclusive) way to interpret the function of MT anchoring could be to locally regulate the rate of MT nucleation and polymerization, given the fact that nucleation promoting factors (e.g. MT polymerases and de-polymerases, motor proteins, activating enzymes) are also found at SDAs (Huang et al., 2017; Kodani et al., 2013; Miyamoto et al., 2015; Soung et al., 2003; Uzbekov and Alieva, 2018). Importantly, both DAs and SDAs are built in a hierarchical, LEGO-like form, with specific proteins making the basis of the appendages (thus most proximal to the centriolar wall) and others

forming the tip (i.e. the actual anchoring point) (Huang et al., 2017; Mazo et al., 2016; Tanos et al., 2013; Yang et al., 2018) (Figure 1.4). Although it may seem rather unimportant, this could mean that parts of the appendages are interchangeable and able to accommodate a variety of proteins, depending for instance on cell type or stage (a good example in Ibi et al., 2011). It is worth mentioning, as it is interesting and relevant to this manuscript, that SDA-components and associated proteins are not present in some classical animal models such as yeast, flies and worms, and they seem to appear first in Deuterostomes (Borrego-Pinto et al., 2016; Carvalho-Santos et al., 2011; Hodges et al., 2010). This strongly suggests that MT organization in this evolutionary lineage demands more mechanistic specialization.
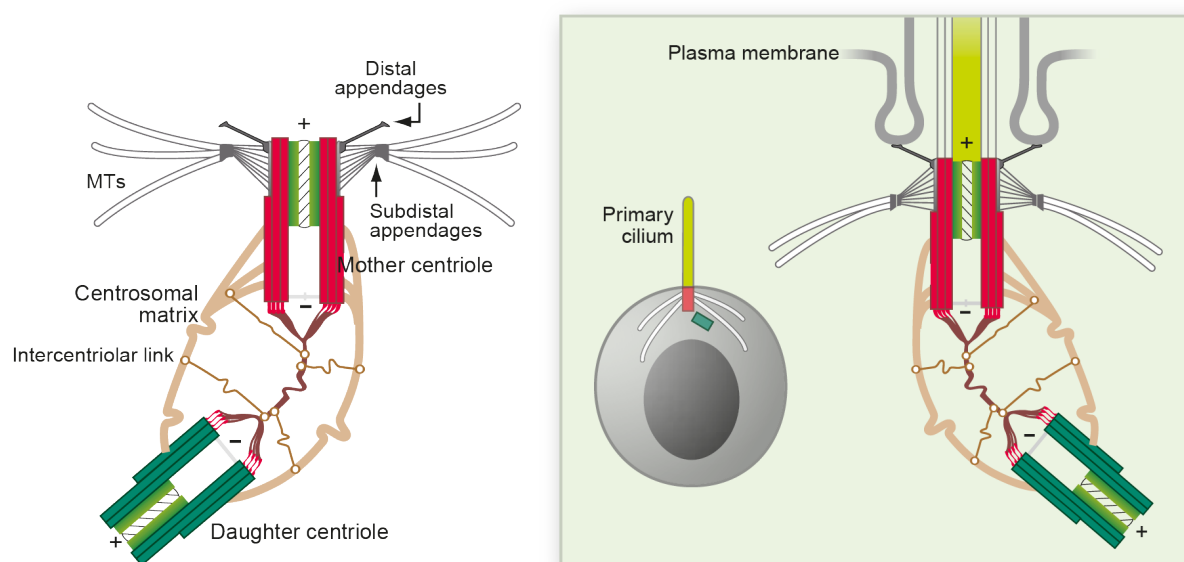
Figure 1.4: **The centrosome of vertebrata.** The centrosome is composed of two centrioles and a protein rich (pericentriolar) material. The older mother centriole has DAs and SDAs. DAs anchor the centrosome to the plasma membrane and facilitate formation of primary cilia or related structures. MTs are organized and their dynamics partly regulated at SDAs during interphase. Both centrioles are joint by a proteinaceous linker that dissolves during cell division to allow segregation of mitotic spindles. However, spindles can form without centrioles because MTs are also nucleated from the PCM and mitosis can thus occur. This occurs naturally in meiosis or when centrioles are physically (e.g. by laser ablation) or genetically (gene knock-out) disrupted. DAs, distal appendages; MTs, microtubules; PCM, pericentriolar material; SDAs, subdistal appendages. From The Centrosome in Cells and Organisms, Michel Bornens, Science, 27 Jan 2012: 422-426. Reprinted with permission from AAAS."

The functions of centrosomes in RGCs and migrating young neurons has been (in principle)

well documented, unlike its role in BPs, where knowledge is rather scarce (for examples see Wilsch-Bräuninger et al., 2010, Paridaen et al., 2013). During interphase, centrosomes of RGCs build the basal body of primary cilia, and organelle crucial for sensing a number of potent morphogenic extracellular molecules important to maintain stemness (Wilsch-Bräuninger et al., 2010; Johansson et al., 2013; Falk et al., 2008; Fliegauf et al., 2007). The primary cilia of RGCs could (in principle) also help to interpret mechanical forces and shear stress from the CSF (Park et al., 2017). During karyokinesis of RGCs, the mitotic centrosomes that make the spindle can help determining the cell cleavage angle (Insolera et al., 2014) which in turn may balance the distribution of intracellular and membrane bound cues to the daughter cells, as seen in Drosophila neuroblasts (Knoblich, 2008). This distribution can be symmetric or asymmetric, and consequently influence the output of the division (i.e. two NSCs, or one NSC and a BP) (Costa et al., 2008; Kosodo et al., 2004). However, it is debatable, if the cleavege angle per se is the master event that dictates fate choice. On the one hand, manipulation of polarity proteins like Inscutable (which regulate spindle orientation) as well as AJ-components or some centrosome- and MT-associated proteins induces randomization of cleavage angle leading to increased non-self-renewal divisions and the concomitant depletion of progenitor cells, including adult stem cells (Asami et al., 2011; Costa et al., 2008; Culurgioni et al., 2018; Falk et al., 2017; Konno et al., 2008; Postiglione et al., 2011; Tylkowski et al., 2015). On the other hand, evidence indicate that, under normal conditions, in most cases, RGCs make planar divisions with the apical domain segregating symmetrically, and only later one cell (the most apical and devoid of basal process) delaminates to become a BP (Konno et al., 2008; Shitamukai et al., 2011). Manipulation of mitotic centrosome associated LGN/Gpsm2 and NuMA, despite changing the division plane and inducing delamination, had no effect on neuronal differentiation (Konno et al., 2008; Peyre et al., 2011; Shitamukai et al., 2011). Something similar is observed when centrioles are eliminated in the developing forebrain (but not PCM, which, importantly, still forms and is able to nucleate MTs in interphase and mitosis), since spindles get misoriented with divisions occurring all directions, and progenitor cells are found scattered throughout the tissue including the CP, but their fate seems unaffected (Insolera et al., 2014). Furthermore, Costa et al showed that cell polarity regulatory proteins Par3 and Par6, which are also associated to centrosomes (Burunte et al., 2017; Costa et al., 2008; Dormoy et al., 2012; Kodani et al., 2010), in contrast to Inscutable, promote stem cell maintenance, as overexpression increases proliferating Pax6 positive RGCs and downregulation has an opposite effect (Costa et al., 2008). Finally, RGCs of Cdc42-cKO

mice (a Rho-GTPase that regulate MT polymerization and stability) lose apical junctions and delaminate prematurely. Concomitantly, there is an increase in BP generation at the expense of RGCs, however, cleave plane orientation is unaffected (Cappello et al., 2006). Therefore, the bottom line is that manipulation of different centrosomal associated factors can generate different phenotypes and thus, the conclusions drawn upon their manipulation may need to take in consideration additional processes. This will help to reconciliate apparently contradictory observations.

In migrating young neurons (of the embryonic and adult brain), a role for centrosomes is also not unified. On the one hand, it has been shown that centrosomes can determine the orientation of somal movements and are needed for nuclear translocation. One mechanism uses the primary cilium to sense attractive molecules, so that cells can navigate correctly towards their end-location (Baudoin et al., 2012; Higginbotham et al., 2012). Another mechanism needs the action of the centrosome- and MT-associated dynein and dynactin complexes, and the microtubule-associated proteins (MAPs) Lis1 and Doublecortin (Dcx), which couple the nucleus to the centrosome via MTs. The minus-end directed locomotion of dynein/dynactin together with Lis1 and Dcx pulls the nucleus towards the centrosome. Since neurons move in a saltatory manner with the centrosome moving ahead within the leading cell process followed by the nucleus, loss of function of the mentioned proteins or de-stabilization of the complexes has negative effects on the perikaryal MT cage and concomitantly hinders its forward translocation (Tanaka et al., 2004; Tsai et al., 2005; Tsai et al., 2007; Wynshaw-Boris and Gambello, 2001). On the other hand, however, it was also reported that nuclei and centrosomes of migrating neurons move independently from each other and the centrosome does not persistently lead during neuronal migration (Distel et al., 2010; Umeshima et al., 2007). How can this difference be explained? Centrosomal-based microtubule nucleation is gradually deactivated during neuronal differentiation, through downregulation or re-localization of MT nucleation and anchoring proteins to noncentrosomal compartments such as the Golgi apparatus, the cell cortex and in the cytoplasm (Lechler and Fuchs, 2007; Sánchez-Huertas et al, 2016; Sanchez and Feldman et al., 2016; Stiess et al., 2010; Tanaka et al., 12; Wu and Akhmanova 2017; Yonezawa et al., 2015; Zhang et al, 2016). This most likely allows local nucleation far away from the centrosomes in the axons and dendrites while giving some independence to the centrosome to move freely and, for example, re-locate the primary cilium. Since neuronal differentiation and migration occurs simultaneously, the above-mentioned incongruences are probably just a

matter of observations made at different developmental stages.

1.2   Neurogenesis in the adult mouse brain

After birth and at adult stages, neurogenesis continues in the mouse brain in at least three areas, namely in the lateral wall of the lateral ventricle below the ependymal zone (thus called the subependymal zone, SEZ) (Figure 1.5), in the dentate gyrus of the hippocampus and in the hypothalamic nuclei (Götz et al., 2016; Kokoeva et al., 2005; Ming and Song, 2011; Robins et al., 2013). Curiously, the areas of adult neurogenesis are not always the same in all species but may vary. In birds (canaries) for instance, new neurons are constantly replaced in vocal control nuclei in the telencephalon, the area where seasonal song-learning is done and processed (Paton and Nottebohm, 1984; Paredes et al., 2016 and see Altman, 2011 for a historical review on the discovery of adult neurogenesis). In rabbits, neurons are also added at noncanonical neurogenic regions such as the striatum, amygdala and cerebellum (Feliciano et al., 2015). In humans, the story is more controversial with reports suggesting absence of adult neurogenesis (Sorrells et al., 2018) and others showing that new neurons can be generated in the striatum and hippocampus (Boldrini et al., 2018; Ernst at al., 2014).

What is the source of adult (a)NSCs, and how are these, and the whole neurogenic process, ontologically related to their embryonic counterpart? In the mouse, adult SEZ NSCs were shown to originate largely from RGCs from the ventral forebrain (more specifically the LGE, see Figure 1.5) (Fuentealba et al., 2015; Merkle et al. 2004), while hippocampal aNSCs derives also from RGCs but from the ventral embryonic hippocampus (Berg et al., 2018; Li et al., 2013). As in the developing brain, activated aNSCs turn into intermediate transient amplifying progenitors (TAPs) that serve to enlarge the pool of daughter cells and subsequently turn into young neurons. Possibly, as is the case in the embryo, besides proliferation, the life of a TAP may also permit many cell biological changes such as cytoskeletal, cell-surface or metabolic rearrangements (Llorens-Bobadilla et al., 2017). Newborn neurons (neuroblasts) then migrate tangentially as a stream within a tunnel-like structure made of astrocytes - and possibly some blood vessels - rostrally towards the olfactory bulb (OB) (Figure 1.5) (Ming and Song, 2011). Once they reach the OB, migration turns radially so that neurons move and colonize the different neuronal layers where they

finally mature. Many - if not most - of the cells from the adult SEZ differentiate into GABAergic inhibitory interneurons in the granule cell layer (Calzolari et al., 2015), but few others colonize different layers of the OB (Brill et al., 2008; Calzolari et al., 2015; Hack et al., 2005; Merkle et al., 2007) and even some belong to the glutamatergic excitatory type (Brill et al., 2009). This heterogeneity is perhaps a reflection of their embryonic specification and may have led to the belief that adult neurogenesis would be a mere recapitulation of embryonic neurogenesis. There are, however, clear differences that argue against this idea. First, and perhaps the most important, adult neurogenesis happens in a context that rather favors gliogenesis, and in addition, adult newborn neurons must adapt to existing neuronal circuits that are not yet formed at embryonic stages. At the molecular level, although aNSC look morphologically similar (radial-like morphology with end feed facing the ventricle with a primary cilium, in the case of SEZ cells) their gene expression profile rather nears mature astroglia cells (Beckerfordersandforth et al., 2010). It is in fact the progeny (TAPs) which are alike to RGCs, in respect at least to gene expression (Götz et al., 2016; Beckerfordersandforth et al., 2010; Pinto et al., 2008). So, in other words, aNSCs must change their program from mature astroglia-like to neuronal progenitor/precursor. On top of that, even under the neuronal program, adult neurogenesis uses additional gene regulatory circuitries not found in the embryo (Brill et al., 2008; Hack et al., 2006, Ninkovic et al., 2010; Ninkovic et al., 2013). It is, however, quite interesting that aNSCs are poised to do so, as they have relatively high levels of transcripts for neuronal fate determinant (compared to other nonneuronal cells) but not the corresponding proteins (Beckervordersandforth et al., 2010; Götz et al., 2016; Sirko et al., 2013). How this is kept in check is still unresolved, yet an obvious way would include epigenetic mechanisms mediated by noncoding RNAs or histone modifiers as these could allow transcription of fate determinants to occur while keeping off their translation (see for example Cheng et al., 2009; de Chevigny et al., 2012; Ninkovic et al., 2013; Lim et al., 2009; Pons-Espinal et al., 2017; Ramos et al., 2015; Shibata et al., 2011). Thus, in conclusion, although the basic stem cell biology is conserved, adult neurogenesis has its own particular requirements.
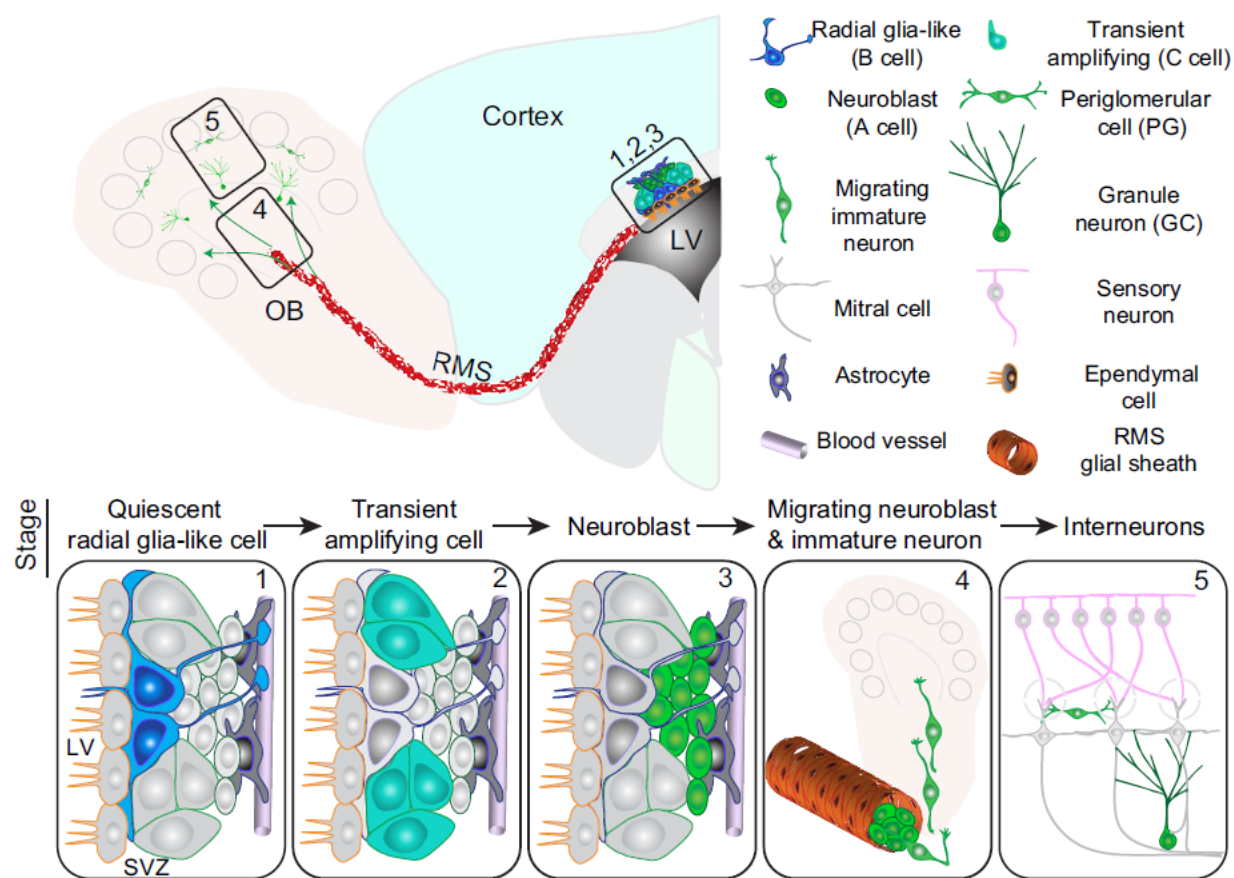
Figure 1.5: **Olfactory bulb adult neurogenesis.** In the adult rodent brain, new neurons are added throughout live to the olfactory bulb. They derived from aNCSs (B cells) at the lateral ventricle. These are astroglia-like cells with radial morphology located below ependymocytes, with primary cilia contacting the ventricle and end-feed contacting blood vessels. Upon activation, aNCS transform into proliferating TAPs (C cells), and these in turn differentiate into neuroblasts (A cells) that migrate tangentially towards the OB along the RMS, a pathway made of astrocytes. There, they migrate radially towards their target layer and mature into diverse type of neurons according to their origin (see below). aNSC, adult neural stem cell; OB; olfactory bulb; RMS, rostral migratory stream. Adapted by permission from Elsevier, Neuron, (Guo-li Ming,Hongjun Song), 4433051253500, (2011), https://doi.org/10.1016/j.neuron.2011.05.001

1.3 Noncoding RNAs and neurogenesis

In contrast to protein coding genes, noncoding regulatory RNAs have just recently emerge as key factors regulating aspects of stem cell biology such as self-renewal versus differentiation. In the case of the neurigenic systems in the developing and adult brain, or in embryonic stem cell (ESC) derived neural progenitors, mostly the roles of microRNAs
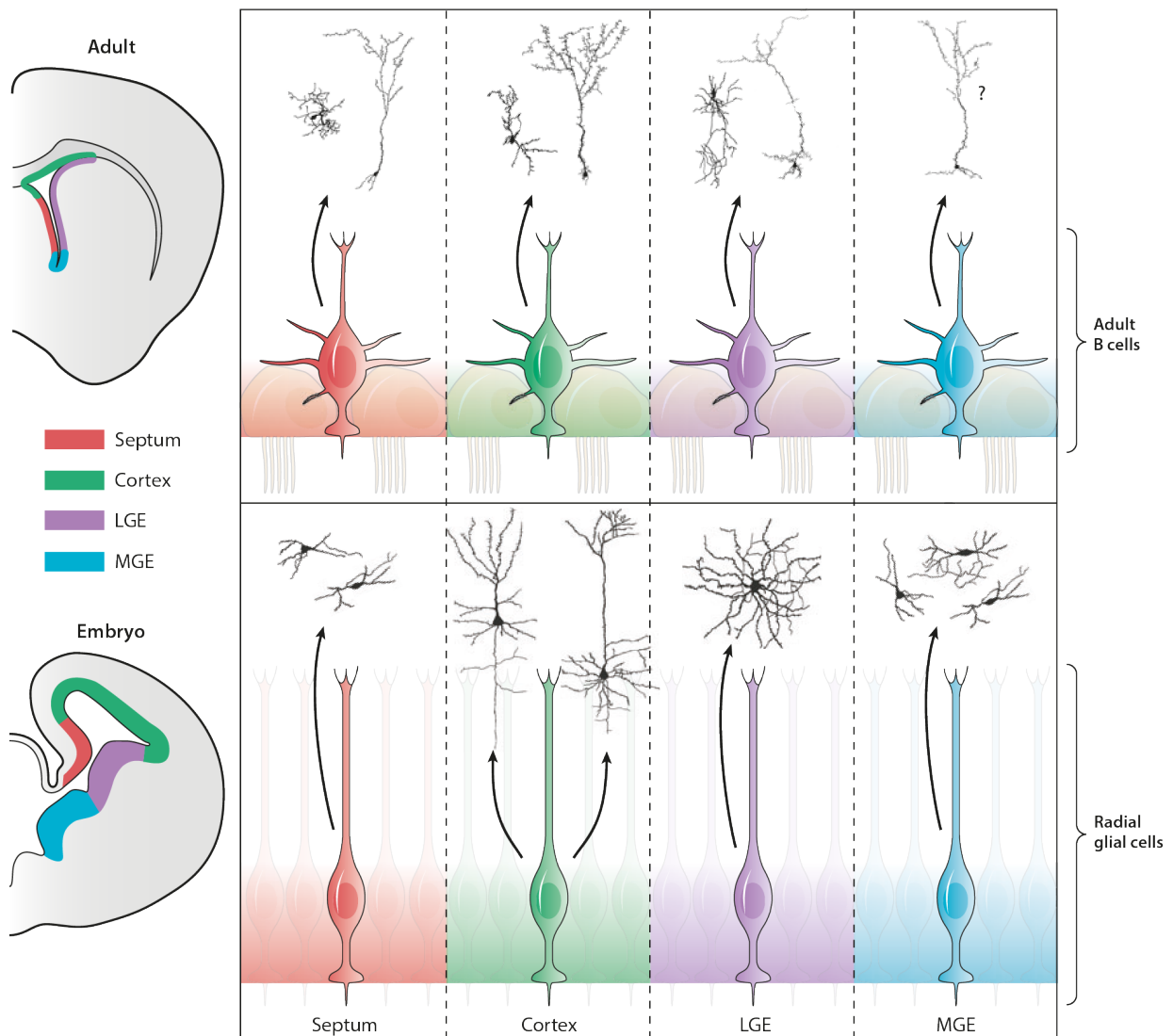
Figure 1.6: **Adult neural stem cells come from radial glia cells.** Subsets of neurogenic progenitor cells located in at different parts of the dorsal and ventral germinal zones (demarcated in colors) are the source of the future aNSCs. In the mouse brain, a large proportion of them derive from the LGE, while fewer come from the MGE and the cortex, and rather few from the septum. Interestingly, aNSC conserve their embryonic identity and consequently produce neurons of the same lineage they do during development. However, in contrast to their embryonic counterpart, aNSC have to transit first from a astroglia-like state (i.e. a differentiated cell) to a progenitor cell type, to then again turn into a (differentiated) neuron. aNSC, adult neural stem cells; LGE, lateral ganglionic eminence; MGE, medial ganglionic eminence. Adapted by permission from Annual Reviews: Annual Review of Neuroscience, (Kriegstein and Alvarez-Buylla, 2009), 4433050101491, (2009), https://doi.org/10.1146/annurev.neuro.051508.135600

(miRNAs) and long-noncoding RNAs (lncRNAs) have been described (see Aprea and Calegari, 2015, Ebert and Sharp, 2012; and Rajman and Schratt, 2017 for excellent reviews). Certainly, however, other regulatory RNAs that may have been not studied in detail, could have critical roles regulating neurogenesis (see Cech and Steitz, 2014; and Palazzo and Lee, 2015 for detailed description of noncoding RNAs in eukaryotic and bacterial cells, and Figure 1.7 for an overview). One can for instance imagine that diffences in abundance or post-transcriptional modifications of transfer RNAs (tRNAs) could have a big impact in the translational rate of fate determinats along the differentiation cascade (e.g. RGC vs. BP, or neurogenic vs. gliogenic RGC differentiation), which in turn could contribute to the definition of the final identity output (see for instance Gingold et al., 2014; and Van Bortle et al., 2017 for such a scenario).

MiRNAs are 20-22 nucleotide long and have the overall function of regulating the levels of transcripts through complementary base pairing to the 3' UTR of mRNAs, if i a protein coding gene, or at any other position in the case of noncoding RNA species. This binding leads wether to degradation of mRNA trascripts or block of their translation (Figure 1.7). LncRNAs are by definition longer than 200 nt and, different than miRNAs, have a broader spectrum of functions. They can, for example, recruit proteins to subcellular locations such as specific genomic loci in the nucleus and nucleolus (transcription factors, chromatin re-modelers, polymerases) to regulate transcription or genome architecture (Cech and Steitz, 2014; Militti et al. 2014; Rinn and Chang, 2012) (Figure 1.7). They can also serve are miRNA precursor transcripts and even act as miRNA-sponges and sequester these from their original targets, the effect being dependent on the number of lncRNA transcripts (Aprea and Calegari, 2014).

It is particularly interesting, in one hand, that noncoding RNAs have very often a remarkably cell type specificity even within the same organ and cell type, suggesting that their role is largely to fine-tune global cellular pathways at, and with, defined spatiotemporal resultion. On the other hand, to date, the data suggest that the brain is the organ with the highest abundance in noncoding transcrips, thus highlighting the extensive regulation that it employs (Adlakha and Saini, 2014; Aprea and Calegari, 2015 and references therein; Ludwig et al., 2016). A nice example of this is miR-92; it targets the 3' UTR of Btg2/Tis21 and delicately regulates its expresssion making it specific to BPs in the developing fore-
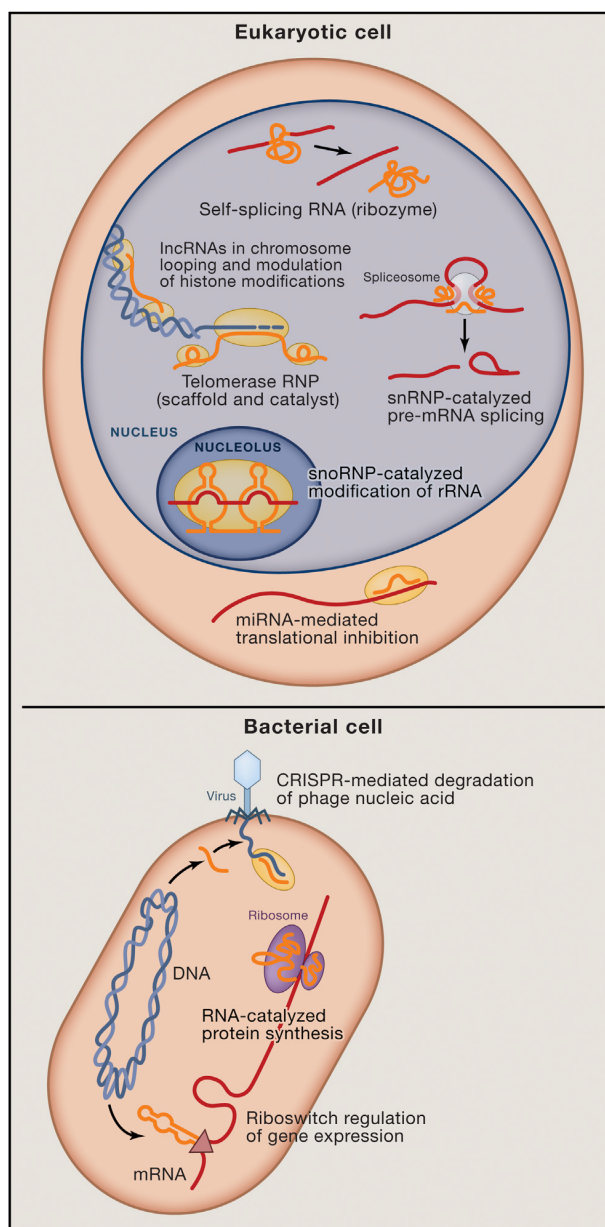
Figure 1.7: **Noncoding RNAs and their roles in eukaryotes and bacteria.** Noncoding RNAs regulate genes expression at different levels (e.g. transcription, translation, splicing) and participate in genome organization and stability, both in prokaryotic and eukaryotic cells. Among the best known functions in bacteria are the CRISPR-based immune response against phages and the regulation of translation by riboswitches during the adaptation to changing environmental conditions. Transfer (t)RNAs are found in ribosomes of all living beings, where they function as adaptor molecules between mRNA and amino acids during the formation of polypeptide chains. In eukaryotic cells, such as mammalian stem cells, other roles encompass for instance: inhibition of miRNA-mediated inhibition of gene expression through sponging (linear or circular ncRNAs), recruitment of transcription factors and chromatin remodelers to genomic loci to activate, repress or fine tune transcription, scaffolding of multiprotein complexes to form higher-order intracellular structures, and control of mRNA splicing (with proteins or alone). CRISPR, Clustered Regularly Interspaced Short Palindromic Repeats; RNP ribonucleoprotein; snRNP, small nuclear ribonucleoprotein. Adapted by permission from Elsevier, Cell, (Thomas R. Cech,Joan A. Steitz), 4433060070863, (2014), https://doi.org/10.1016/j.cell.2014.03.008

brain. As a matter of fact, a mouse model laking the binding site for miR-92 shows defects in corticogenesis as Tis21 cannot be silenced in proliferating RGC, resulting in premature differentiation, exhaustion of the RGC pool and consequently microcephaly (Fei et al., 2014). Other miRNAs have equally essential roles in neuronal development; most known are miR9, miR124, miR128, miR204 (Lang and Shi, 2012), but there are surely many other unexplored candidates. Similarly, the roles of some lncRNAs in neurogenesis have uncovered, ranging from transcriptional control of pro-neurogenic and pro-gliogenic factors through miRNA sponging (Ramos et al., 2015), to maintenance of the epigenegic status of their protomoters (Berghoff et al., 2013; Cajigas et al., 2015), and mediation of RNA splicing (Aprea et al. 2013). The latest example is of great relevance as it uncovered a novel mechanism regulating BP generation in the developing cerebral cortex based on a noncoding RNA species. Miat, as it is called, is highest expressed in Tis21 positive differentiating RGCs and BPs where it contribubes to splicing of genes important for neuronal differentiation.

As with miRNAs, the field of lncRNA research is rather young and many more candidates and mechanism are awaiting to be discovered, also - if not specially - in the brain.

1.4 Novel factors regulating generation of intermediate neuronal progenitors and precursors

In search for a better understanding regarding (a) how intermediate progenitors are generated, (b) what the principal events taking place in them are and (c) are the molecular mechanisms regulating those events are, our lab and others have done pioneering genome-wide examination of the transcriptional landscape of different population of murine neural stem and progenitor cells of the developing and adult brain (Aprea et al., 2013; Becker-vordersandforth et al., 2010; Codega et al., 2014; Lim et al., 2006; Llorens-Bobadilla et al., 2017; Pinto et al., 2008; Ramos et al., 2013). This has led to the identification of novel players controlling common aspects of adult and embryonic neurogenesis, including IP generation (Pinto et al., 2009; Ramesh et al., 2016; Stahl et al., 2013). The nuclear protein Trnp1 for instance dictates if RGCs amplify or make BPs in the developing cerebral cortex, as forced expression increases the number of RGCs and its downregulation greatly expands

BPs and bRGCs resulting in the folding of the otherwise smooth mouse brain (Stahl et al., 2013). Not surprisingly, Trnp1 is expressed in the gyrencephalic brain of ferrets in a block-wise manner typical of genes involved in brain folding (De Juan Romero et al., 2015). There, Trnp1 expression defines the period of oSVZ formation, i.e. oSVZ RGCs generation (Martínez-Martínez et al., 2016). Importantly, it may also play an important role in adult SEZ neurogenesis where it is highest expressed in tangentially migrating NBs of the RMS. The mechanism by which Trnp1 exerts its role is not yet well understood, but perhaps it helps to rearrange or shape the nuclear architecture in a constantly changing context - i.e. constantly changing cell fates. This could explain why it is also expressed in neurons of the CP of the developing cortex (Stahl et al., 2013). Another important gene regulating BP fate is the transcription factor Tfap2c (AP2-gamma) (Pinto et al., 2009), which in a region and layer specific manner controls the expression of pro-neurogenic BP genes in the developing cortex at mid-neurogenesis. LOF by genetic ablation leads to miss-specification of BPs and cell death in the visual cortex of the mouse, specifically affecting upper layer neurons.

1.5   Aim of the study

In a similar fashion to the discoveries mentioned above, a novel candidate gene was found enriched in the germinal areas of the developing forebrain and in the adult SEZ neurogenic system. This gene is called AT-hook transcription factor Akna (KIAAA1968). Intuitively, it was a very promising candidate gene to investigate due to its reported role in regulating the expression of surface antigens in lymphocytes and knock-out mice showed exacerbated immune reaction under challenging conditions with perinatal dead (Siddiqa et al., 2001; Ma et al, 2011). Furthermore, there were also indications that Akna is associated with autoimmune diseases and certain types of cancer (Mao et al., 2011; Moliterno and Resar, 2011; Perales et al., 2010; Suram et al., 2013). Nonetheless, no study had interrogated the role of this gene in neurogenesis, providing thereby an opportunity for novel discoveries. So, our laboratory asked what its role in embryonic corticogenesis could be. Initial manipulations in vivo (gain and loss of function) by previous members of our group showed strong effects in neuronal differentiation (described later in the results part), which impulsed the obvious question on how Akna works at the molecular level. That became the focus of my studies. The main questions were therefore: (a) What kind of protein is Akna (this,

given that available antibodies did not performed well)? (b) Which are the interactions partners? (c) What kind of cellular events does it regulate? (d) How is it itself regulated? (e) Is its role similar or different in adult neurogenesis?

In the following part, I will present the results of my work and the new and exciting lessons we, and the field, have learned from this gene.

Chapter 2

Results

Introductory remark
Some data shown in this section were derived by or done together with co-authors of the study and are essential for the understanding and the flow of the manuscript. In such cases, the respective person is acknowledged in the figure legend.

2.1 Identification of Akna as centrosomal protein

Akna expression was highest in E14 CTX tissue compared to E9 forebrain and E18 CTX tissues, i.e. the peak of SVZ generation via BPs, as well as in RGCs fated to generate BPs compared to those that will proliferate or generate neurons directly (Pinto et al., 2008) (Figure 2.1 a-c). RNA-ISH showed that Akna transcripts were also enriched in the germinal zone of the ventral telencephalon, but as in the CTX, rather low in more mature neurons (lying basally) (Figure 2.1 d,e). This is in agreement with RNAseq data from the Calegari lab (MPI CBG, Dresden; Aprea et al., 2013) showing highest levels of Akna in differentiating RGCs (Tis21+/Tubb3-) compared to proliferating RGCs (Tis21-/Tubb3-) and neurons (Tis21-/Tubb3+) (Figure 2.1 c). This strongly suggested that Akna is involved in BP generation and thus, mouse and rat monoclonal antibodies were generated against recombinant mouse Akna protein or two peptides, yielding antibodies that recognize Akna from different mammalian species such as mouse, rat, ferret macaque and human. Stablished clones were validated by RNAi (Figure 2.1 f). Notice that Akna, though having a molecular weight (MW) of 153 kDa, is detected at a higher MW. This may be due to the

relatively low isoelectric point (6.1) and posttranslational modifications (discussed later). To my surprise, I could never detect nuclear immunoreactivity and instead I observed always signal at centrosomes, in different cell types and different species (Figure 2.2 a-f). This localization at centrosome was validated by RNAi and GFP-tagged BAC transgenic cells lines (GFP-tagging in the endogenous c-terminus) (Figure 2.2 d,f). In addition, analysis of subcellular fractions by Western Blot (WB) and mass spectrometry showed enrichment of Akna in the centrosomal fraction but not in the nuclear portion (Figure 2.2 g,i). Electron microscopy with immunogold labeling and STED nanoscopy allowed to pin down the specific location of Akna within the centrosome, namely at the most outer part SDAs and to a minor degree at the PEs (Figure 2.2 h,j-k'). Not surprisingly, and as mentioned previously, since SDAs are not present during mitosis, Akna IF-signal was not detectable at any time during this cell cycle phase (Figure 2.3 a and see mitotic cell in Figure 2.2 f). In contrast, Akna is detected at all stages of interphase (Figure 2.3 a). Importantly, immunoblots of synchronized cells showed no obvious protein degradation during M-phase, meaning that Akna is de-localized from the centrosome but not degraded (Figure 2.3 b).

2.2   Targeting of Akna to centrosomes

I asked next if localization of Akna from centrosomes in mitosis would be regulated by phosphorylation, as has been shown for other SDA proteins. Treatment with 0.5 μM ocadaic acid (OA) for 3-4 hours, to block protein phosphatases 1 and 2 (PP1/PP2), and thus promote phosphorylation, led to delocalization of Akna from centrosomes in primary cortical cells (Figure 2.3 c), suggesting that phosphorylation by serine/threonine kinases (PP1/PP2 are serine/threonine phosphatases) is involved in its localization at centrosomes. Notice in Figures 2.3 d,e that phosphorylation is partly responsible for the delay in migration in immunoblots (as mentioned above, Akna should be detected at 153 kDa, but is observed at around 190 kDa): a shift towards higher MW is observed upon treatment with OA for 4 hours. In contrast, immunoblots of protein lysates dephosphorylated by calf Intestinal alkaline phosphatase (CIP) showed a band at the predicted MW (Figure 2.3 e). Importantly, at later time points after treatment (for instance, 5 hours) or with higher doses if OA (1 μM) the increased phosphorylation induced protein degradation (Figure 2.3 f). Lower doses, which should specifically inhibit only PP2, do not seem to affect migration
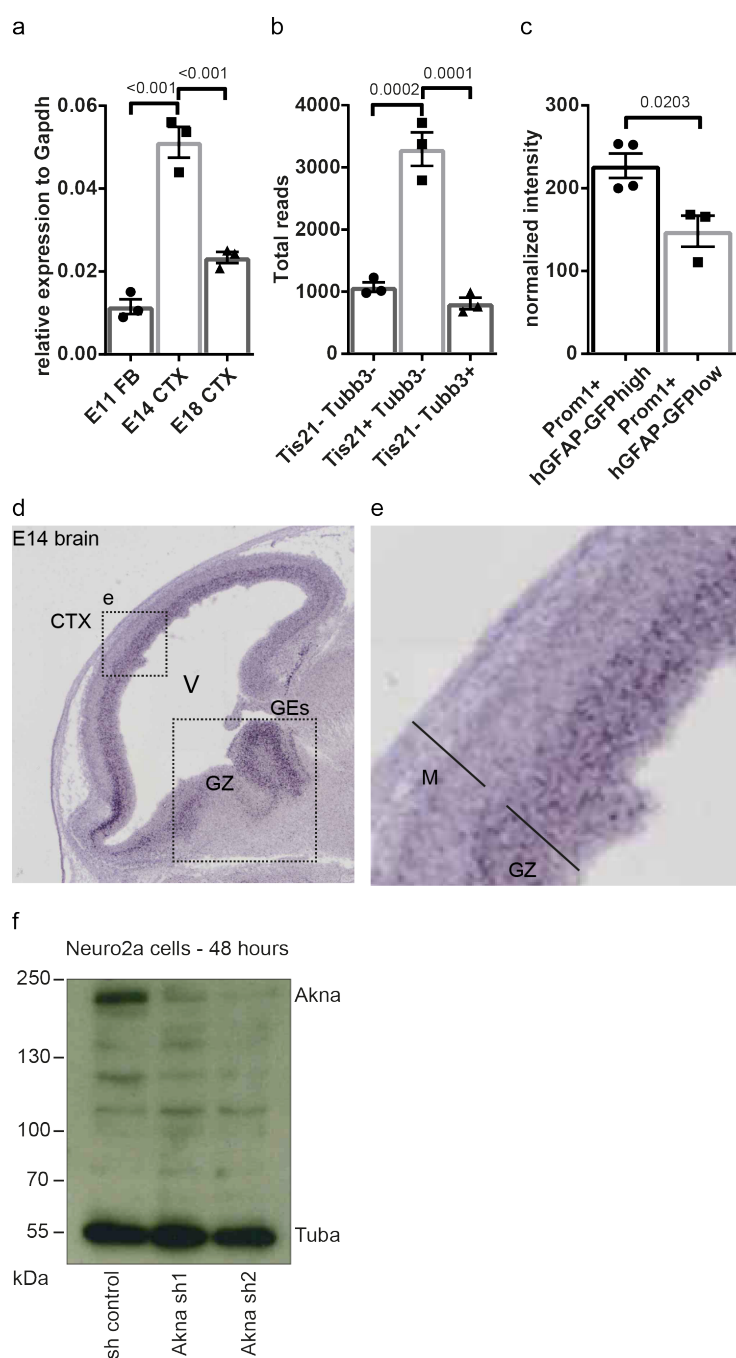
Figure 2.1: **Akna mRNA levels in the developing mouse brain.** (a) RT-qPCR results showing Akna transcription at the start (E11), mid- (E14) and end (E18) of neurogenesis. (b) RNAseq data in proliferating non-differentiating RGCs (Tis21- Tubb3-), differentiating delaminating RGCs and BPs (Tis21+ Tubb3-) and neurons (Tis21- Tubb3+) (Aprea et al., 2013; publish available). (c) Levels of Akna transcript in RGCs that will generate BPs (Prom1+ hGFAP-GFP high cells) and RGCs that will not make BPs (non-differentiating RGCs or RGCs doing direct neurogenesis) (Prom1+ hGFAP-GFP high cells) (Pinto et al., 2008, published microarray data). (d,e) RNA ISH of E14 mouse sections showing higher levels of Akna transcripts in the GZ of the dorsal and ventral forebrain at E14 compared to the M. Adapted by permission from PLOS: PLOS Biology, (Diez-Roux et al., 2011), Open Access article distributed under the terms of the Creative Commons Attribution License, (2011), https://doi.org/10.1371/journal.pbio.1000582. (f) WB of Akna knockdown using a control empty plasmid or two different anti Akna shRNAs. CTX, cortex; GE, ganglionic eminence, GZ, germinal zone (VZ+SVZ); M, mantle (IZ+CP+MZ); V, ventricle. Statistical analysis (a-c) is student t-Test.
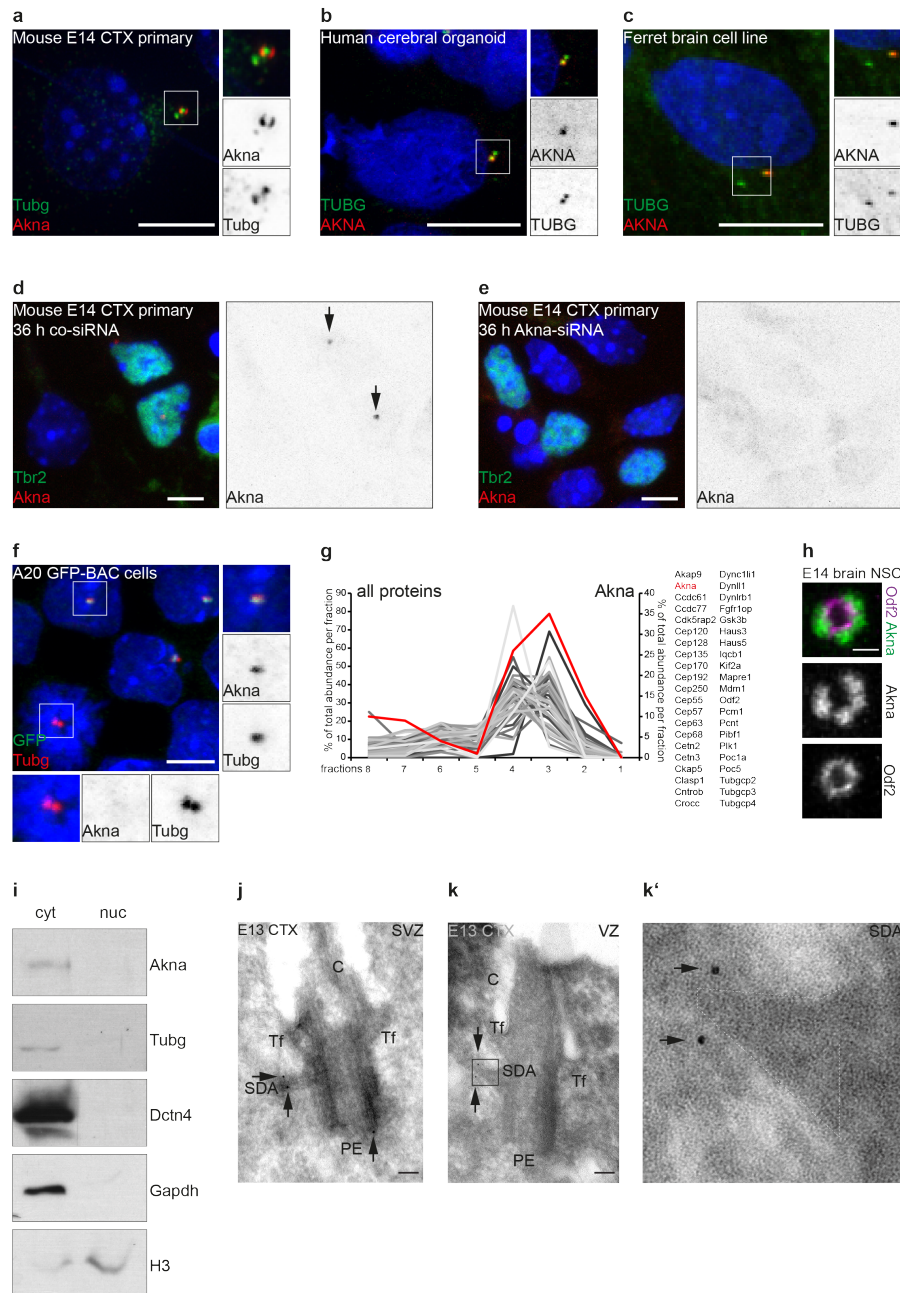
Figure 2.2: **Akna localization at centrosomes.** (a-c) IF of Akna in neural cells from different species. Notice enrichment of Akna signal at one (mother) centriole in all three examples. (d,e) Akna IF in murine E14 primary cortical cells after siRNA mediated knockdown showing. (f) BAC transgenic A20 cells (B lymphocytes) in which GFP was tagged at the endogenous C-terminus. Akna IF signal is not observed in the spindle, as exemplified in the lower left cells. (g) Mass spectrometric analysis of cellular fractions of A20 cells. Akna (red) is enriched in the centrosomal fraction. (h) STED image of SDA protein Odf2 and Akna indicating the relative position at the SDAs (Odf2 is most proximal to the centriolar wall, Akna is rather distally). (i) Importantly, Akna was not detected in nuclear fractions, suggesting that it localizes mostly at centrosomes. (j-k') Immuno-gold EM of Akna in RGCs (VZ) and BPs (SVZ) in E13 CTX tissue. Notice the signal at distal parts of the SDAs (arrows). In occasions there was also immuno-signal at PEs. EM pictures by MWB. C, cilium; CTX, cortex; BAC, bacterial artificial chromosome; IF, immunofluorescence; NSC, neural stem cell; PE; proximal end; SDA, subdistal appendage; SVZ, subventricular zone; Tf, transitional fiber (i.e. distal appendages); VZ, ventricular zone. Scale bars: 5 μm (a-f); 0.1 μm (h, j-k')
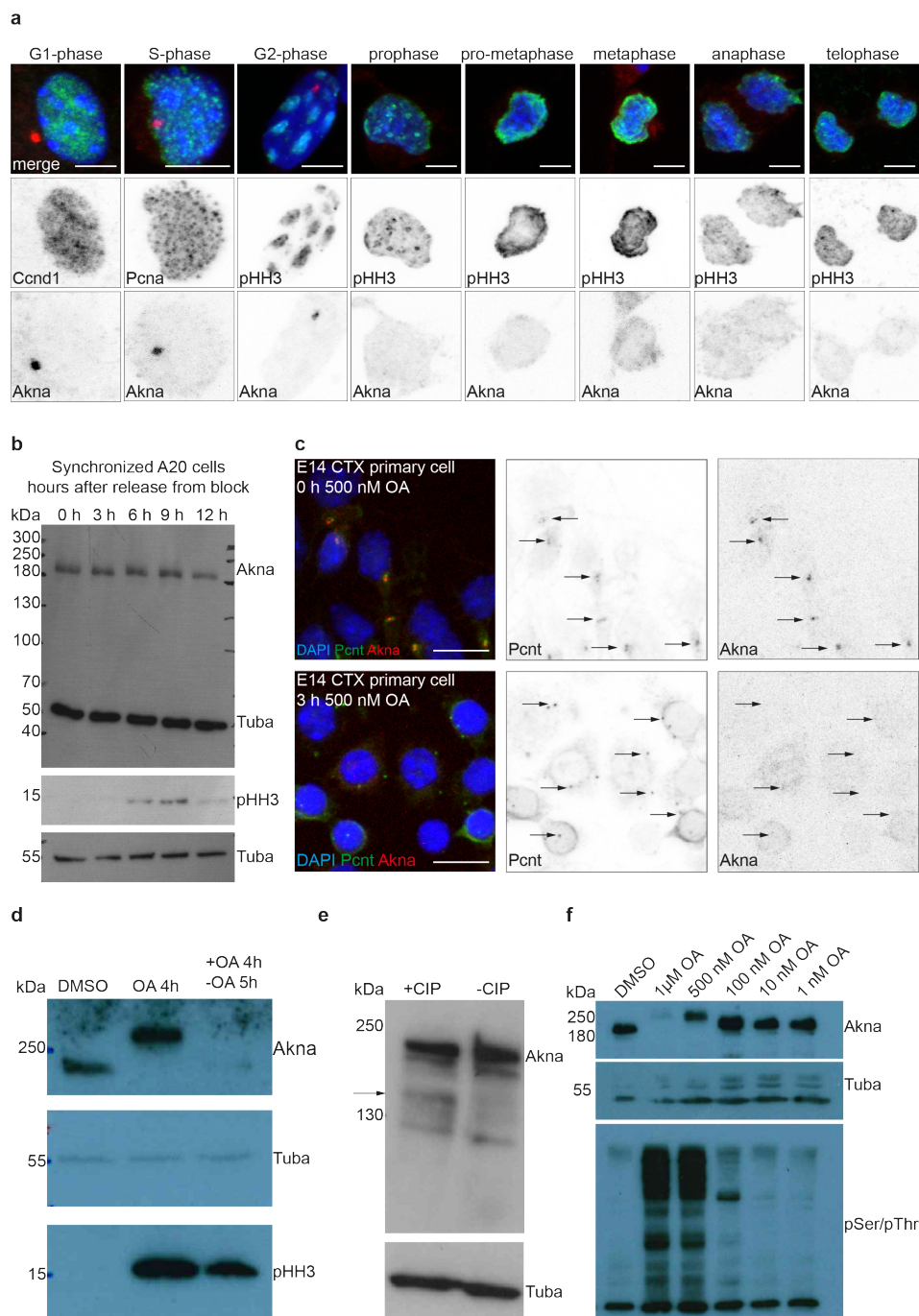
Figure 2.3: **Regulation of Akna localization at centrosomes.** (a) IF staining of Akna in E14 CTX primary cells at all stages of the cell cycle as identified by corresponding phase marker. (b) WB of synchronized A20 cells previusly block by double thymidine treatment. (c) Immuno-staining of Akna and Pcnt in cells treated with OA (PP1 and PP2 inhibitor). (d) WB of E14 brain proliferating progenitor cells treated with OA and 5 hours after drug wash-out. Notice delay in migration and reduction in protein leves after 5 hours. (e) Dephosphorylation of protein lysates with CIP induces a migration shift towards a lower molecular weight (arrow). (f) phosphorylation also regulates protein stability; a decrease in protein is seen 5 hours after wash-out (d) or with higher doses (e.g. 1 μM) (f). Lower doses of OA, which blocks specifically PP2) has no effect in protein migration in WBs. CIP, calf alkaline phosphatase; OA, okadaic acid. Scale bars: 5 μm (a); 10 μm (c)

in WBs and localization at centrosomes (Figure 2.3 f, and data not shown). This therefore indicates that PP1 is a key factor regulating the phosphorylation status, and thus, the protein stability and localization of Akna.

The localization of many SDA proteins such as Ninein depends on its interaction with MTs or MT-associated factors such as the Dynein/Dynactin complex (Dammermann and Merdes, 2002). I asked, therefore, if Akna's enrichment at SDAs would be MT-mediated, because otherwise it would suggest that Akna is an integral component of centrioles. Treatment of E14 primary cortical cells with 3.3 μM Nocodazole or 5 μM Taxol, to block MT polymerization or MT de-polymerization (hence more stable), respectively, showed no effect in the localization of Akna at centrosomes (Figure 2.4 a-c). Furthermore, overexpression of the Dynactin subunit 2 (Dctn2/p50), which leads to de-stabilization of Dynein/Dynactin complexes (Burkhardt et al., 1997), also did not affected the localization of Akna (Figure 2.4 d). To investigate if Akna is an integral part of centrioles at SDAs, E15 brain slices of Sas4 knock-out neocortices (see methods), in which centrioles have been eliminated (Insolera et al., 2014), were immunostained for Akna. This revealed that in the absence of centrioles, but not pericentriolar material (as this was still present, given Pcnt-positivity), Akna IF-signal at centrosome in the VZ was absent (Figure 2.4 e,f). Next, Odf2 KO cell lines were generated via Crispr Cas9 mediated genome editing (Figure 2.4 g). These cells were analyzed to determine if the localization of Akna at centrosomes was impaired in the absence of SDAs due to Odf2 loss (Ishikawa et al., 2005). In these cells, Akna was also not detectable at centrosomes (Figure 2.4 h,i), thus confirming that it is a constituent of centrioles and SDAs rather than being just recruited there by MTs or MAPs.

2.3 The centrosomal targeting domain of Akna

Considering the above-mentioned observations, I thought that perhaps knowing what region of Akna is important for localization at centrosomes could help to understand and explain what may have gone wrong in the original description of Akna as a transcription factor (Siddiqa et al., 2001). Towards that end, I generated expression constructs encoding truncated variants (Figure 2.5 a) and tested them in E14 primary cortical cells. As shown in Figure 2.5 b,c, the c-terminal quarter (amino acids (AA) 1031-1401) of Akna is necessary and sufficient for centrosomal localization, since (a) it alone can localize there
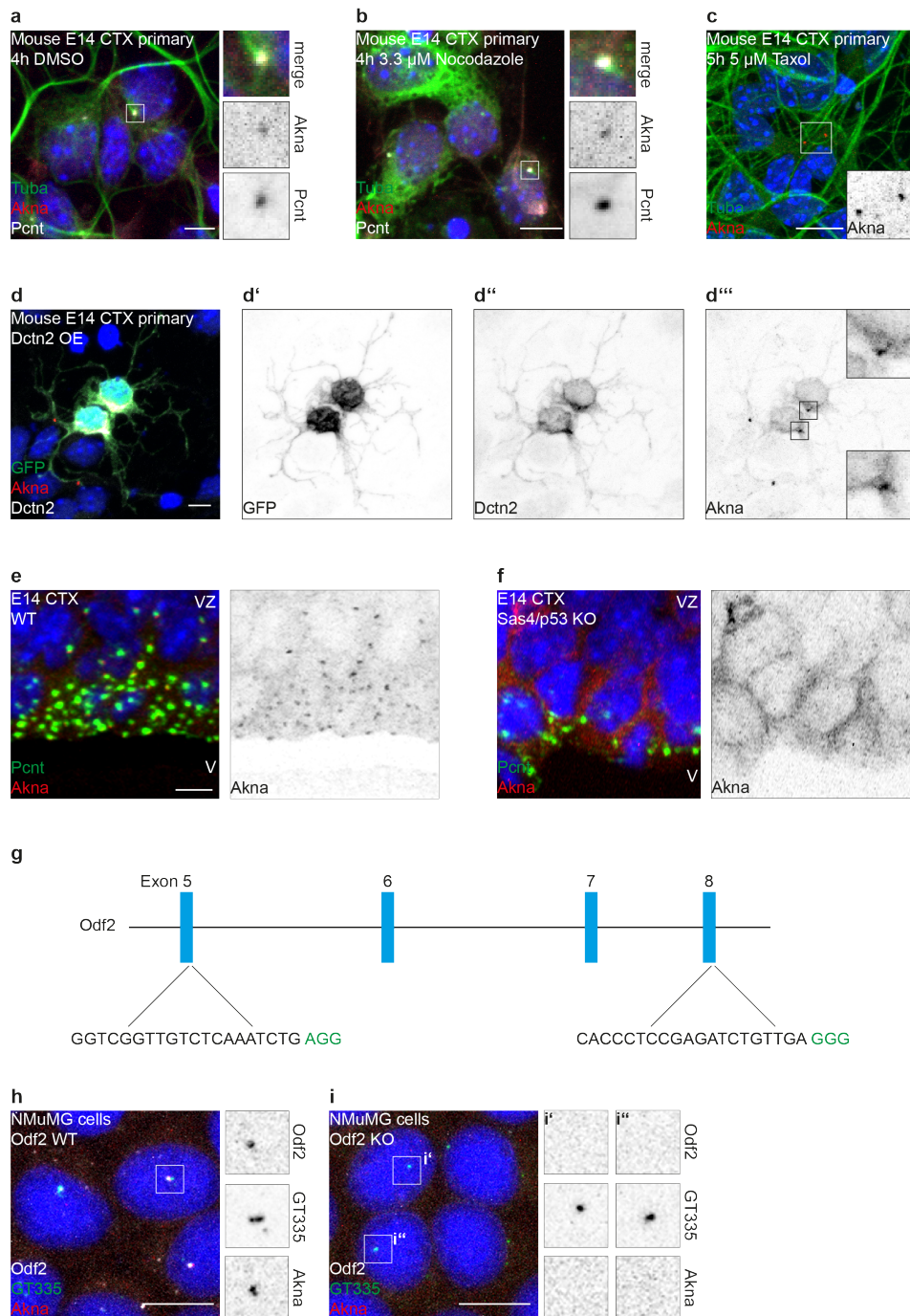
Figure 2.4: **Akna is an integral component of centrosomes.** (a-c) Micrographs of E14 CTX primary cells treated with DMSO, Nocdazole or Taxol. (d) Primary cortical cells transfected with Dctn2 plasmids. (e,f) Centrosomes of E15 apical progenitors in WT and sas4/p53 double knock-out mice. These lack centrioles but preserve PCM (Pcnt reactivity). (g) Strategy to knock out Odf2 in NMuMG cells via Crispr/Cas9. DNA sequences are the genomic targets (correspondingly the gRNAs) with PAM sequence in green. (h,i) Akna IF in WT and Odf2 knockout NMuMG cells. GT335 staining identifies centrioles. CTX, cortex; KO, knockout; PCM, pericentriolar material; V; ventricle; VZ, ventricular zone; WT, wild type. Scale bars:5 μm (a-f); 10 μm (h,i)

and (b) without it Akna is found in the cytoplasm (Figure 2.5 c-f). It is very curious, that a construct harboring the first halve of Akna (AA 1 - 707), but not the first three quarters (1- 1080), shows partial enrichment in the nucleoplasm (Figure 2.5 e,f). It is possible that the peptide generated by that construct (AA 1 - 707) would have a tertiary conformation that could be interpreted by the cell as nuclear localization sequence. Notice that the clone used by Siddiqa et al., 2001 (Figure 2.5 g,h) lacks the first 761 amino acids (blue color), i.e. almost half of the protein, and the c-terminal part containing the last 211 amino acids (green/red colors) does not correspond to the actual sequence of (human) Akna. Therefore, that clone encodes a version of Akna that has no domain for centrosome localization and possibly other important domains.

This lead to the obvious question: has Akna really an AT-hook DNA binding domain? AT-hooks contain obligatory the core amino acid sequence GRP (glycine-arginine-proline), surrounded by several lysine (K) and arginine (R) residues (Filarsky et al., 2015) (Figure 2.6 a for example). In mouse (Figure 2.6 b) and non-mammalian species such as like zebrafishes (Danio rerio), frogs (Xenopus tropicalis), sea squirts (Ciona intestinalis) and echinoderms (where it first apears), the GRP sequence is absent. However, it is present in humans, and thus, to check if the AT-hook would be a feature acquired in primates, I compared the region around the GRP motif in all primates in the ENSEMBL genome browser (Figure 2.6 c). Interestingly, this comparison revealed that GRP-sequence is not found in many primates (16 out of 22 have it). The presence or absence of the sequence does not seem to reflect an evolutionary relationship, since for instance, Orangutan has it (98.19% protein identity) but not Bonobo (98.22% identity). Thus, GRP sequences in AKNA are likely not primate specific. Finally, it is worth mentioning that, in general, the region around the putative GRP is not rich in K/R (not shown).

2.4 Akna is expressed in subtypes of neuronal progenitors

To understand the function of Akna in the developing cerebral cortex, I first checked which cells have Akna-positive centrosomes. Consistent with RNA levels (Figure 2.1 a), centrosomes of NECs and RGCs prior (E9) or at the end of neurogenesis (E18) had low to
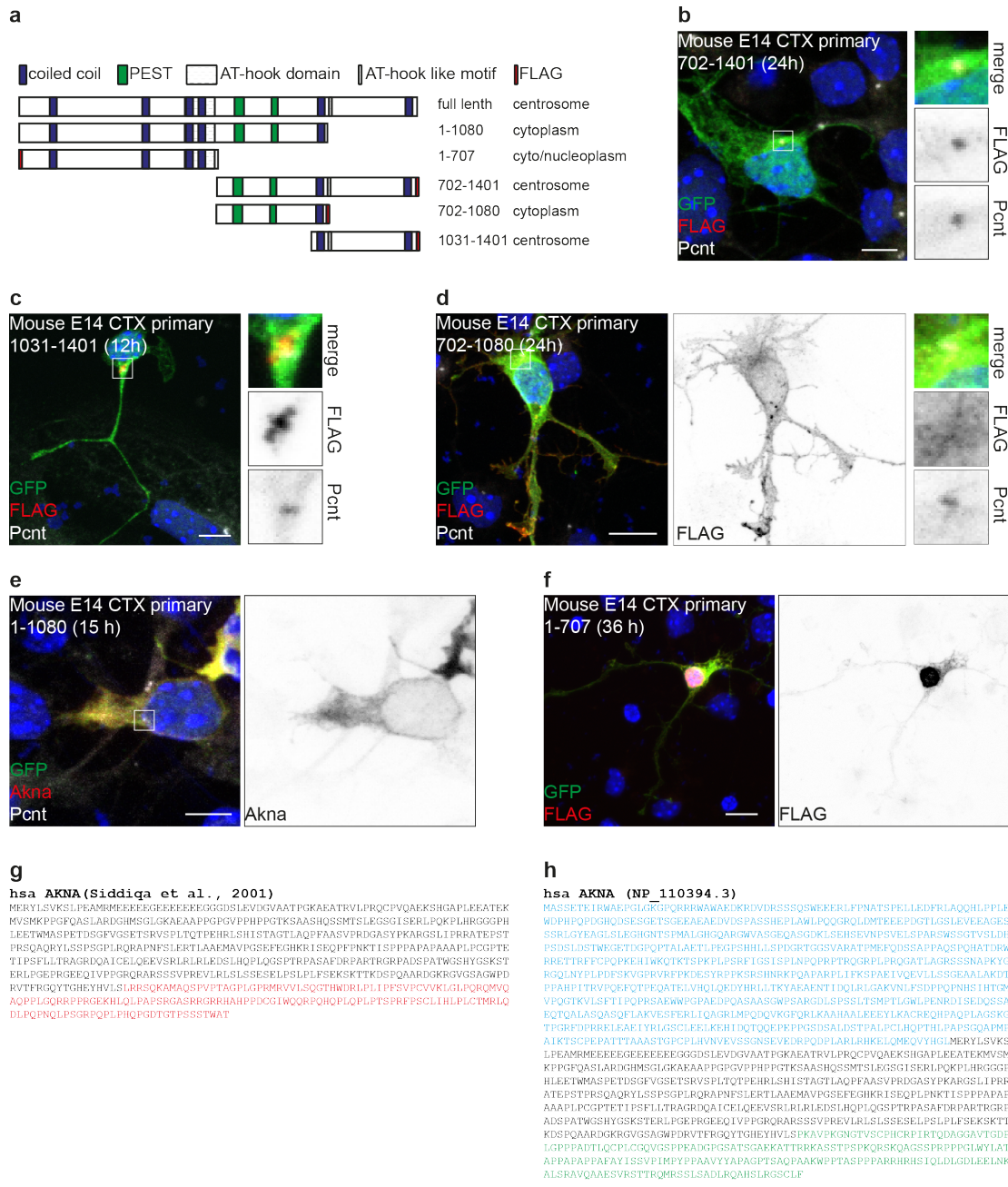
Figure 2.5: **Centrosome targeting region of Akna.** (a) Graphical description of the truncated Akna constructs. FLAG-tagging is depicted in red. (b-f) Expression of truncated versions of Akna in E14 primary cortical cells and co-localization with centrosomes (if needed). Akna monoclonal antibodies recognize variants 1-1080 and 1-707. (g) Protein sequence of the clone used in Siddiqa et al., 2001. (h) Full-length correct sequence of human AKNA. Notice that the N terminal part (blue in h) is missing in (g), which makes basically half of the protein. The correct c-terminus of AKNA (green in h) is missing in the original clone (red in g) and instead another unknown polypeptide sequence has been inserted. Scale bars: 5 μm (a-f)

a
AT-hook domains of Hmga1
. . . KRGR**GRP**PRKQP . . .
. . . KRPR**GRP**KGSK . . .
. . . RKPR**GRP**KKLE . . .

b
mouse AT-containing transcription factor domain of Akna (pfam12443)
QDQIKSLEQL**R**AAHMALEAEYLQAC**R**EELLD**P**QLDASQ**G**S
PR**TLNLC**R**ELEAEIYHL**G**Q**R**LEELQDHMDQTQ**R**ETEPC**RP**
DLQDST**P**TMSFL**P**QSAHLSM**P**S**G**PV

mouse AT-hook-like domain of Akna (UniProtKB/Swiss-Prot: Q80VW7.1)
. . . QTQEKL**G**SS . . .

c
GRP motifs of AKNA in primates

Homo sapiens (Human)	RPARTR**GRP**ADSPATW
Colobus angolensis (Angola colobus)	RPARTR**GRP**ADSPATW
Rhinopithecus bieti (Black snub-nosed monkey)	RPARTR**GRP**ADSPATW
Pan paniscus (Bonobo)	RPARTR**GWP**ADSPATW
Otolemur garnettii (Bushbaby)	RPTQTR**DRP**ADSLTSW
Cebus capucinus (Capucinus)	RPTRTR**GRP**ADSPAPW
Pan troglodites (chimpanzee)	RPARTR**GRP**ADSPATW
Propithecus coquereli (Coquerel's sifaka)	RPAGTR**DRP**ADSSAAW
Macaca fascicularis (Crab eating macaque)	RPARTR**GRP**ADSPATW
Mandrillus leucophaeus (Drill)	RPARTR**GRP**ADSPATW
Nomascus leucogenys (Gibbon)	RPTRTR**GRP**ADSPATW
Rhinopithecus roxellana (Golden snub-nosed monkey)	RPARTR**GRP**ADSPATW
Gorilla gorilla gorilla (Gorilla)	RPARTR**GRP**ADSPATW
Aotus nancymaae (Ma's night monkey)	RPARTR**GRP**ADSPATW
Macaca mulatta (Macaque)	RPARTR**GRP**ADSPATW
Microcebus murinus (Mouse Lemur)	HPARTQ**DRP**RDSSATW
Papio anubis (Olive baboon)	RPARTR**GRP**ADSPATW
Pongo abelii (Orangutan)	RPTRTR**GRP**ADSPATW
Macaca nemestrina (Pig-tailed macaque)	RPARTR**GRP**ADSPATW
Cercocebus atys (Sooty mangabey)	RPARTH**SRP**ADSPATW
Carlito syrichta (Tarsier)	HPARTR**DRP**ADSPAAW
Chlorocebus sabaeus (Vervet-AGM)	RPARTR**GRP**ADSPATW

Figure 2.6: **Analysis of the AT-hooks of Akna.** (a) Sequences of the three AT-hooks of Hmga1 as an example of a protein with proven AT-hooks. Notice the defining core sequence GRP characteristically surrounded by several K and/or R residues. (b) Murine Akna has no GRP core sequence. (c) Comparison of GRP motifs of Akna in different primates showing that in many of them, even in close relatives to humans, such as Bonobos, the GRP is missing. In addition, region surrounding the putative GRP core is not rich in K and/or R residues. This indicates that AT-hooks are not present in Akna and the GRP in humans may be coincidental.

undetectable levels of Akna (Figure 2.7 a,b). In contrast, many centrosomes of RGCs at E14 were strongly immunopositive for Akna at the VZ and their number increased in the SVZ/IZ (Figure 2.7 c,d). The Akna+ centrosomes at the apical processes at E14 (ie, in RGCs) made approx. 46% of the total Pcnt+ centosomes, as quantified by IF, showing an interesting heterogeneity (Figure 2.8 a). Importantly, this heterogeneity could also be observed by EM. FACS-sort of Prom1+ (CD133) RGCs showed that the Akna+ population corresponds to Pax6+ Tbr2+ nascent BPs, while the non-differentiating fraction of RGCs (Pax6+ Tbr2-) have low to undetectable levels of Akna at centrosomes (Figure 2.8 b). Immunocytochemistry (ICC) of E14 cortical primary cells confirmed this observation and further revealed that Pax6- Tbr2+ BPs is the population that more abundantly contains Akna+ centrosomes, while only a minor fraction of Tbr1+ (deep layer) neurons (which are relatively mature) are immunopostive (Figure 2.8 c). Furthermore, in the SVZ and IZ, where the great majority of Akna+ cells reside (Figure 2.9), there are still few centrosomes without Akna. These are in part interneurons born in the ventral telencephalon and tangentially migrating in these areas of the cerebral cortex, as observed by immunostaining of GAD65-EGFP brain slices (Figure 2.10 a). Furthermore, the centrosomes of cells in the CP (neurons) had low to undetectable Akna IF-signal (Figures 2.7 c, 2.9 b and 2.10 b), suggesting that expression is gradually down regulated at later stages of neuronal differentiation. In fact, co-staining with the early neuronal marker Tubb3 in cells and tissue revealed that Tubb3-low cells are still Akna positive, while Tubb3-high cell are not (Fi 2.10 b,c). These data are in complete agreement with mRNA expression profile of our lab and others (Figure 2.1 c) (Aprea et al., 2013; Diez-Roux et al., 2011; Pinto et al., 2008). In conclusion, Akna has an unprecedented subtype-specificity for a centrosome associated protein, largely restricted to differentiating RGCs and BPs. It is important to mention at this point, that the cell type specificity of Akna has no relation with the proliferative nature of the cells, since it localizes at centrosomes only in interphase also in post-mitotic cells. Instead, it may be an indication of a previously overlooked cellular process taking place during RGC differentiation.
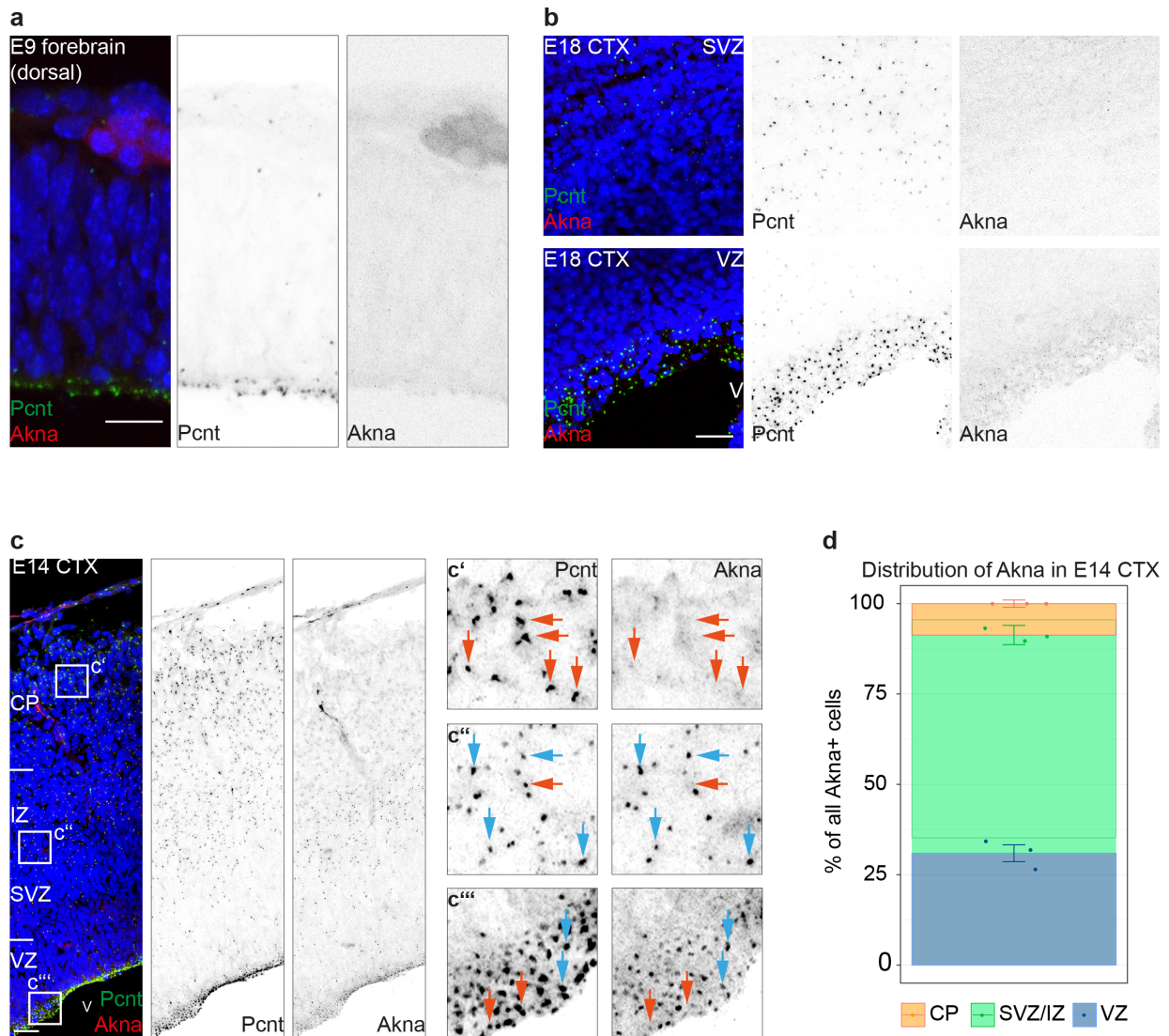
Figure 2.7: **Akna is heterogeneously expressed at mid-neurogenesis.** (a) Akna and Pcnt immuno staining in a E9 forebrain section (dorsal part). (b) Micrograph showing Akna and Pcnt IF in the E18 cortical VZ and SVZ. (c,d) IF staining and quantification of Akna+ centrosomes in the CTX at E14. The micrographs show that Akna is detected in a fraction of centrosomes in the apical surface at the VZ (i.e. RGCs). In the SVZ/IZ Akna IF is observed in the majority of centrosomes, while in the CP it is not detected. The quantification in (d) confirms that most cells with Akna+ centrosomes are in the SVZ/IZ, in agreement with previously mentioned RNA data. CP, cortical plate; CTX, cortex; IZ, intermediate zone; SVZ, subventricular zone; VZ, ventricular zone. Orange and blue arrows indicate Akna- and Akna+ centrosomes (co-labeled with Pcnt), respectively. Scale bars: 10 μm (a); 20 μm (b,c)
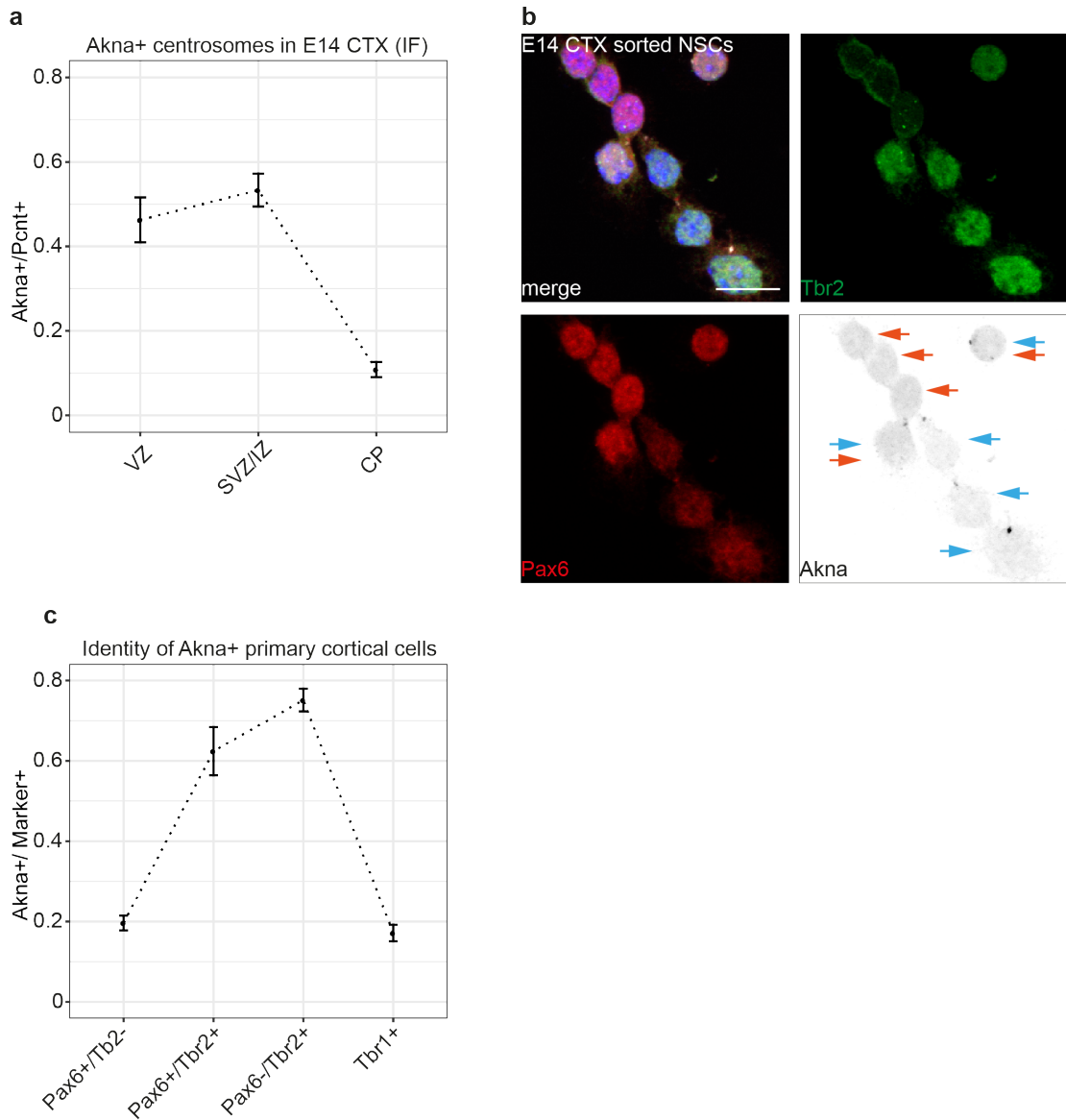
Figure 2.8: **Distribution of Akna+ centrosomes and subtype specificity.** (a) Quantification of Akna+ centrosomes in the E14 CTX by indirect IF. This confirms that a fraction of centrosomes in RGCs (VZ) have immune-positive Akna signal. In delaminating RGCs, BPs and new-born neurons (SVZ/IZ) there is a higher proportion of Akna+ centrosomes, while in the CP the numbers are low. (b) FACS sorted RGCs immunostained for Pax6 (red arrows) and Tbr2 (blue arrows). (c) Identity of Akna+ cells in E14 primary cortical cells in vitro, confirming the observations made in tissue and in sorted populations. CP, cortical plate; IZ, intermediate zone; SVZ, subventricular zone; VZ, ventricular zone. Orange and blue arrows indicate Pax6- and Tbr2+ cells. Scale bar: 10 μm (c)
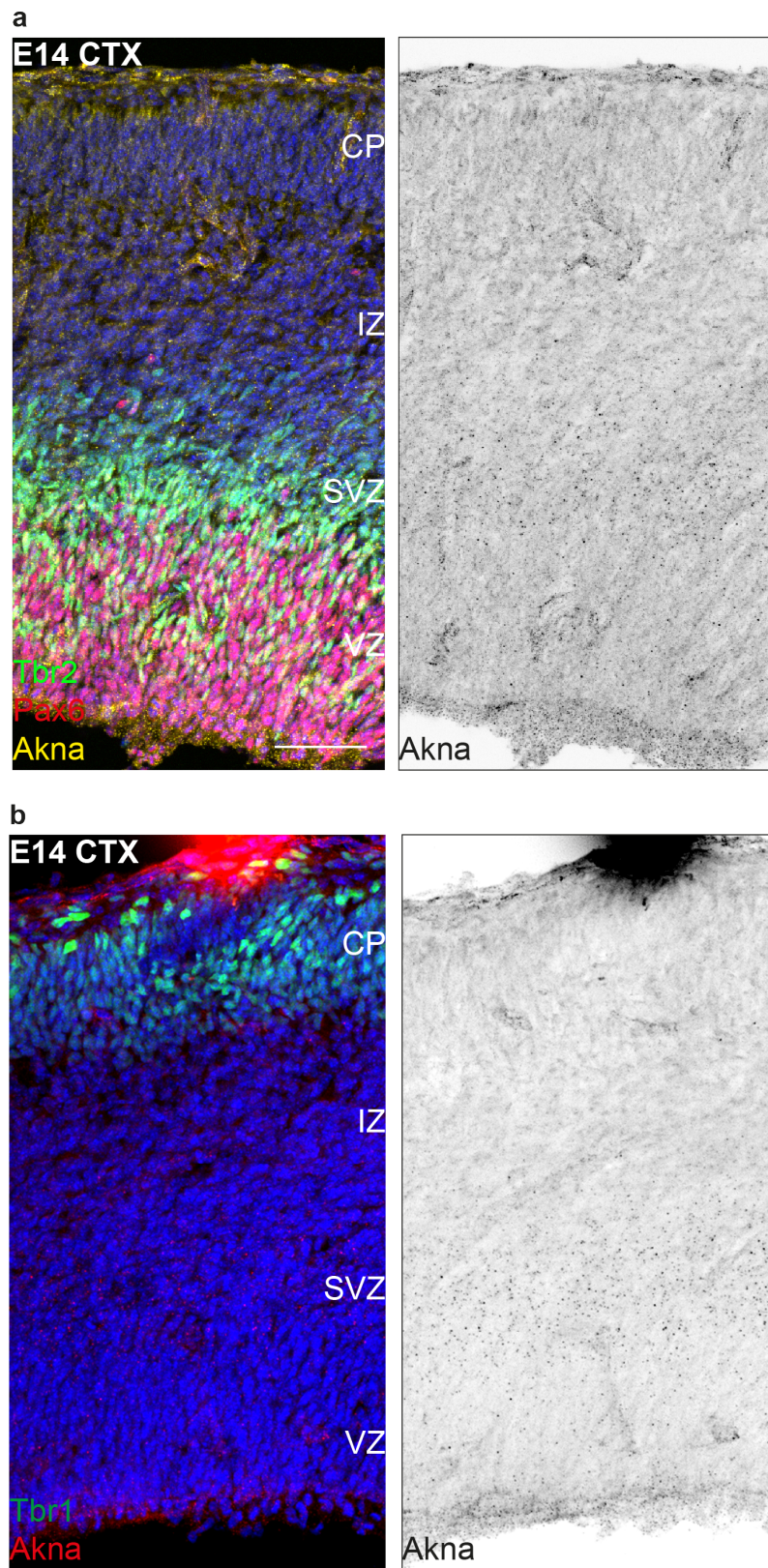
Figure 2.9: **Spatiotemporal expression pattern of Akna in the CTX at E14.** (a) Co-labeling of Akna with Pax6 and Tbr2. Akna is found in the apical surface in the VZ and mostly in the SVZ, as marked by Tbr2. It is also obvious that centrosomes in the area where Pax6 and Tbr2 overlap (delaminating cells) are also immunopostive. Akna is also enriched in the lower IZ where many cells are Tbr2 negative. (B) Tbr1 staining makes it clear that Akna is virtually absent from the CP where more mature neurons reside. Scale bars: 50 μm (a,b)
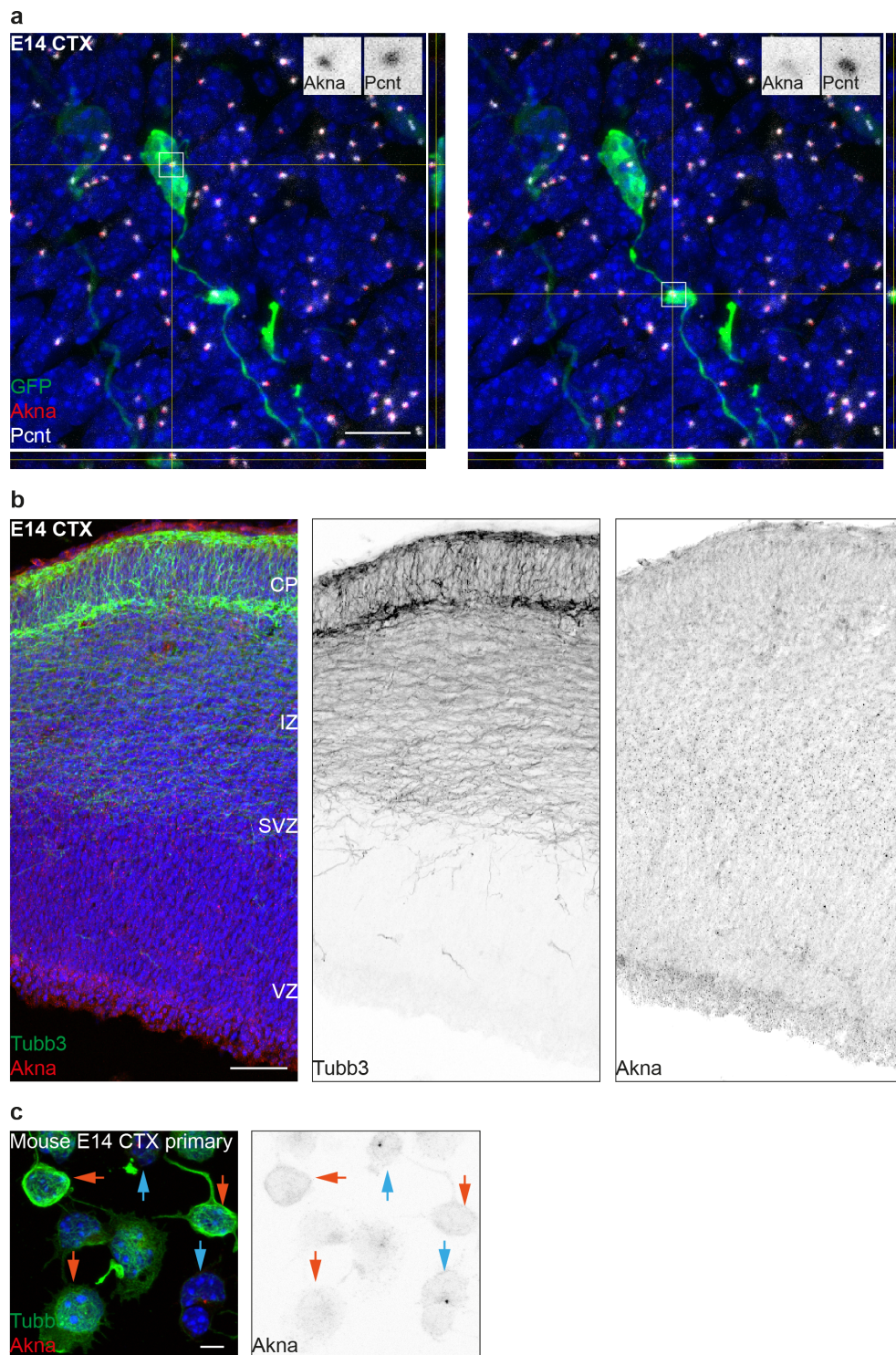
Figure 2.10: **Akna expression in neurons in vivo.** (a) Microgropah showing Akna staining in GAD65-GFP mice. Orthogonal view shows that centrosomes of GFP+ interneurons in the CTX (picture in the right) do not express Akna. The picture in the left shows an Akna+ centrosome from a neighboring GFP- cell. (b) Tubb3 and Akna staining in E14 CTX section. Tubb3+ signal in the upper SVZ and IZ co-localizes with Akna. Hence, Akna is downregulated in the process of leaving the IZ and entering the CP. (c) Co-staining of Akna and Tubb3 in E14 primary cortical cell. Tubb3 low cells (blue arrows) express Akna, Tubb3 high do not (red arrows). CP, cortical plate; IZ, intermediate zone; SVZ, subventricular zone; VZ, ventricular zone. Scale bars: 50 μm (b); 25 μm (a); 5 μm (c)

2.5 Akna is required for delamination of RGCs into the SVZ

To investigate the function of Akna and the role of MT-organization during BP generation, loss- and gain-of-function (LOF and GOF, respectively) experiments were done via in utero electroporation (IUE) in the developing cerebral cortex. Short hairpin RNA- (shRNA, sh) based Akna knockdown at E13 led to marked retention of RGCs in the VZ and SVZ when compared to control cells two days after electroporation, many of which were already migrating into the CP (Figure 2.11 a,b). Importantly, this phenotype was observed with two different shRNAs (see Figure 2.11 b). Furthermore, the proportion of Pax6+/Tbr2- cells increased upon knockdown, while Pax6-/Tbr2+ BPs decreased. The number Pax6+ Tbr2+ double positive cells (differentiating RGC) remained unchanged (Figure 2.11 c). Notably, Akna knockdown triggers apoptosis as observed by TUNEL staining. This effect is characteristic upon loss of function of centrosome-associated proteins and is mainly mediated by p53 up-regulation or activation (Bazzi & Anderson, 2014; Meitinger 2016; Mikule et al., 2007). Co-electroporation of Akna shRNAs and p53-miRNAs rescued the cell death and demonstrated that the block in delamination of RGCs from the VZ is not a secondary effect of apoptosis (not shown). Therefore, Akna knockdown impairs RGC delamination and, in accordance to the positional changes, blocks lineage progression towards BP fate.

Conversely, Akna overexpression induced strong and fast delamination of RGCs from the VZ into de SVZ already one day after electronation at E13 (Figure 2.11 d,e). This resulted in premature differentiation of RGCs, as elucidated by reduced numbers of Pax6+ and Ki67+ cells, and an increase in the proportion of Tbr2+ BPs and NeuN+ neurons (Figure 2.11 f,g). Importantly, the delamination caused by overexpression was evoked by retraction of the apical process without undergoing mitosis (28%, n=33 compared to 3%; n=165, in controls) as observed via imaging of cortical slices. Hence, the delamination triggered by Akna is not based on changing the orientation of cell division, as is the case with other centrosome associated protein (see introduction), but instead takes place during interphase, in complete agreement with its localization at centrosomes during the cell cycle.

The next obvious question was if Akna, being a centrosomal protein, would by itself promote neuronal differentiation. For that, overexpression was done in E14 cortical primary
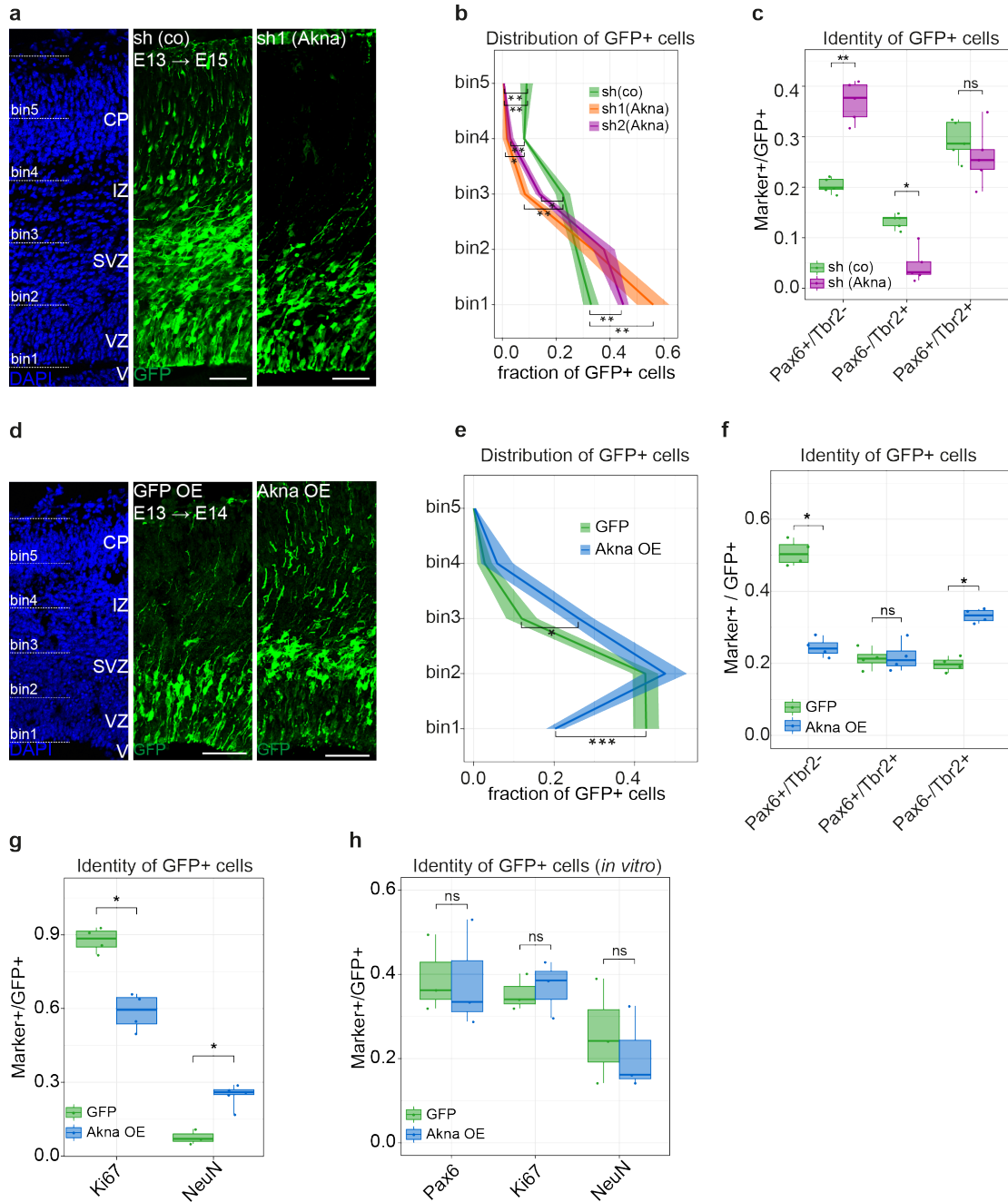
Figure 2.11: **Akna loss and gain of function in vivo.** Micrographs showing the effect of Akna knockdown in cortical cells via IUE of shRNAs. (b) Distribution of electroporated GFP+ cells in the CTX upon Akna knockdown with 2 different shRNAs. (c) Identity of cells in vivo upon Akna knockdown shows an increase in non-differentiating RGCs (Pax6+ Tbr2-) and a decrease in BPs (Pax6- Tbr2+). (d) Micrographs showing the effect of overexpression in the CTX via IUE of Akna cDNA. (e) Distribution of cells in the CTX upon Akna overexpression. (f) Identity of cells in vivo upon Akna gain-of-function shows a decrease in Pax6+ Tbr2- RGCs and an increase in BPs (Pax6- Tbr2+). The proportion of Pax6+ Tbr2+ RGCs did did not significantly change. (g) Accordingly, the number of proliferating Ki67+ progenitor cells also decreased upon Akna overexpression, and the proportion of NeuN+ neurons increased. (h) Cell identity after Akna overexpression in vitro in E14 primary cortical cells, showing that, in contrast to the in vivo phenotype, there is no effect on differentiation in dissociated cells cultures. CP, cortical plate; IUE, in utero electroporation; IZ, intermediate zone; SVZ, subventricular zone; VZ, ventricular zone. Data of this figure were generated by SF and PJ, except for (h). Scale bars: 50 μm (a,d)

cells (48 hours) and in adult SEZ derived neurospheres (7 days; not shown) in vitro and cell identity was analyzed. In none of both systems, however, there was no change in cell fate (Figure 2.11 h) compared to controls, suggesting that the differentiation phenotypes in the cerebral cortex upon Akna manipulation may derive from perturbations in the spatiotemporal positioning of the progenitor cells; overexpression relocate RGCs prematurely in a pro-differentiative environment (the SVZ/IZ) while knockdown keeps them in the pro-proliferative, anti-differentiative niche (the VZ). Which cell biological process regulated by Akna is then responsible for RGC delamination?

2.6 Akna regulates centrosomal MT organization and growth

To answer this question, one needs to comprehend the function of Akna at centrosomes. Given its localization at SDAs, where MTs are anchored and many MT-polymerization factors are enriched, it was logical to ask if and how Akna would affect these two processes. Towards this end, MT regrowth was monitored in nocodazole wash-out assays in E14 primary cortical cells upon Akna gain- and loss-of-function. Nocodazole binds to Tubulin-beta and blocks addition of further tubulin subunits, thereby inhibiting polymerization. Thus, only MT catastrophe can occur, and this ultimately leads to total disappearance of Tubulin-polymers. This effect is reversible and MTs regrow after the drug is washed out (Figure 2.12 a), allowing therefore to analyze e.g. the origin of MT nucleation and speed of polymerization (growth).

Overexpression of Akna leads to formation of blobs after reaching a threshold, very similar to phase separated bodies (Rai et al., 2018), which can liquid-merge and are dissolved during mitosis as seen by time lapse imaging. The regrowth assay revealed that those structures can organize and nucleate MTs, since MT asters grew from each one of them (Figure 2.12 b) in a size dependent manner, demonstrating that Akna can confer MTOC activity. The ectopic Akna bodies did not induce overduplication of centrosomes (Figure 2.12 c). Instead, they seem to sequester the MT nucleation and organization machinery away from the centrosome (Figure 2.12 c; compare MT aster sizes in GFP+ cell and neighboring untransfected cell). The gamma-Tubulin Ring Complex (gTuRC), as shown by Tubg and Tubgcp4 IF, localized to Akna polymers, while Pcnt, Nedd1 and Camsap2 (a

minus end capping protein) where not recruited (Figure 2.12 d-h). This indicates (a) that the recruitment effect is specific, (b) that recruitment of gTuRCs by Akna is independent of Nedd1 in these cells, and (c) that MTs capped by Camsap2 at the minus end do not bind Akna and may therefore belong to a different pool. Furthermore, in nocodazole wash-out experiments under knockdown conditions the proportion of cells with centrosomal MT regrowth was significantly reduced (around 25%) compared to control conditions (Figure 2.13 a-c) and the remaining cells that still grew centrosomal MTs had an overall reduction in the length of the MT fibers (Figure 2.13 d). Moreover, EB1 (Mapre1), Dctn1 (Dynactin complex), Dyn (Dynein complex) and Odf2, which participate in MT organization at SDAs (Askham et al., 2002; Ibi et al., 2011; Kodani et al., 2013; Yan et al., 2006), were observed together with Akna bodies (Figure 2.14 a-d), and they co-precipitated with Akna (Figure 2.14 f), thus suggesting that they cooperate to organize MTs. However, Tubgcp2 did not co-precipitate, and thus indicates that the recruitment of gTuRCs is not mediated by Akna directly, but through its interaction partners. Unexpectedly, a strong accumulation of another member of the Camsap family, Camsap3/Nheza, was observed in Akna bodies (Figure 2.14 e). Importantly, this was also the case in epithelial cells in vitro. Indeed, Camsap3 was readily found in Akna+ centrosomes as well as in the cytoplasm (Figure 2.14 g). These data then suggest that Akna can organize MTs that are coated by Camsap3 at the minus end. This type of MTs are thought to be released from centrosomes and distributed in the cytoplasm or transported to AJs (Dong et al., 2017; Jiang et al., 2014). Yet, in contrast to neurons, neuronal progenitor cells have mainly centrosome-centered MT organization, as observed in nocodazole wash-out experiments with FACS-sorted cells (Figure 2.15 a,b), suggesting therefore that in RGCs and BPs, Akna and Camsap3 could compete for binding to MT minus ends. In fact, Akna can bind Tubulin in vitro in its polymerized form, but not as dimers (Figure 2.15 c), indicating that competition could be for MT binding. Alternatively, Akna could recruit Camsap3 to the centrosome to stabilize MTs there.

To investigate if Akna controls MT organization in vivo in RGCs and to understand how it thereby promotes delamination, EB3-GFP MT comets were followed under control conditions and Akna overexpression. As expected, and in agreement with previous observations (Tsai et al., 2010), in RGCs electroporated with control plasmids most MTs grew with an apical to basal direction into the basal process and, thus, near perpendicular to the apical surface (average angle of 78°) (Figure 2.16 a,b). In contrast, upon overexpression the angle
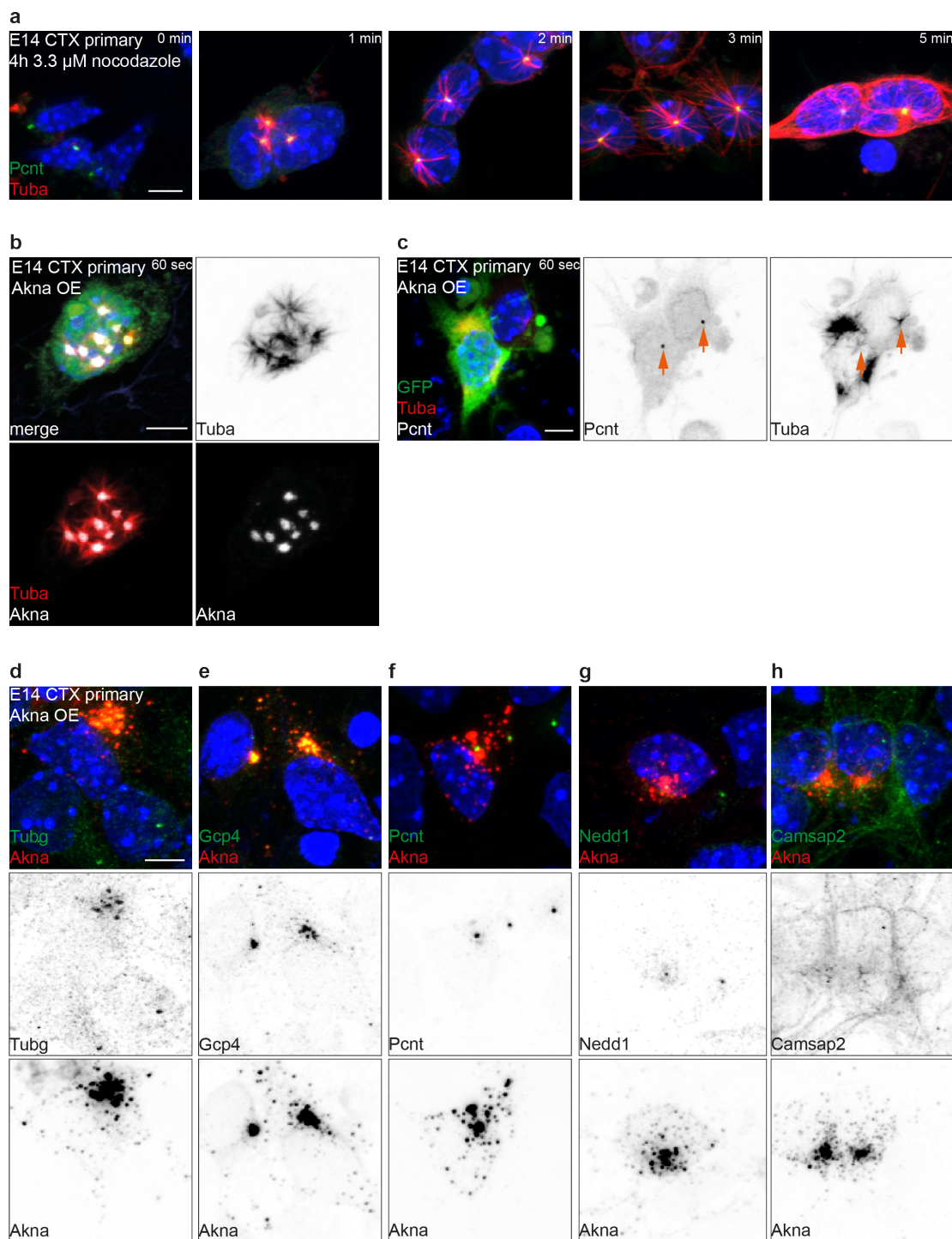
Figure 2.12: **Akna promotes MT nucleation.** (a) Example of MT regrowth in E14 primary cortical cells after nocodazole wash-out. (b) MT regrowth upon Akna overexpression in vitro showing that MT asters arise from each Akna speckle in a size dependent manner. (c) Nocodazole wash-out experiment indicating that ectopic MT asters do not come from supernumerary centrosomes but solely from Akna bodies. Arrows indicate the centrosome. Notice that MT nucleation at the centrosome of the cell overexpressing Akna is weaker compared to the neighboring GFP- cell. This indicates that Akna can recruit the factors required for MT nucleation and polymerization even away from the centrosome. APlease also compare MT nucleation in the neighboring untransfected GFP-negative cell. Note that in this cell, nucleation (at steady state conditions) is not as robust as with Akna OE. This indicates that Akna, in addition of being able to sequester the centrosomal portion of MT nucleation factors, is also capable of recruiting the free available cytoplasmic pool of them, such as the gTuRC (d,e). Recruitment is not an artifact since not all centrosome associated proteins accumulate there (f-h). Scale bars: 5 μm
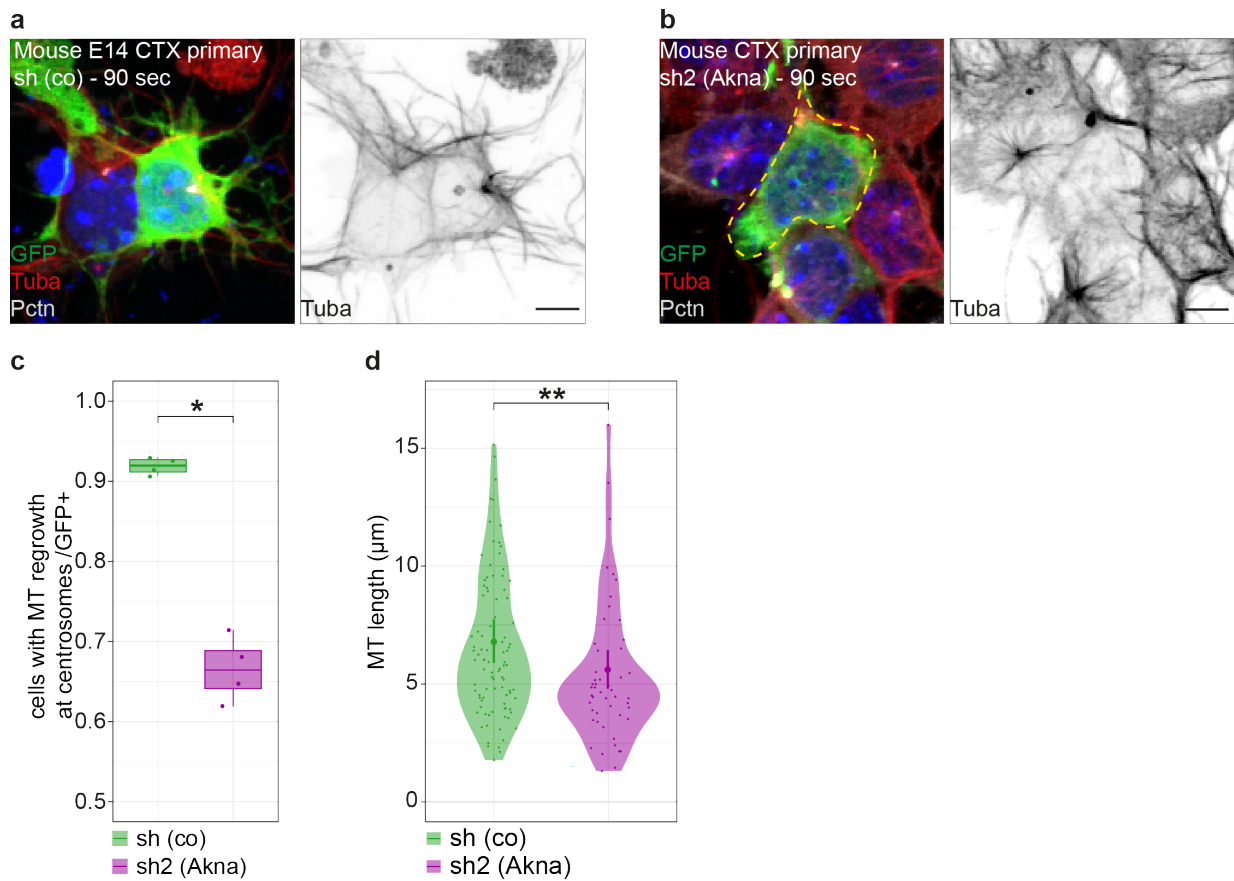
Figure 2.13: **Akna knockdown impairs MT nucleation in cortical cells.** (a,b) Examples of MT regrowth assays in E14 CTX primary cortical cells transfected with control or Akna shRNAs. Dotted yellow line in (b) depicts a cell without MT regrowth upon Akna knockdown. (c) Quantification of cells with centrosomal MT regrowth in control or knockdown conditions in vitro. (d) Length of MTs in those cells that could still growth centrosomal MTs. Scale bars: 5 μm
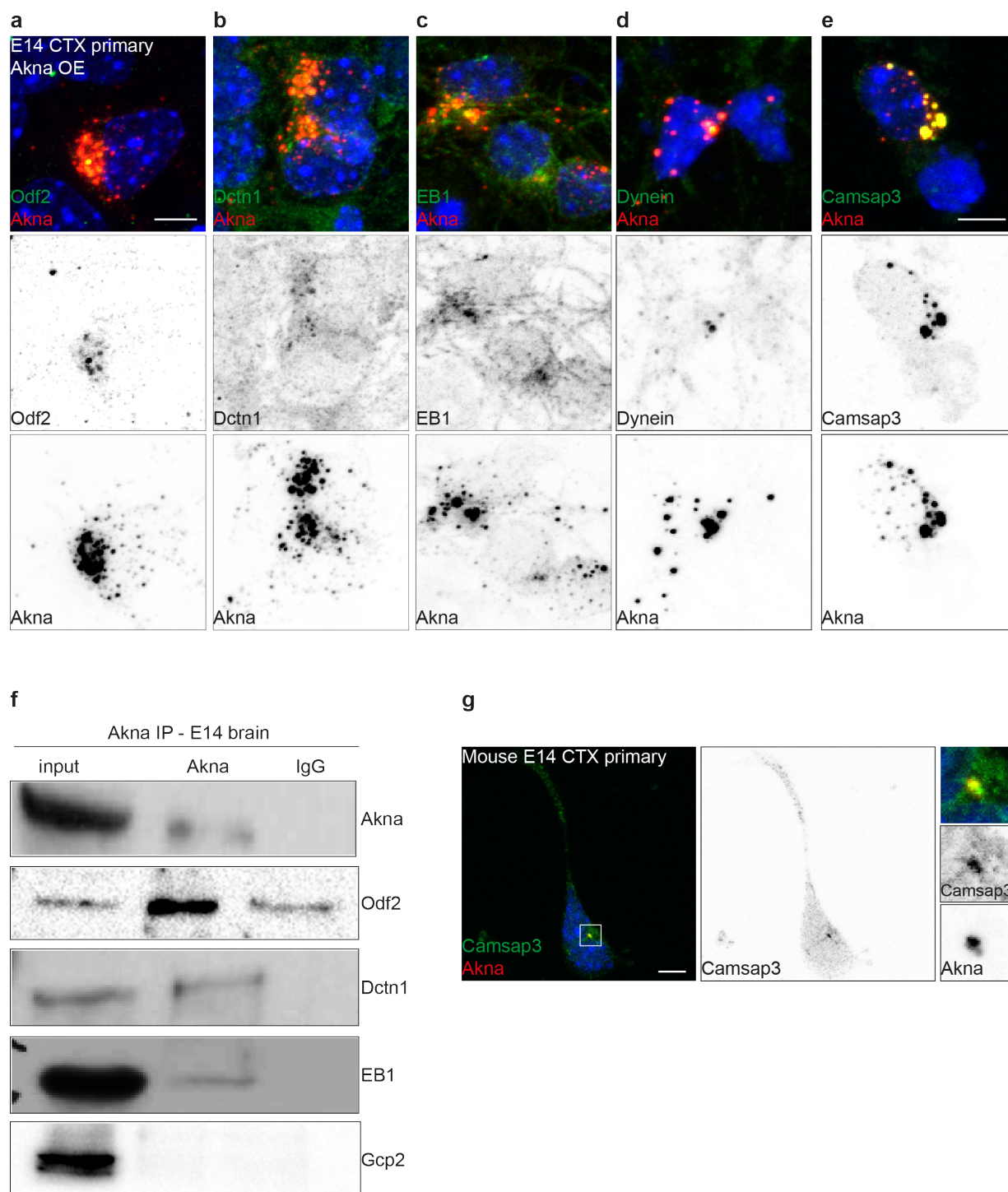
Figure 2.14: **Akna can recruit factors for MT organization.** (a-d) Micrographs showing that proteins involved in MT organization at SDAs are concentrated at Akna bodies after overexpression, indicating that Akna can also attract these. (e) Also the MT mins-end binding protein Camsap3 is strongly attracted to Akna foci. (f) Immunoprecipitation of Akna from E14 CTX brains showing that MT organizing factors co-precipitated with Akna, while the gTuRC (Gcp2) does not. (g) Example of a cell from E14 cortical cultures indicating that Akna and Camsap3 can be found in the same centrosome. Scale bars:
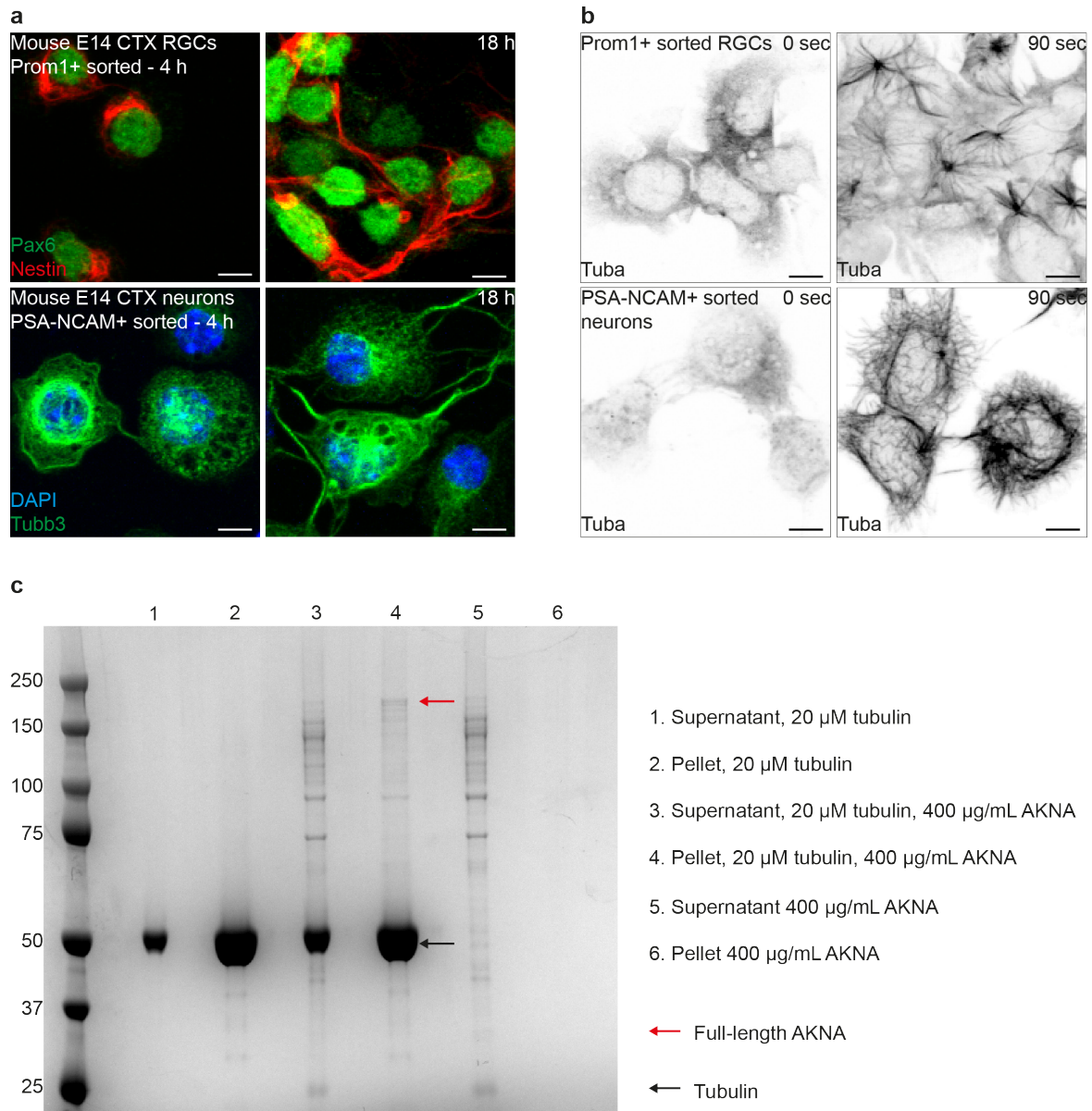
Figure 2.15: **Akna binds microtubules and regulate their network in vivo.** (a,b) MT regrowth assay in sorted E14 CTX progenitor cells and neuros. The pictures demonstrate that progenitors growth MTs mostly from then centrosomes while neurons have largely noncentrosomal MT nucleation. (c) MT co-sedimentation assay with recombinant Akna protein showing that full length Akna (red arrow) binds (only) to polymerized MT (black arrays). Experiment in (c) was done together with WH. Scale bars: 5 μm

of growth was more oblique (in average 55°), indicating a change in the orientation of MT growth and repositioning of the MTOC to non-apical locations, resembling the type of MT organization of BPs (compare MT tracks in Figure 2.16 a,c). So, high levels of Akna promote the re-organization of the centrosomal MT network in RGCs towards a more BP-like condition. To confirm that MT growth is affected by Akna manipulation, speed of EB3-GFP commets was measured from the above mentioned in vivo analyses after Akna overexpression in progenitor cells. This showed that MT growth in cells that overexpressed Akna was in average slightly but significantly higher compared to controls (Figure 2.16 d), which means altogether that Akna promotes polymerization of MTs and regulates their organization and nucleation at centrosomes in RGCs and BPs, and this is required and sufficient to induce delamination. But, is this a general cell biological mechanism?
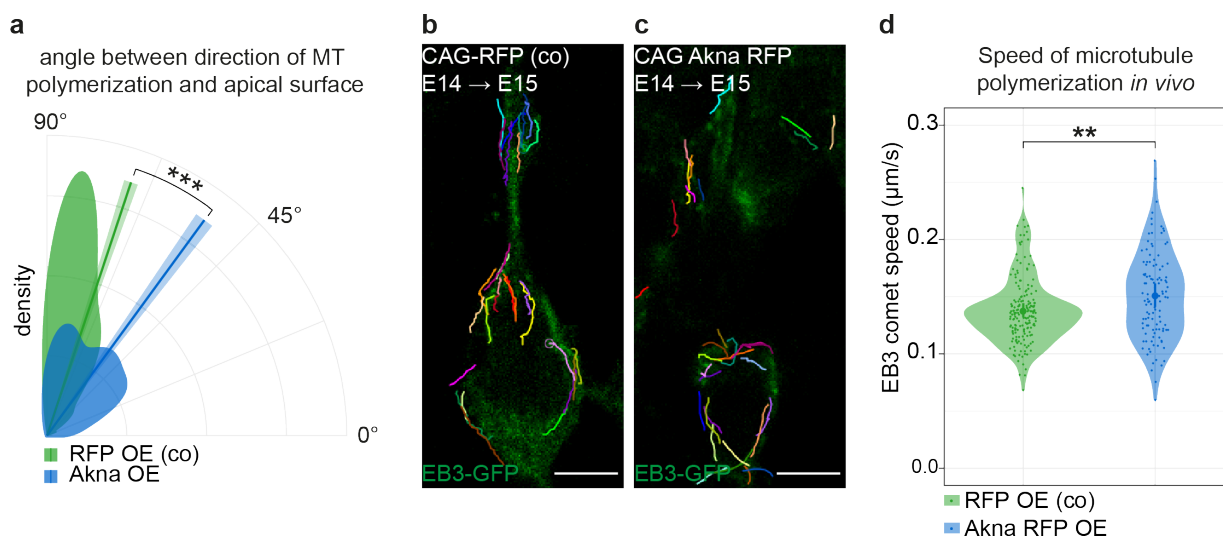
Figure 2.16: **Akna contributes to re-organization of MT growth orientation.** (a) Measurement of the angle of MT growth relative to the apical surface upon control or Akna overexpression in vivo in RGCs. (b,c) Tracks of EB3-GFP comets in control and overexpression conditions showing that Akna gain of function can contribute to the re-organization of the MT growth direction in RGCs. (d) Quantification of MT growth upon Akna overexpression in vivo by calculating the EB3-GFP comet speed. Data in this figure was generated by EP. Scale bars: 5 μm

2.7   Akna is required for EMT

It is known that delamination of RGCs follows a remarkably similar program to that of epithelial cells undergoing EMT in development and disease (such as cancer metastasis), and in fact many EMT key drivers also govern RGC delamination and differentiation (Itoh et al., 2013; Singh et al., 2016; Zander et al., 2014). Moreover, the transition from multi-polar to bipolar morphology in neurons and their subsequent migration seems to resemble the opposite process, mesenchymal to epithelial transition (MET) (Singh et al., 2016). On this basis, it was logical to ask if Akna would have a role, beyond the developing forebrain, during EMT in general; with other words, if the mechanisms that are controlled by Akna during RGC delamination are also important for EMT in other epithelial cells. Towards this end, murine NMuMG mammary epithelial cells undergoing TGFb1-induced EMT were monitored (Sahu et al., 2015; Tiwari et al., 2013). While untreated cells have low levels of Akna, TGFb1-treatment led to its up-regulation, with a peak at day 2 and decreasing levels thereafter (Figure 2.17 a-d). Given that epithelial cells have largely noncentroso-mal MT nucleation prior to EMT (Tanaka et al., 2012; Toya et al., 2016), Akna could re-direct MTOC activity to the centrosome at the start of EMT, similar to differentiating RGCs, and thus be critical for EMT progression. This hypothesis was tested by Akna RNA-interference in TGFb1-treated NMuMG cells for 2 days (when cells have flattened elongated morphology instead of cuboidal morphology, and cell-cell contacts start to dissociate) and 4 days (when cells display more mesenchymal fibroblastic morphology and downregulation of epithelial E-Cadherin was nearly complete) (Figure 2.17 e-g). Interestingly, while normal activation of core EMT transcription factors such as Zeb1 and Twist as well as the mesenchymal marker FN1 (Fibronectin) was observed upon siRNA-knockdown (data not shown), the tight junction component ZO1 and the Cadherin interactor and stabilizer p120/Ctnnd1 (Delta catenin) were more abundant upon Akna knockdown than in control siRNA transfected cells at 2 and 4 days (Figure 2.18 a-d). Consequently, cells remained closer together with many of them retaining ZO1 at cell-cell junctions and attenuated rearrangement of the actin cytoskeleton (from the AJs to stress fibers), as visuallized by Phalloidin staining (Figure 2.19 a-c). Hence, Akna plays an important role for the disassembly of junctional coupling during EMT.

Finally, to understand the cause of the observed phenotype upon Akna knockdown I analyzed the longevity of MTs, as this has been previously shown to fine-tune factors that

regulate the maintenance of junctional coupling and the actin cytoskeleton such as Rho-GTPases or their effectors (Heck et al., 2012; Krendel et al., 2002; Nagae et al., 2013). Immunoblots of NMuMG cells after 4 days of TGFb1 treatment revealed an increase in Tubulin de-tyrosination upon Akna loss-of-function, indicating that MTs become longer-lived in such conditions. No obvious changes were observed in the levels of Tubulin tyrosination, suggesting that Akna knockdown specifically affects the pool of longer lived MTs, perhaps through their stabilization or inhibiting their catastrophe rate (Figure 2.18 e,f). In agreement with this, Akna overexpression in N2A cells reduced the levels of de-tyrosinated Tubulin, while the levels of tyrosinated Tubulin and acetylated Tubulin were unchanged (Figure 2.18 g-j).Therefore, Akna levels have an impact on the life of MTs, that affect junction disassembly and actin cytoskeleton dynamics.

2.8   Akna maintains cells in SVZ

As demonstrated in section 4, the MT organization in progenitor cells and neurons is different and this can be linked to the gradual downregulation of Akna during neuronal differentiation. It is also known that MTs become longer lived and more stable upon neuronal maturation (see discussion), and this is important for neuronal repolarization and axon specification and formation (Aillaud et al., 2017; Cappello et al., 2012; Pongrakhananon et al., 2018; Witte et al., 2008). It seemed therefore logical to ask, if maintaining high levels of Akna (and hence promoting centrosomal MT nucleation with reduced levels of long lived detyrosinated tubules) would have a negative effect in cells progressing from a multipolar state in the SVZ to a bipolar migratory phase entering the CP in vivo. This was evaluated by overexpression of Akna via IUE at E13 under control of the Doublecortin (Dcx) promoter, that is active in late BPs and neurons, and analyzed 5 days later. While most of the control GFP+ cells had progressed into the CP, approximately half of the GFP+ cells overexpressing Akna remained below the CP, at the SVZ/IZ (Figure 2.20 a-c). Despite their ectopic localization (Figure 2.20 d), they could differentiate and extend callosal projections (Figue 2.20 e and not shown), indicating that neuronal differentiation occurred normally. On the other hand, miRNA-mediated Akna knockdown in the same conditions did not have an obvious effect in CP seeding of electroporated cells and was similar to controls regarding aspects such as speed of migration (Figure 2.20 f) or frequecy of pausing during migration. Therefore, the conclusion is that the physiological downregulation of Akna in neurons is
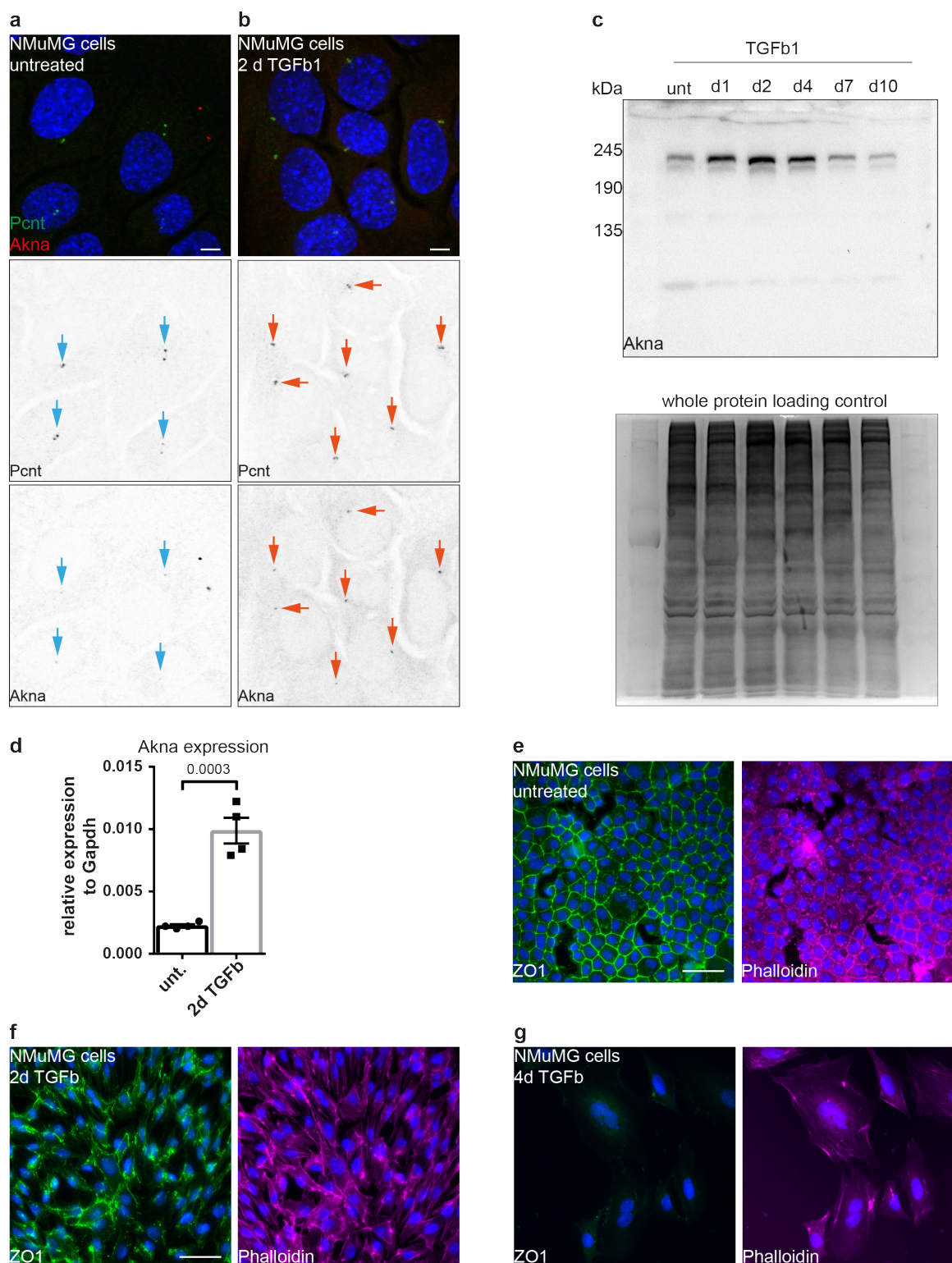
Figure 2.17: **Akna is upregulated at the onset of EMT.** (a,b) IF stainings in NMuMG epithelial cells showing low to undetectable Akna immunoreactivity at centrosomes in untreated cells (blue arrows) or positivity in TGFb1 treated cells (2 days). (c) Immunoblot showing Akna protein levels at different time points of TGFb1 induced EMT. WB by SKS. (d) RT-qPCR of Akna in untreated and TGFb1 induced cells for 2 days. (e-f) Example of re-arrangement of cell-cell contacts (ZO1) and the actin cytoskeleton (Phalloidin) in NMuMG during EMT. Notice that the cells change from a cobblestone to a fibroblastic morphology and this is accompanied by dissolution of cell adhesion proteins and re-localization of cortical Actin to stress fibers. Statistical analysis (d) is student t-Test. Scale bars: 5 μm (a,b); 50 μm (e-g)
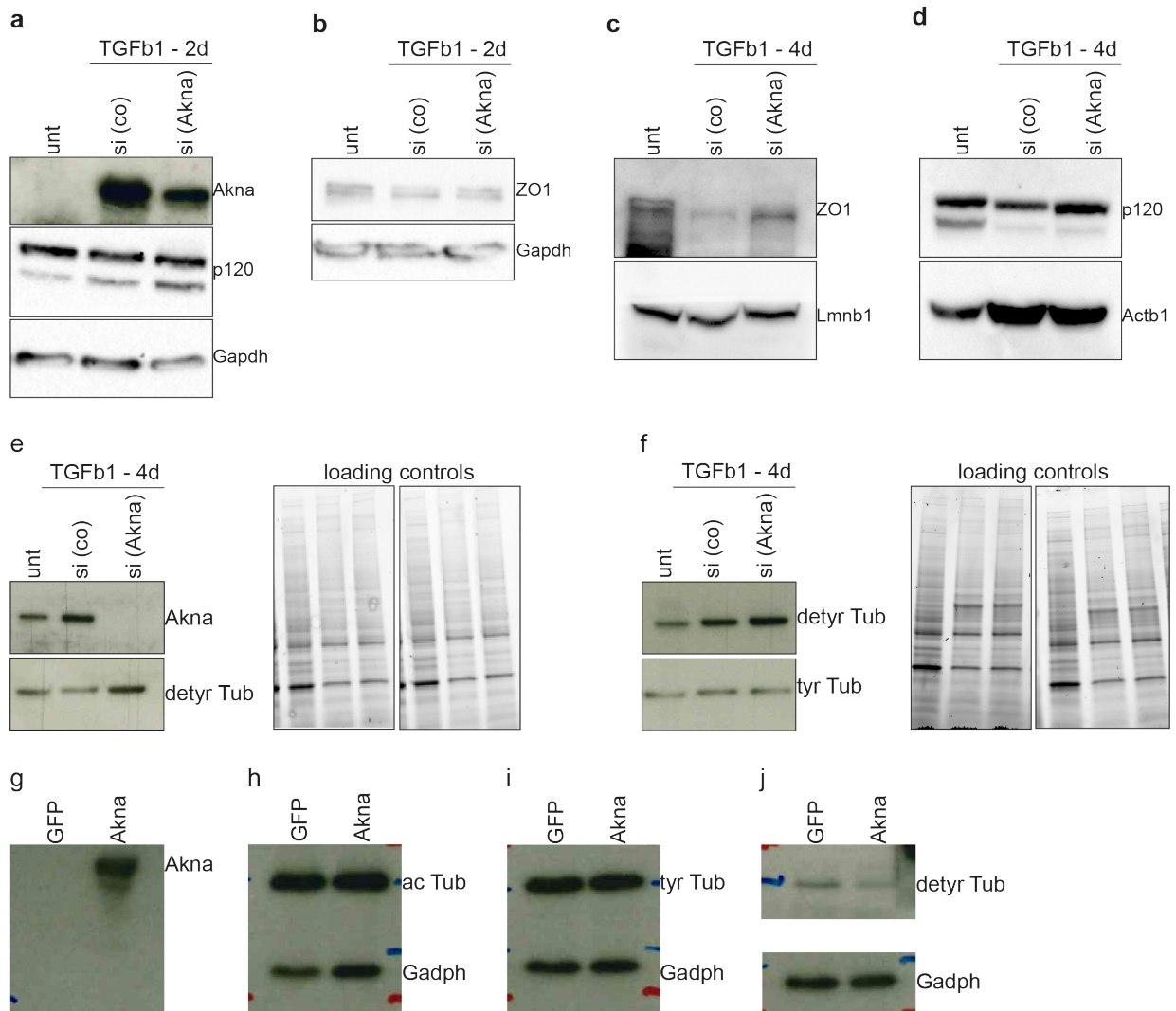
Figure 2.18: **Akna is required for dissolution of cellular junctions during EMT.**(a-d) Immunoblots of cell adhesion components ZO1 (tight junctions) and p120 (adherens junctions) in untreated and TGFb1 treated NMuMG cells (2 and 4 days) in control and Akna knockdown conditions. (c,d) by SKS. (e,f) Immunoblots of detyrosinated Tubulin in untreated and TGFb1 treated NMuMG cells (4 days) in control and Akna knockdown conditions, indicating increased levels upon loss-of-function. Two different representative examples are shown. (i-l) Immunoblots of Tubulin post-translational modifications upon GFP or Akna overexpression in Neuro2a cells (12 hours post transfection).
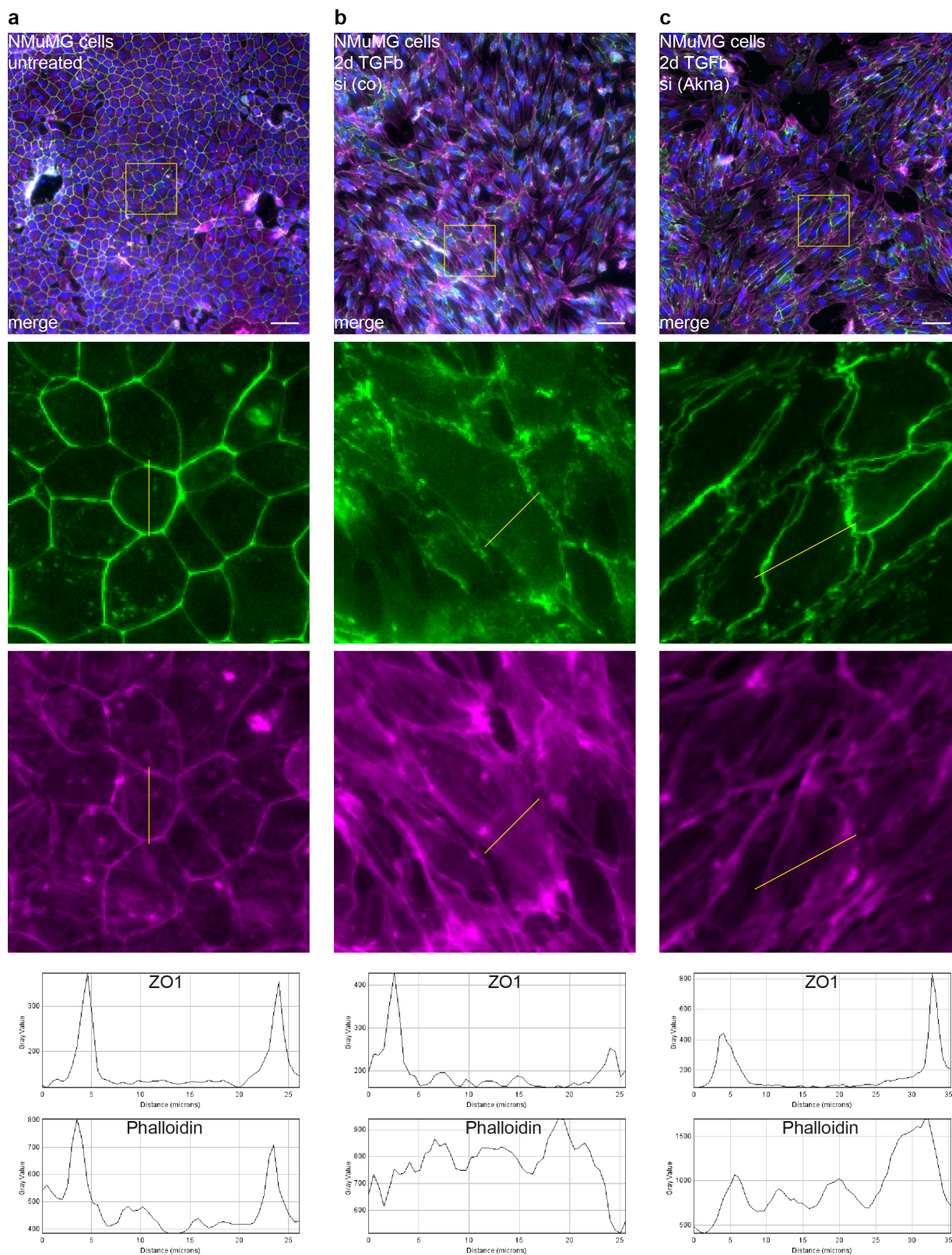
Figure 2.19: **Cell junctions and Actin cytoskelleting upon Akna knockdown**(a-c) ZO1 or Phalloidin (F-Actin) staining in untreated or TGFb1 treated NMuMG cells 2 days after transfection with control or Akna siRNAs. At the bottom, representative summary plots of line scans of fluorescent intensity at cell borders (cell with yellow line across). Scale bars: 50 μm (e-g)

crucial for the migration into the CP. To investigate if neuronal re-polarization is affected, taking in consideration the above-mentioned implications of microtubule polymerization, organization and longevity, live imaging in cortical slices was done upon Akna overexpression or knockdown. These experiments showed that Akna downregulation promoted the transition from multipolar to bipolar migrating neuronal morphology (Figure 2.20 g,h). Conversely, cells in which Akna was overexpressed remained longer in a multipolar state and displayed less migration during the time frames analyzed (Figure 2.20 i,j). All in all, the results demonstrate that the key cellular role of Akna is to promote the entrance of progenitor cells into the SVZ and to retain them therein. Since this is a tightly controlled mechanism critical for proper neuronal development, the question that next arises is, what is up-stream of Akna?

2.9   Sox4 and Tcf12 are positive upstream regulators of Akna

As mentioned in the introduction, delamination and neuronal repolarization resembles EMT and MET, respectively, and are controlled by the same family of (transcription) factors. I therefore asked next if Akna expression is induced by genes commonly involved in RGC differentiation and EMT (see introduction). Towards that end, N2A cells were transfected with Scrt1, Scrt2, Sox4, Tcf12 and Btg2, and Akna transcriptional levels checked by RT-qPCR approximately 36 hours afterwards. While Scrt2 had no effect, Scrt1 reduced Akna expression (Figure 2.21 a,b). Furthermore, Sox4, Tcf12 and Btg2 were able to upregulate Akna transcription significantly (Figure 2.21 c-e), indicating that they are positive regulators. In fact, Akna has DNA binding motifs for both Sox4 and Tcf12 in its promoter (Figure 2.21 f). The binding motif of Btg2 has not been defined, and its subcellular localization is also unclear (see discussion). Of notice, the conclusion is further supported by the fact that Akna, Sox4, Tcf12 and Btg2 are expressed in the same population of cells not only in the developing cortex, but also in the germinal zones of the developing ventral forebrain as well as in the migrating SEZ neuroblasts of the adult brain and in immune cells (data not shown and Beckervordersandforth et al., 2010; Pinto et al. unplublished). Furthermore, since the levels of Akna in E14 CTX tissue from the Pax6-mutant mouse Small eye (Sey) are elevated, as observed by microarray (Holm et al., 2007; Walcher et al., 2013), and in these animals there are –in addition to changes in mitotic cleave angle
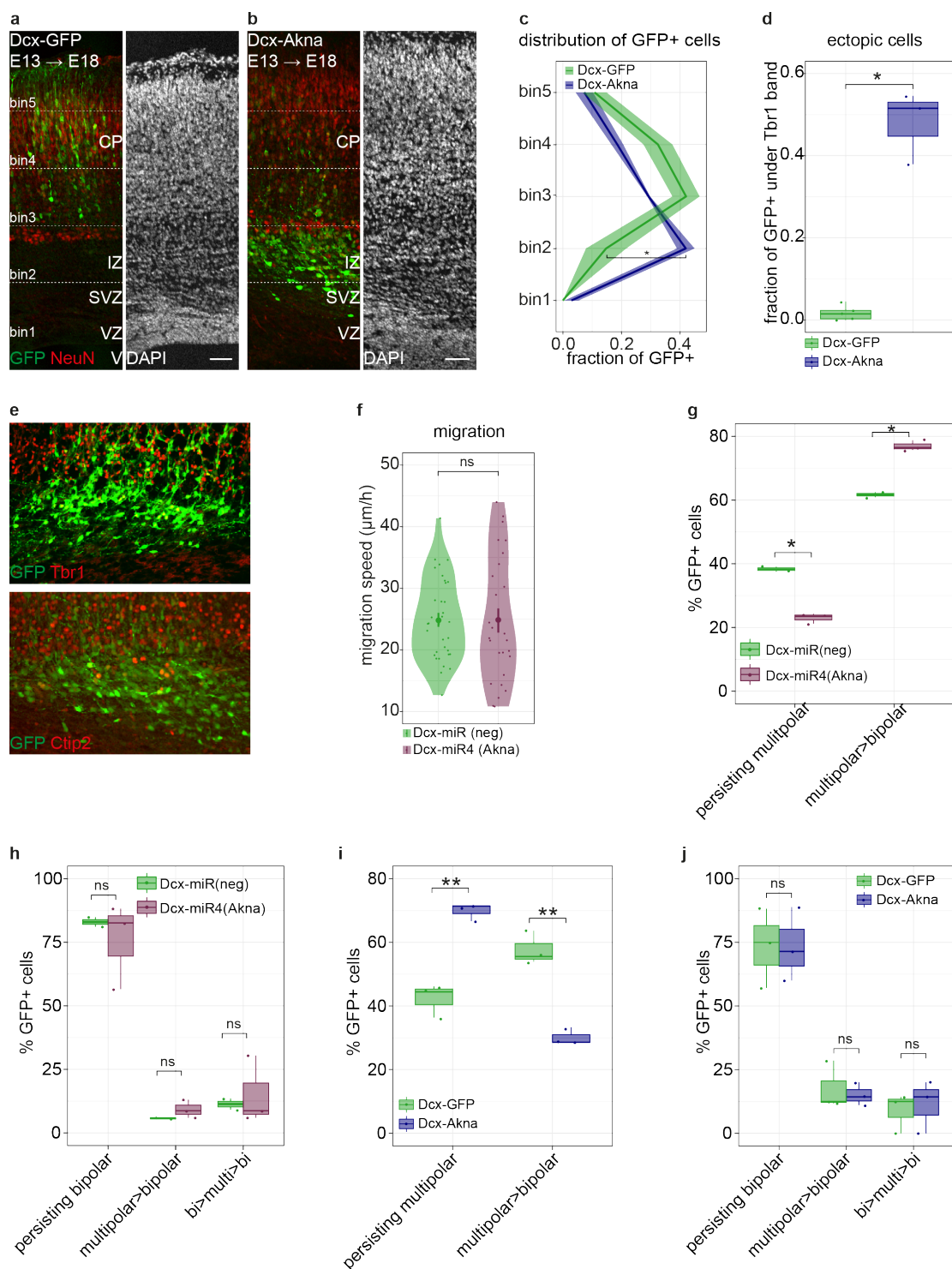
Figure 2.20: **Akna downregulation is necessary for exit of the SVZ/IZ.** (a,b) Micrograph of GFP or Akna overexpression with Dcx driven promoters in neurons (5 days after IUE) showing retention of cells in the SVI/IZ upon Akna gain of function. (c) Quantification of the distribution of GFP+ cells in the CTX after GFP or Akna overexpression (5 days after IUE). (d) Quantification of ectopic cells below the CP as marked by Tbr1 (early born, deep layer neurons). (e) IF staining for GFP and neuronal markers Ctip2 and Tbr1 demonstrating that ectopic cells (after Akna overexpression) can differentiate to neurons of different layers. (f, g) Quantification of the percentage of cells that do multipolar to bipolar transition upon Akna loss and gain of function. Data from SF and PJ (a-e), and EP (f-j). Scale bars: 50 μm (e-g)

–abnormal levels of cell-adhesion molecules (including p120), increased delamination and more BPs (Asami et al., 2011; Duparc et al., 2006; Tylkowski et al., 2013), it was reasonable to check if Pax6 overexpression would have an influence on Akna. This was, however, not the case, but instead it downregulated Sox4 although not singificantly (Figure 2.21 g). It remains to investigate if Pax6 overexpression has repressive effect in Tcf12 or Btg2. All together, the results are compatible with a mechanistic model with Sox4, Tcf2 and Btg2 acting upstream of Akna early at the onset of neuronal commitment. Pax6 would control the balance between RGC self-renewal at the VZ and their delamination and subsequent differentiation, as shown by others (see for instance Asami et al., 2011), through repression of Sox4.

Lastly, I asked how the proposed transcriptional circuitry could be fine-tuned or shut down for instance during neuronal maturation when Akna levels are decreased. For that, I considered the involvement of miRNAs, because they can efficiently do both tuning and knockdown in a remarkably cell type and developmental stage specific manner. Thus, I checked miRNAs that are up-regulated in neurons using microarray data from our laboratory with samples taken at different time points during neuronal differentiation of embrynic stem cells (unpublished data). Among several cadidates I decided to analyse miR-129 because: (a) upregulated specifically in neurons (which I could confirm by qPCR in differentiated P19 cells; Figure 2.21 h,i), (b) in the developing cerebral cortex it is expressed at higher levels in the mantle compared to the germinal zone (Cao et al., 2012) and (c) it has been reported to regulate the expression of Sox4, and other centrosome and MT associated factors (Cao et al., 2012; Wu et al., 2010 among others) and also have putative target sites for Akna.

Overexpression of miR129 (by cloning the miR129-2 locus into an expression vector) in N2A cells demonstrated that it is capable of reducing the levels of endogenouse Sox4-protein, but had not effect on Akna (Figure 2.21 j). So, it is a negative regulator of Sox4 and this in turn could indirectly interfere with Akna gene expression. At this point, it is worth mentioning that during these experiments I repeatedly noticed that cells in which miR129 was overexpressed grew slower than in controls. The cells did not have abnormal (apoptotic) morphology, though p53 protein levels increased (not shown). Preliminary analysis of DNA content by flow cytometry suggests that they are arrested in G1 phase (Figure 2.21 k-m), which can be a consequence of p53 activation through Akna mediated

knockdown, as observed in the developing cortex. This effect is therefore in agreement with its expression pattern and a putative role as (a) promoter of cytoskeletal re-arrangements in post-mitotic maturing neurons through targeting of Sox4 and (b) anti-proliferative factor.
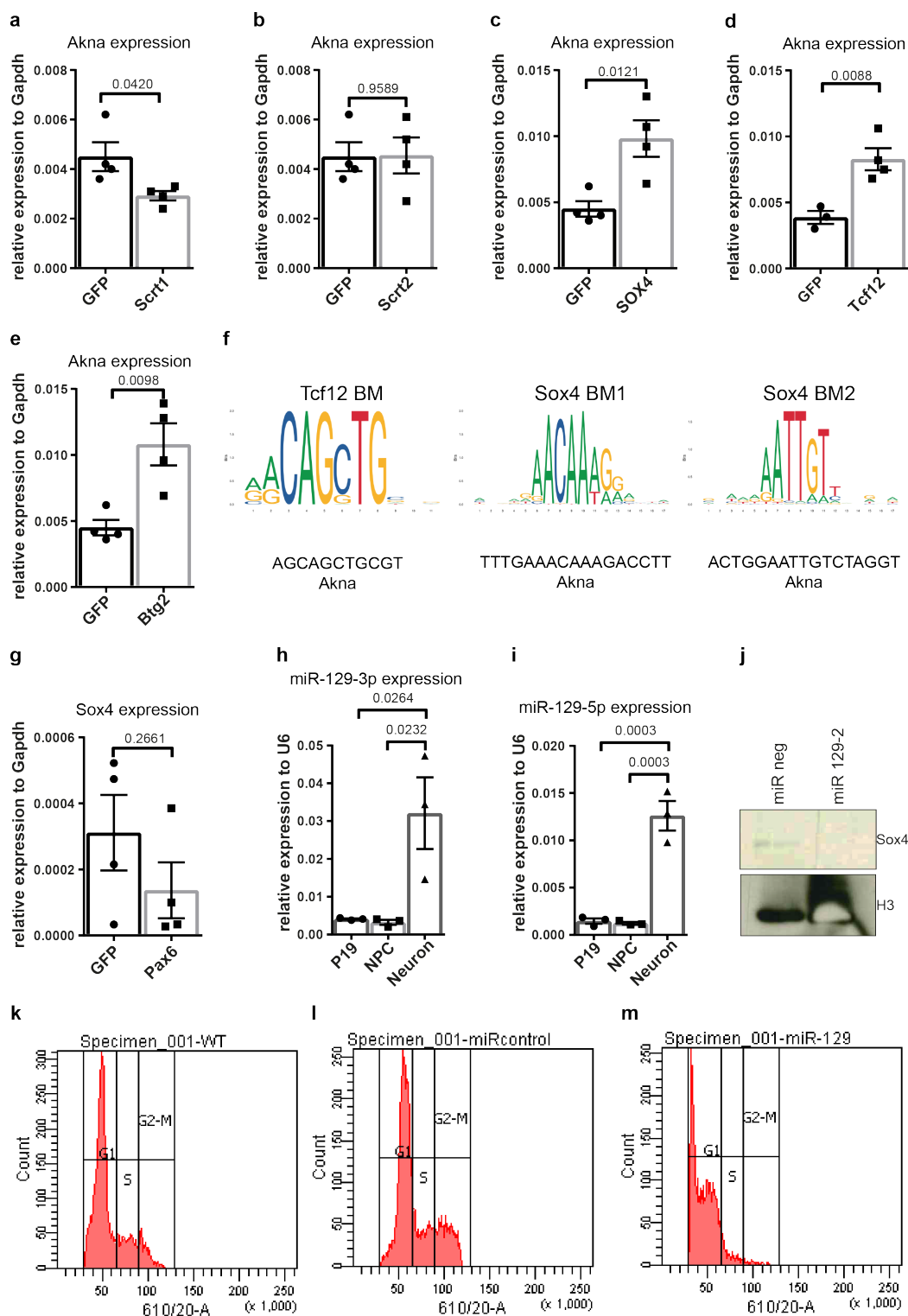
Figure 2.21: **Up-stream regulation of Akna by EMT-promoting factors.** (a-e) RT-qPCR of Akna in N2A cells upon overexpression of known factors that promote EMT. (f) Binding motifs (BM) of Tcf12 and Sox4 in the Akna promoter. (g) RT-qPCR of Sox5 upon Pax6 overexpression in N2A cells. (h,i) RT-qPCR of miR-129 during neuronal differentiation of P19 cells. (j) Immunoblot of Sox4 in N2A cells upon control or miR-129 overexpression. (k-m) DNA content analysis of untransfected, control and miR-129 transfected N2A cells. Statistical analysis (a-c) is student t-Test (a-e, g) or Mann-Whitney with Tukey´s post hoc test (h,i). (a-e, g) done together with TS; (j) done together with JW.

Chapter 3

Discussion

3.1   Akna is a new centrosomal protein

My studies uncovered the true nature of the wrongly designated AT-hook transcription factor Akna and demonstrated that it is in fact a novel integral part of the centrosome in mammalian cells. The present work characterized the function of this protein and revealed thereby hitherto unknown cell biological aspects controlling neurogenesis and EMT.

Using an array of techniques and tools, most critically in-house generated monoclonal primary antibodies, I uncovered the unexpected localization of Akna at centrosomes. As indicated in the results, the cloned sequence used in the first description was incomplete and missed the centrosomal targeting region; which explains why it was misinterpreted. I have also suggested that the GRP sequence in human Akna and some other primates may be coincidental and not the core of a true AT-hook. This sequence is also absent in rodents, amphibians and fishes and likely other species. Whene does Akna first appears in evolution? In agreement with the recent observation that SDAs and its associated proteins are not present in C. elegans and Drosophila (Carvalho-Santos et al., 20111; Hodges et al., 2019), both of which are protostomes, Akna is found first in echinoderms (Strongylocentrotus purpuratus SPU_020662, Lytechinus variegatus LVA_004041, Parastichopus parvamensis PPA_014634; www.echinobase.org) and chordates, including tunicates (Ciona intestinalis gene KH.C9.661.v1.B.SL1-1). This suggests that Akna, and maybe SDAs, are a special feature that could have evolved in deuterostomes.

3.2 Akna expression correlates with centrosomal MT organization

Furthermore, Akna concentrates at SDAs and, to a smaller degree, at PEs of the centrioles. MTs are nucleated in the PCM but also at SDAs and anchored there when the centrosome is the main MTOC (Uzbekov and Alieva, 2018). Otherwise MTs can be severed, capped, transported and anchored in noncentrosomal compartments. Given the number of participants (much more than a dozen) it is reasonable to assume that anchoring, and thus organization, of MTs is a strictly coordinated yet remarkably dynamic process. Akna is a new player in this process and shows many features that make it outstanding: Its levels correlate with the type of MT organization, namely high when the centrosomes is, or becomes, the main MTOC, as in the case of the differentiating sub-group of RGCs, BPs, B-cells and epithelial cells early during EMT. In contrast, Akna levels are low in cells with large pools of non-centrosomaly organized MTs such as in neurons and untreated epithelial cells (Cunha-Ferreira et al., 2018; Sanchez and Feldman, 2017; Stiess et al., 2010; Toya and Takeichi, 2016 and my own observations). It is therefore possible to anticipate what kind of cell expresses Akna depending how the MT network is organized, or, on the contrary, how is the MT network organized depending on the levels of Akna. Not surprisingly tangentially migrating adult brain SEZ neuroblasts, N2A cells, and spleenocytes (most of which are immune cells) are rich in Akna and have centrosome-based MT organization, while mature OB neurons and fibroblast have lower levels of Akna and many noncentrosomal MTs (data not show). Certainly, it will be particularly interesting to understand why tangentially migrating interneurons in the developing cortex and the proliferating non-differentiating fraction of RGCs have fewer Akna, but perhaps this means that their MT organization is partly different (see below).

3.3 Centrosomal localization of Akna is cell cycle dependent

During mitosis, in the cells analyzed so far (from mouse, ferret and human brains, naive immune cells from the spleen, A20, Neuro2a, 293HEK and NMuMG mammary epithelial cells), Akna was not detected at the mitotic spindle. Disappearance from centrosomes

happens at the transition from G2 to prophase, before sister centriole separation and nuclear envelope break down, because in roughly 10% of cells with not-yet-condensed but pH3-positivity, Akna was still detectable at centrosomes. This coincides with the time in which mitotic kinases such as Nek2 and Plk1 (and possibly also Cdk1/Ccnb1 and Aurka) antagonize PP1-function allowing disassembly of centrosomal components such as the centriole linker (that unites sister centrioles) and SDAs through phosphorylation of their constitutive proteins (Mardin et al., 2011; Nigg and Stearn, 2011). Not surprising, treatment with OA to block PP1 led to separation of centrioles and disappearance of Akna from centrosomes. It is therefore possible that Akna's dissociation from the centrosome during mitosis is triggered by mitotic kinases. Why are SDAs dismantled during mitosis? As mentioned in the introduction, SDAs participate in the regulation of both MT organization (anchoring and nucleation) and it is therefore not surprising to find Tubg protein enriched there, but also factors that influence dynamics such as the MT de-polymerase Kif2c (my own observation). Yet, SDAs are found only in the mother centriole, thus generating an asymmetry. In mitosis, in order to break that asymmetry and ensure that both mitotic centrosomes can function equally and separate chromatin properly (otherwise there would be aneuploidy), SDAs should be broken down. Not surprising other SDA proteins such as Ninein, Nlp and Cep170 are also undetectable during mitosis (Casenghi et al., 2004; Graser et al., 2007; Ohama and Hayashi, 2009), though some studies have shown centrosomal staining in spindles (Paridaen et al., 2013); perhaps these observations derived from their localization at proximal ends of both mother and daughter centrioles. In contrast, proteins from the DAs such as Cep164 still remain at the mother centriole in M-phase (Graser et al., 2007), possibly because this structure does not have a major influence in MT organization and hence would not disturb MT dynamics in the spindle. The problem of SDA asymmetry could be circumvented in cells with intense MT nucleation at centrosomes and very fast cell cycle, like activated lymphocytes (8 hours), and both mitotic spindles would be decorated by SDAs.

3.4   Akna can confer MTOC activity

I found here Akna can potently confer MTOC activity in interphase, even in the absence of centrioles, meaning that although it is part of them, it can function independently. It does so (at SDAs) by recruiting the gTuRC and the MT nuclease/polymerase Ckap5/chTOG

(mammalian homologue of XMAP215) (Thawani et al., 2018) in coordination with other proteins involved in MT organization and anchoring such as EB1, Odf2, Dctn1/p150Glued and possibly the Dynein complex (Askham et al., 2002; Ibi et al., 2011; Kodani et al., 2013; Yan et al., 2006; Yang et al., 2017). As a matter of fact, the interactome of EB1 has been discerned by Jian and colleagues in 2012 and it includes the Dynein and Dynactin complexes, chTOG and Akna, consistent with the observations in the present study. The recruitment of the above mentioned centrosome- and MT-associated proteins is specific, because Pcnt, Nedd1, and Camsap2 were not observed at Akna bodies. This indicates that differentiating RGCs and BPs may use a different set of proteins to organize MTs at their SDAs. It is fair to say, in my personal opinion, that composition of centrosomes in the different cells of the developing and adult brain, as well as the dynamic of MTs, are practically unknown territory and certainly waits for further characterization that shall reveal unexpected aspects. As an example, and in defence of my arguments, loss-of-function of Ninein in RGCs or the overexpression of its neuronal splice variant have the opposite effect compared to Akna, namely promoting delamination (Asami et al., 2011, Shinohara et al., 2013; Zhang et al., 2016). Besides, careful inspection of the literature (see for instance Shinohara et al., 2013, Figure 1) clearly shows also a heterogeneity regarding Ninein expression, with clear absence in centrosomes of delaminating RGCs. Furthermore, it needs to be elucidated by profiling experiments such as proximity biotinylation and immunoprecipitation with mass spectrometry and/or other classical ways such as yeast-two-hybrid, if Akna has other interacting partners.

3.5   RGC delamination requires MT organization by Akna

Why do delaminating RGCs and BPs required more centrosomal MT organization, mediated by Akna, than non-differentiating RGCs and neurons? The results suggest that Akna promotes delamination from the apical surface and movement into the SVZ, given that cells stay longer in the VZ upon Akna loss-of-function or, on the contrary, transit faster into the SVZ upon Akna overexpression. This happens during interphase, when Akna is present at centrosomes, and was observed by imaging of cortical slices (not shown), indicating that delamination per se can be independent from mitosis. Although it is clear that mitotic cleavage orientation can play a key role in delamination and definition of the of

daughter cell fate (Kosodo et al., 2004, but see Insolera et al., 2014) our lab and others (Shitamukai et al., 2011) have observed that RGCs at mid neurogenesis often divide with both daughter cells inheriting the apical domain symmetrically, and just then one or both undergo delamination. This fits well with the function of Akna mediating delamination in interphase.

At the molecular level, delamination could be partly explained by the increase in MT nucleation, reflected by the changes in Akna levels. Indeed, Akna overexpression in vitro demonstrates its capacity to promote nucleation and organize MTs through recruitment of g-TuRCs, independent of centrioles, while in vivo it contributes to the rearrangement of the MT network in RGCs. Akna knockdown in vitro in primary cortical cells reduced the number of cells able to grow centrosomal MTs, further supporting its involvement in MT nucleation. The cells, where growth still occurred, had slightly shorter MTs, suggesting an additional role of Akna in MT polymerization, which could be confirmed in cortical progenitors in vivo by measuring the speed of fluorescent EB3 upon Akna gain-of-function. It is noteworthy that cells with very high nucleation activity, such as immune cells, have mainly centrosome MT nucleation, more dynamic MTs and, at the same time the highest levels of Akna expression. It is also important to bear in mind that fast migrating and constantly polarizing cells, again such as immune cells, delaminating RGCs, BPs and adult brain neuroblasts, have these characteristics. Thus, there is a clear connection between the type of MT organization, the level of polymerization and dynamics, the migratory behavior and the expression of Akna. Not surprisingly, work from the Norden lab (Icha et al., 2016) showed in the zebrafish developing retina that RGCs have more acetylated stable MTs in the apical process and these are less dynamic than in (basal) progenitors. This accumulation of acetylated tubulin in the apical process of murine cortical RGCs can be also observed in Cappello et al., 2012.

Moreover, one observation in particular is key in understanding the relevance of Akna's mediated MT organization for delamination of RGCs; Camsap3, but not Camsap2, is strongly recruited to Akna speckles upon overexpression (both in primary cortical cells and mammary epithelial cells). Differential effects and roles of Camsap2 and 3 have been previously reported (Akhmanova and Hoogenraad, 2015; Noordstra et al., 2016; Hendershott and Vale, 2014). In vivo in the developing dorsal forebrain at E14, all three Camsap

proteins are expressed (Aprea et al., 2013; RNAseq data), and Camsap2 and 3 can be found at AJs in RGCs. However, Camsap3, but not Camsap2, was seen at centrosomes in vivo and in vitro including Akna+ centrosomes. Work by the Takeichi lab and colleagues showed that Camsap3 is normally found in the pericentrosomal area and together with Katanin and cytoplasmic Dynein, accompanies MT release from the centrosome allowing their tethering to AJs by p120/Ctnnd and Plekha7 (Dong et al., 2017; Meng et al., 2008). Thus this could be the case in RGCs before delamination, since these proteins are found there. In epithelial cell lines, knockdown of Camsap3 (and 2) destabilizes AJs and potently enhances centrosomal MT organization and polymerization (Dong et al., 2017, Jiang et al., 2014; Nagae et al., 2014; Noordstra et al., 2016; Tanaka et al., 2012). Destabilization of AJ in general, for example by E-cadherin knockdown, enhances centrosomal MT nucleation (Dong et al., 2017). But, could it also work the other way around? Meaning, could intensified centrosomal MT nucleation have a negative impact in AJ stability by sequestering Camsap3 away, hence similar to its loss of function?

How the dynamics of Camsap proteins look in delaminating RGCs and BPs is not known, but the results presented here support a model in which both proteins could compete for more MTs at centrosomes during delamination, given that an increase in nucleation activity, and a larger recruitment of Camsap3 away from AJs could weaken cell adhesion and trigger delamination. Importantly, this concept is supported by the effects of Akna knockdown in epithelial cells undergoing EMT: Akna loss of function during EMT impairs disassembly of cell adhesion proteins such as p120 (AJs) and ZO1 (tight junctions), which may be the reason why the characteristic cell scattering during EMT is partly inhibited, with more cells being attached to each other upon knockdown.

An additional effect could take place at the level of the Actin cytoskeleton: analysis of de-tyrosinated Tubulin during EMT showed that levels increase if Akna is knocked down, again, suggesting that they become longer lived and possibly more stable (more acetylated). Stable long-lived MTs promote the binding of the Rho-GTPase effector Arhgef2/GEF-H1 (Heck et al., 2012; Krendel et al., 2002) which in turn is unable to activate RhoA (and possibly Rac1 and Cdc42), affecting thereby stress fiber formation (F-Actin formation). In epithelial cells stress fiber formation occurs during EMT and indeed, it diminishes upon Akna knockdown, with more Actin at the cell border at the junction, where it normally

regulates strength of adhesion (Vasioukhin and Fuchs, 2001). Actin is also found enriched at AJs in RGCs and it is known that it controls cell adhesion (i.a. Capello et al., 2006; Cappello et al., 2012; Kasioulis et al., 2017) and loss-of-function of Arhgef2 in RGCs impairs their differentiation, with more cells retained at the germinal zones and less cells seeding the CP (Gauthier-Fischer et al., 2009; Ravindran et al., 2018). Thus, certainly the effects of Akna on microtubule stability could lead to the impairment of Rho-GTPase signaling and consequently delamination in both RGCs and epithelial cells during EMT. Finally, it is important to emphasize that Akna does not exert its effects via cilia-mediated mechanisms, which also can regulate delamination of RGCs (Paridaen et al., 2013; Wilsch-Bräuninger et al., 2012), because neither Akna loss- nor gain-of-function have any apparent effect on cilia growth, maintenance or position in cortical progenitors neither in vivo nor in vitro (Figure 3.1 a,b and not shown).

It is fair to mention that mechanisms mediated by Akna outlined here are partly complementary to previously reported studies of NEC delamination, specially the observations by Das et al., 2014 and Kasioulis et al., 2017. These studies have shown that centrosomal MT nucleation is important for delamination of neuroepithelial cells of the chicken spinal cord, by controlling what they termed abscission (of the ciliary membrane) from the apical surface, or apical abscission. This requires dissolution of AJs and an intensified MT nucleation from the centrosome of the NECs to build, together with an Actin cable, a cage that facilitates the retraction of the centrosome and constriction of the ciliary membrane. My results would suggest that Akna is the factor mediating these processes. However, it is important to add, the fact that delamination during mid cortical neurogenesis occurs at the RGC stage and generates, mostly, BPs that segregate immediately from the VZ. In the studies by Kasioulis delamination is studied in NECs and must be induced by overexpression of transcription factors that promote direct neuronal differentiation (i.e. Neurog2). In the mouse developing cortex direct neurogenesis is rather rare at mid neurogenesis. Furthermore, the delamination observed in those studies seem to relate mostly to the retraction of the apical process, since the cell soma remains largely in place in the periods described by the authors. This suggest therefore that Akna coordinates more processes beyond the constriction of the centrosome, for example in cells that have already delaminated, i.e. in BPs.

3.6 Akna mediates retention of cells in the SVZ

In addition to the role in delamination, Akna has a crucial role for the retention of multi-polar cells (BPs and new-born neurons) in the SVZ. Gain-of-function using the promoter of the early neuronal gene Dcx to drive expression of Akna inhibits neuronal migration into the CP and neurons remain stuck in the SVZ/IZ, where they mature despite their ectopic location. Loss-of-function, in contrast, has basically no effect on neuronal migration. Nonetheless the change from multi- to bipolar morphology is accelerated if Akna is precociously downregulated in neurons and is slowed upon overexpression, which explains why they are blocked en route to the CP, as this step is essential for neurons to successfully define their orientation of migration and to specify the leading and trailing processes of bipolar neurons, and ultimately the future axon. What mechanism could be behind this effect? For this, one must go back to the discussion above regarding MT organization and dynamics in neurons, taking into account the changes MT upon Akna manipulation. Firstly, it is known that MTs are stabilized in neurons as they mature, given the increase in acetylation, de-tyrosination and non-tyrosinable delta-2 Tubulin, including neurons of the developing neocortex (see figures in Capello et al., 2012n but also see Aillaud et al., 2017), and thus turn less dynamic. This is important for neuronal polarization (e.g. for axon and dendrite specification) (Song and Brady, 2014; Witte et al., 2008). Importantly, this is concurrent with inactivation of centrosomes as MTOCs (see Stiess et al., 2010). The molecular mechanisms of centrosome inactivation are not well understood, but re-localization of nucleating and anchoring factors such as Tubg, Cdk5rap2 (i.e. gTuRCs), Ninein and the Haus complex as well as the down-regulation of Nedd1 (Cunha-Ferreira et al., 2018; Sakakibara et al., 2014; Yonezawa et al., 2015; Zhang et al., 2016), and now Akna, have been implicated. It is possible that Akna could coordinate all this players. Furthermore, Akna gain-of-function decreases MT de-tyrosination and make MTs more dynamic, while knockdown has the opposite effect. Therefore, by keeping the levels of Akna high in neurons, and henceforth maintaining the centrosome active and inhibiting MT stabilization, re-polarization can be impaired. In knockdown conditions re-polarization may occur faster because centrosome inactivation and MT stabilization would be accelerated.

In summary, together with the above mentioned observation that Akna gain-of-function in RGCs induce the re-arrangement of the microtubule cytoskeleton towards a conformation that is alike to delaminating cells and BPs, and the effects observed in young neurons,

suggest that Akna's role as MT organizer is essential for mediating the changes in polarization when bipolar RGCs transit to multipolar BPs (requiring high Akna levels) and when multipolar cells in the SVZ progress towards bipolar migrating neurons (requiring gradual downregulation of Akna levels). It is known that both re-polarization events are largely controlled by the microtubule (and actin) cytoskeleton in the developing brain (Cooper, 2014 and refs. therein), for example to properly relocate organelles like the Golgi apparatus and centrosomes themselves. These features are generally conserved in other developing organs and epithelial cell lines undergoing EMT (Burunte et al., 2017), where Akna also has regulatory functions. In this study, the key factor that links those processes with MT organization and their dynamics has been revealed by identification and characterization of the function of the novel centrosomal protein Akna.

3.7   Akna is regulated by EMT transcription factors

The expression pattern of Akna in the developing (and adult) brain is particularly remarkable for a centrosomal protein. It was assumed for many years that centrosome composition would be homogeneous and that just a minor fraction of centrosome associated proteins would vary according to the nature of the cell, for instance Ninein in epithelial cells (Mogensen et al., 2000). Recently, however, many studies have demonstrated that the centrosomal compartment can be occupied by many rather unexpected proteins in different cell types, or depending of cell cycle phase and, most importantly, the type of MT organization (Hintermair et al., 2016; Huang et al., 2017; Ibi et al., 2011). Akna is an excellent example of centrosomal heterogeneity. Yet, how is that heterogeneity transcriptionally wired? The results here showed that Akna expression is co-regulated by the transcription factors Sox4 and Tcf12 and the cell cycle regulator Btg2. Interestingly, Scrt1 had a negative effect on Akna, althought it promotes RGC differentiation and delamination, suggesting that that different EMT-like delamination programs may act in parallel and even cross-regulate each other.

Importantly, Sox4, Btg2 and most likely Tcf12 are not only expressed in differentiating RGCs (in dorsal and ventral germinal areas) but also have been shown to direct their differentiation to BPs (Chen et al., 2015; Fei et al., 2014). In the developing cortex, Sox4 is in addition expressed in more superficial neurons and only partially co-localizes with

Sox11 (which is not expressed in differentiating RGC and BPs), suggesting a different role in neuronal specification during cortical development (Chen et al., 2014), because at adult stages its expression is restricted to migrating SEZ/RMS neuroblast (where Akna is highly expressed) and hippocampal new-born neurons (Mu et al., 2012). For some time, it was thought that Sox4 and Sox11 - both belong to the SoxC family - would have redundant functions (Mu et al., 2012 and refs therein), thus the finding that in the developing forebrain they have differential expression and roles highlights the importance of more careful examination of related genes. Why would a cell spend energy having two genes for exactly the same function? Similarly, the role of the bHLH transcription factor Tcf12 has just started to be uncovered. In contrast to its sibling Tcf4, whose function in neuronal development has been partly characterized (see for instance Chen et al., 2016; Ohtsuka et al., 2011; Schmidt-Edelkraut et al., 2014), the knowledge regarding its participation in forebrain neurogenesis, besides the expression profile (high in neurogenic germinal zones) and the exencephaly phenotype in the loss of function mouse models (Uittenbogard and Chiaramello, 2002), is rather few. In the midbrain it is involved in fate determination of dopaminergic neurons (Mesman and Smidt, 2017). In the hematopoietic system, studies by the Andersson and Zúñiga-Pflücker laboratories have demonstrated that Tcf12 is a fate determinant (a) of early hematopoietic commitment from mesodermal progenitors and (b) of specific subtypes of T-cells (In et al., 2017; Li et al., 2017). The transcriptional regulation of T-cell differentiation by Tcf12 is coordinated, interestingly, by Sox4 (In et al., 2017). Thus, both genes can work synergistically to define cell fate through transcriptional regulation, and as shown here, Akna is one of their common targets. Furthermore, Sox4 and Tcf12 promote EMT through epigenetic mechanisms upstream of Snail, Zeb, or Twist (Tiwari et al., 2013) and repression of cell adhesion components like Cdh1/E-Cadherin in cell lines (Lee et al., 2012). It seems, therefore, logical that Akna is a transcriptional target of both TFs, given its role in promoting delamination and EMT through dissolution of cell-cell contacts via MT organization and dynamics. What other roles Tcf12 would have in the developing brain is not well known, but its interaction with the potent pro-neurogenic Ascl1 (Gradwohl et al., 1996) suggests that it may be a co-regulator of neuronal fate determination. It would be tempting to investigate if forced expression of Tcf12 would be sufficient to transdifferentiate nonneuronal cells, or at least improve the process.

Btg2 is a particularly interesting gene. Its role (and the one of Btg1) in neurogenesis has been well studied. It promotes exit or slowing of cell cycle at G1 phase, where it is highest

expressed (Iacopetti et al., 1999). Not surprisingly it is upregulated upon neuronal commitment in the developing forebrain, where it marks differentiating RGCs and BPs, and gain-of-function induces premature differentiation which ultimately causes microcephaly due to reduced number of cortical neuronal (Fei et al., 2014). In adult brains, loss of function Btg2 and Btg1 triggers activation of quiescent adult SEZ NSCs and concomitantly increases neuronal precursor amplification which ends with the exhaustion of the stem cell pool (Farioli-Vecchioli et al., 2012; Farioli-Vecchioli et al., 2014). Btg2 has been shown to regulate the expression of genes like Id3, Cyclin D, and RARβ (Farioli-Vecchioli et al., 2007; Lin et al., 1996; Passeri et al., 2006) by binding to their promoters. Yet, this is somehow controversial given its cytoplasmic localization (Iacopetti et al., 1999), and other members of the same family were found to be RNA-binding proteins in the cell soma. In fact, Stupfler et al., 2016 reported a function for Btg2 in de-adenylation of mRNA. Maybe is acts in both cellular compartments, but this may need to be revised. Btg2 could therefore regulate Akna by binding to a regulatory region, if it is in the nucleus, or by binding to its transcripts and regulating the lifetime. This would explain in part the sharp regulation of Akna expression in subtypes of progenitor cells only.

In trying to identify negative up-stream regulators of Akna in proliferating RGCs, I hypothesized that Pax6 could be a good candidate because the Pax6 mutant mouse model Small eyes (Sey) shows precocious delamination of progenitor cell due, in part, to aberrant cell adhesion at the apical surface, and most importantly, elevated levels of Akna mRNA. Nonetheless, Pax6 overexpression had no effect on Akna in N2A cells, but it seemed to have one on Sox4, though not statistically significant given large sample variation. This suggests therefore that Pax6 could except a negative regulation on Akna indirectly by controlling the expression of Sox4.

Finally, I show here that mir-129 can regulate the levels of Sox4, and this in turn could in help reducing the levels of Akna at later stages of neuronal differentiation and keeping them low in mature neurons. This is in agreement with previous studies and can be achieved by both arms of the miR (i.e. 3p and 5p) (Huang et al., 2009; Wu et al., 2010). Both mir-129 arms are predominantly and almost exclusively expressed in the brain during development and at adult stages, largely in neurons (Cao et al., 2012; Ludwig et al., 2016; Wienholds et al., 2005) (although a proper comparative analysis with glial cells has

not been done). So, it is obviously contradicting the fact that both Sox4 and miR-129 are expressed in neurons in the developing brain (Cao et al., 2012). Yet, since Sox4 is present in rather the more superficial type of neurons, it is possible that Sox4 and miR-129 could be mutually exclusive, with the microRNA being expressed higher in deeper layer neurons. A second alternative could be that mir-129 just fine-tunes but does not silence Sox4, as shown for Rbfox3/NeuN in hippocampal neurons (Rajman et al., 2017). A third alternative could that the 3´UTR of Sox4 may be differentially polyadenylated in neurons, compared to BPs, making it insensitive to miR-129. Importantly, the Akna interactor EB1 has been proposed to be also targeted by miR-129 (Wu et al., 2010), suggesting that miR-129 could fine tune the levels of centrosome and MT associated proteins in neurons (see also Bijnsdorp et al., 2016 and Cao et al., 2012), and this in turn could facilitate the rearrangement of the microtubule cytoskeleton descripted here (but also in adult neurogenesis). Beyond controlling MTs, and in agreement with neurons becoming post-mitotic, mir-129 overexpression in vitro reduced cell growth, possibly because they get blocked in G1 phase as shown by DNA content analysis by flow cytometry. In fact, targets of miR-129 also include cell cycle regulators such as Cdk6 (Wu et al., 2010) and metastasis-related genes p-FAK, MMP-2 and MMP-9 (Chen et al., 2014). It would be thus fascinating to investigate in more detail the function of this neuronal miRNA, as - curiously - it has remained understudied. The developing cerebral cortex would be a nice system given the feasibility for manipulation of the different populations (progenitors and neurons) and the relative simplicity of readout. How is miRNA-129-2 expression controlled? A detailed explanation goes beyond this manuscript, but pilot experiments suggest that its nearest gene, the long noncoding RNA E531000K10Rik, which is also enriched in the brain, could be an upstream regulator, possibly through recruitment of chromatin remodelers to the CpG island on which miR-129-2 is located.

3.8   Conclusion and future directions

Akna is the first and only known centrosomal protein regulating entry to and exit from the SVZ thereby not only coordinating both of these processes, but also highlighting the importance in the balance of centrosomal versus acentrosomal MT recruitment in this crucial event during ontogeny of the brain and in other epithelial cells undergoing EMT (Figure 3.2), a wide spread process in many developing tissues and cancer. Preliminary analyses

in the developing folded cerebral cortex of ferrets and macaques, as well as 3D models of cortical development (i.e. cerebral organoids), point towards a conserved mechanism regulating the seeding of BPs in the expanded SVZs of those species, therefore suggesting that it has broader implications during phylogeny.

The fact that Akna is also particularly highly expressed in migrating adult brain neuroblast from the SEZ does not scape my consideration (Figure 3.1 c,d). Strikingly, Akna is only detected in the OB in the RMS, but not in other layers (unpublished data), indicating that it is downregulated when cells change from tangential to radial migration. This contrasts with the developing cortex, where radially migrating cells still have some Akna, but tangentially migrating interneurons do not. Hence, are the mechanisms regulated by Akna the same in embryonic and adult neurogenesis? Towards that end, I have generated, on one hand, pseudotyped rabies viral particles to overexpress Akna specifically in adult NSCs using the hGFAP-TVA mouse line. This was done in collaboration with the Conzelmann lab. On the other hand, I also generated an Akna full knockout mouse line (Figure 3.1 d). It's characterization though is presently ongoing and is therefore outside of the scope of this thesis. This mouse line will certainly open the door not only to understand the role in neurogenesis but also in other contexts such as immune system activation, delamination processes in other organs, especially in the lungs where Akna highly expressed in subtypes of epithelial cells.

With a look into future ways to regenerate lost neurons (and why not glia cells?) under pathological conditions, for example through forced neuronal reprogramming, I would like to conclude by emphasising the importance of further investigating and understanding the very basic cell biology of neurogenesis. Have in vitro derived (reprogrammed) cells a similar microtubule cytoskeleton profile as endogenous ones? Are the dynamics and composition supportive (e.g. for intracellular vesicle transport, or proper formation of connections, which rely on MTs), and permit integration in pre-existing neuronal networks? A fascinating time is ahead to answer this and many other interesting questions, and to do striking unappreciated new discoveries.
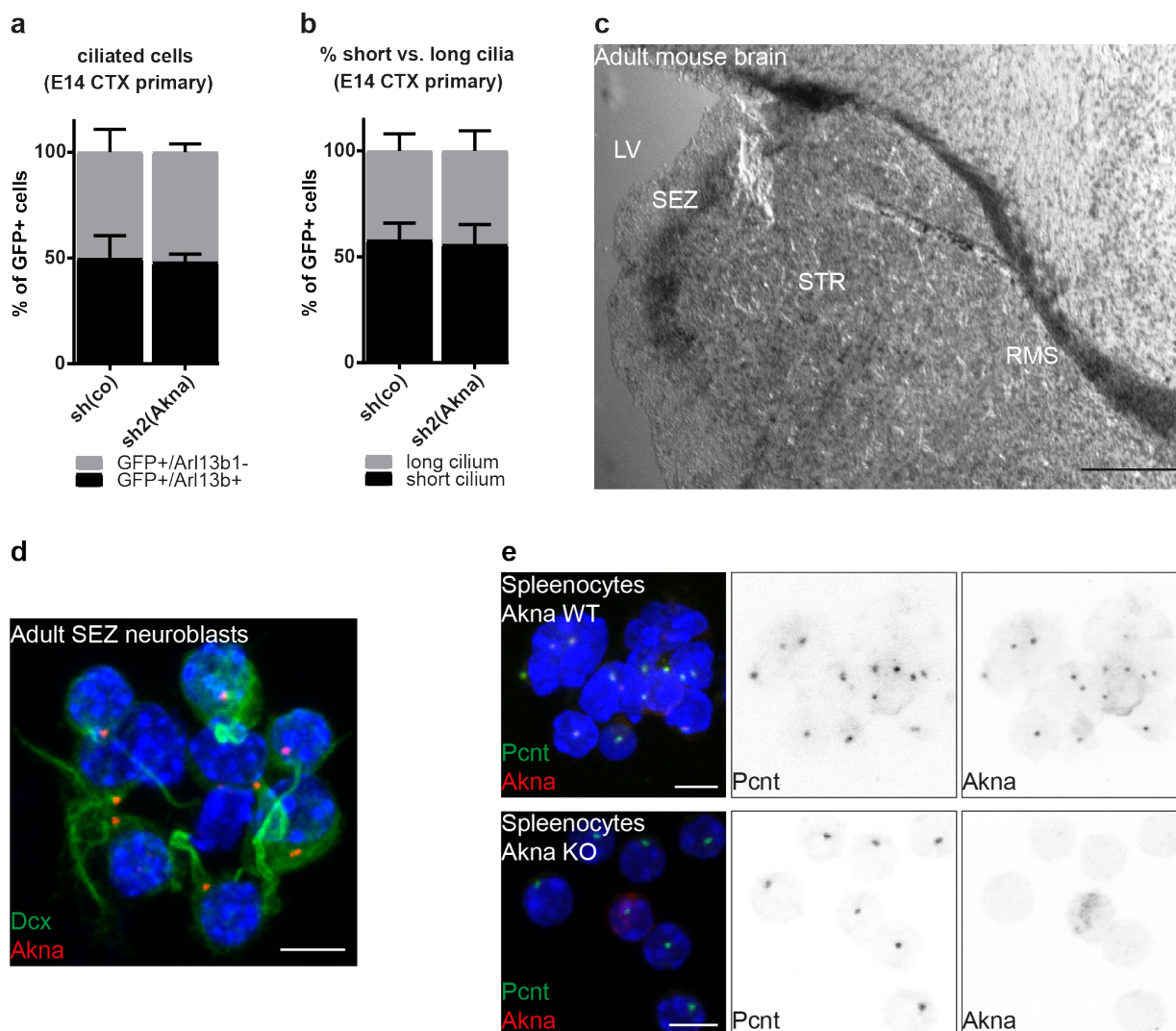
Figure 3.1: **Primary cilia upon Akna manipulation, expression in adult brain neuroblast and Akna KO animals.** (a) Histograms depicting the percentages of ciliated cells (Arl13+) (a, n=3) and short vs. long cilia (b, n=3) in control or Akna shRNA transfected E14 primary cortical cells. Short cilia are defined as dot-like (short axoneme or cilium not fully exposed to cell surface), long as rod-shaped (long axoneme exposed at the cell surface). (b,c) Akna RNA-ISH and IF of adult brain tissue and in primary adult SEZ neuroblasts, respectivelly, showing high expression in migrating neuronal precursor cells. (b) Spleenocytes of Akna WT and KO animals confirming the absence of Akna protein in cell of KO mice. LV, lateral ventricle; RMS, rostral migratory stream; SEZ, subependymal zone; STR, striatum. Scale bars: 3.3 mm (b); 5 μm (d,e)
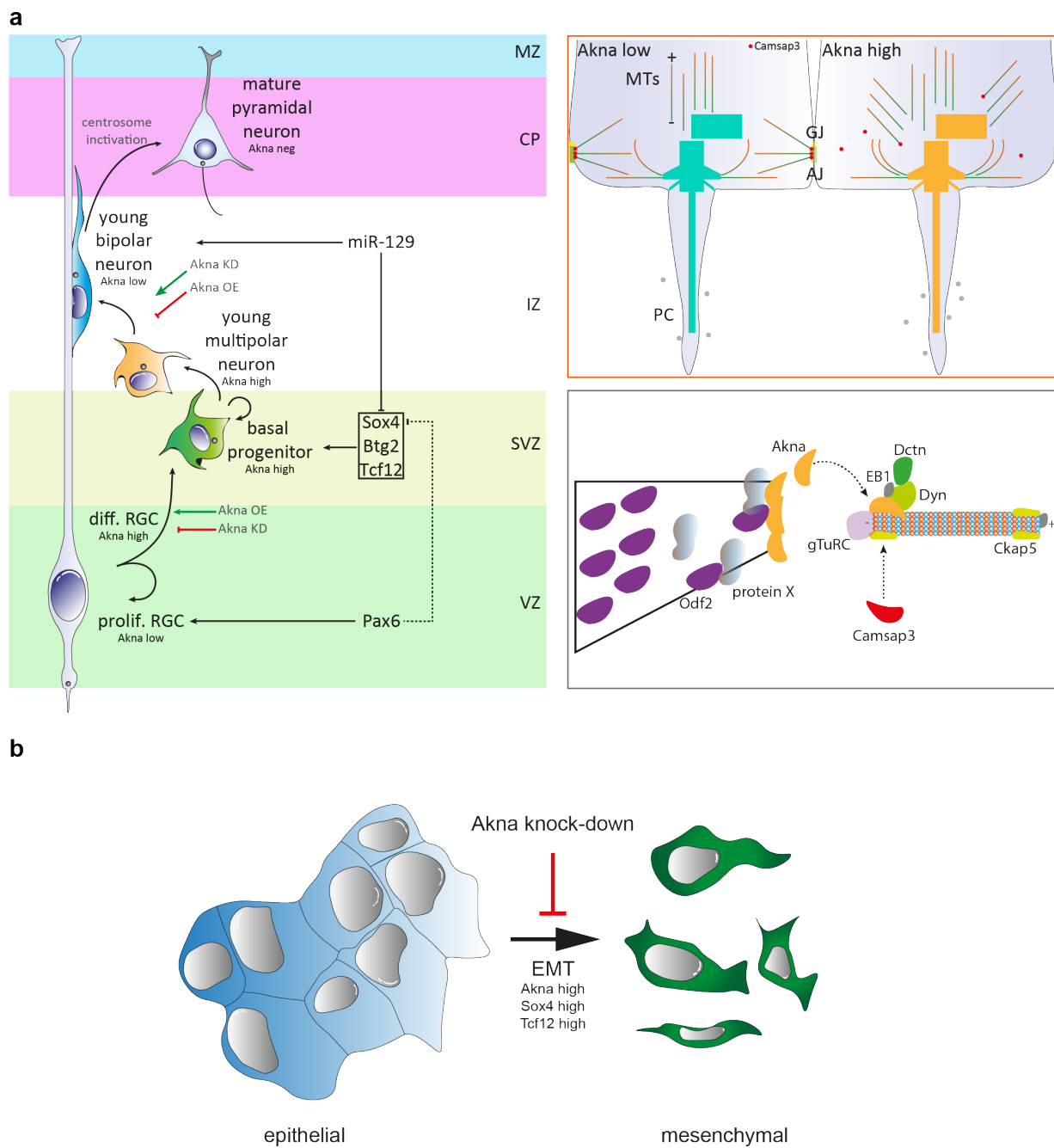
Figure 3.2: **Working model.** Model summarizing the expression of Akna, the phenotype upon manpulation and the changes in MT dynamics and AJs in the developing cererbal cortex (a) and the phenotype in epithelial cells (b).

Chapter 4

Materials and Methods

4.1 Methods

4.1.1 Molecular and biochemical assays

Molecular cloning and plasmids

GIBSON assembly, Gateway cloning (Invitrogen) and conventional restriction enzyme-based molecular cloning were used routinely to generate all expression plasmids, unless otherwise stated, according to manufacturer recommendations. All vectors are described throughout the thesis and maps are found in digital form in the CD-DVD attached to the manuscript. Original full-length murine and human Akna CDSs derive from the IMAGE cDNA clone 30531788 (vector pYXAsc; purchased from Origene) or IMAGE cDNA clone 6143155 (vector pCMVSPORT6; purchased from Dharmacon). Unless stated differently, CDS from genes used in this study were cloned from C57BL/6 mouse embryonic brain derived cDNA. The following plasmid and backbones were gifts from: pETM11LIC (Arie Geerlof, Helmholtz Zentrum München), pCAG-EB3-GFP (Anna Akhmanova, Utrecht University), pCAG-EB3-NeonGreen, Stanislav Vinopal (DZNE, Bonn), pDcx-GFP (Ulrich Mueller, UC San Diego), pCMV-hyPBase (Pentao Liu, Sanger Institute, UK), pRV-CAG-HA-SOX4-IRES-EGFP (Chichung Lie, University Erlangen-Nüremberg) Knockdown experiments were done with shRNAs cloned into the pSUPER.neo+gfp vector (Oligoengine). Parallel Akna knockdown and MT-tracking was achieved by exchange of the EGFP-CDS

from pSUPER.neo+gfp for EB3-NeonGreen. The BAC clone to generate GFP-tagged Akna transgenic cells lines was purchased through the MitoCheck-consortium (BAC ID: MCB 4151). PCR primers for molecular cloning and all PCRs, which count in the hundreds, are deposited in the CD-DVD attached to this work.

Western blot

Fresh tissue or cells were homogenized in 1X RIPA buffer or IP-lysis buffer (1XTBS pH7.6, 1% IGEPAL, 2 mM EDTA, 2 mM EGTA) containing protease (cOmplete, Roche) and phosphatase (PhosSTOP, Roche) by passing it repetitively through a 20G and then a 26G needle using a 1ml syringe. Lysates were incubated on ice for 10-30 min and spin-cleared for 20 min at 4°C at 13000 rpm in a microcentrifuge. Protein concentration was calculated by Bradford assay. The protein was subsequently diluted to the desired concentration in 1X Laemmli Buffer with 10% 2-Mercaptoethanol or DTT. Gel electrophoresis was done with 6%, 7%, 10% and 12% poly-acrylamide SDS gels or 4-15% Mini-PROTEAN TGX Stain-Free Gels (BioRad) depending of the protein molecular size and then transferred to PVDF membranes (pore sizes 0.2 μm or 0.45 μm) (BioRad) for 70 min at 100V. For immmunodetection, membranes were blocked with 5% nonfat dry milk (BioRad) in TBS/T (Tris buffered saline/0.1% Tween-20, pH7.4) for 30 minutes, incubated over night with primary antibodies in 1% nonfat dry milk in TBS/T and next day incubated with HRP-coupled secondary antibodies diluted in 1% nonfat dry milk in TBS/T. Finally, the signal was visualized by ECL method on Röntgen films (Fujifilm).

Protein immunoprecipitation (IP)

E14 forebrains lysates were obtained as mentioned above with ice-cold IP lysis buffer. 10 mg protein lysate was incubated end-over-end with 5 μg purified antibody (clone 25F1) or IgG1 control overnight at 4°C. Next morning, 20 μl pre-cleared Dynabeads Protein G (Invitrogen) were added to the lysate/antibody mix and incubated end-over-end at 4°C for 1 hour. Beads were then separated with a magnet and washed 4 times at 4°C with washing buffer (lysis buffer with 0.25% NP-40), for 10 minutes each time. Alternatively, antibodies were incubated with 100-200 μl pre-cleared Protein G Sepharose 4 Fast Flow for 4-5 hours at 4°C. Beads were washed three times as above, incubated overnight with protein lysates and next day washed 3 times. Proteins were eluted by cooking beads at

70°C on a mixer at 600 rpm for 15 min in 2X Laemmli buffer and separated from the beads with a magnet. In the case of Odf2, 1 ml hybridoma culture supernatant of clone 25F1 or an unrelated antibody of the same isotype (mouse IgG1) were incubated with 200 μl of pre-cleared Protein G Sepharose beads (GE Healthcare Life Sciences) for 5 hours at 4°C. Beads were then collected by centrifugation (3000 rpm, 30 sec, 4°C) and washed three times and thereafter incubated overnight with 3.5 mg protein lysate end-over-end at 4°C. Next day, beads were washed 4 times and protein was eluted at mentioned above.

Subcellular fractionation and centrosomal fraction enrichment

Centrosomal enrichment was performed according to Moudjou and Bornens, 1994 with modifications. Approximately 3.6×10^8 cells were used for the procedure. One hour before lysis cells were incubated at 37°C with 100 ng/ml Nocodazole and 1 μg/ml Cytochalasin D to depolymerize microtubules and Actin filaments, respectively. Cytoplasmic and nuclear extracts were obtained by resuspending cells in Tween20 lysis buffer (25 mM HEPES pH 8, 20 mM NaCl, 2 mM EDTA, 1 mM PMSF, 0.5% Tween20, 1X protease inhibitors, cOmplete, Roche) and incubated on ice for 30 min with gentle vortexing every 10 min. Nuclei were pelleted by centrifugation at 1200 rpm for 10min at 4°C. The supernatant (cytoplasmic fraction) was supplemented with 250 mM NaCl. The nuclear fraction was washed once with 250 μl of lysis buffer, centrifuged at 1200 rpm for 10 min at 4°C, resuspended in 250 μl lysis buffer containing 500 mM NaCl, incubated 15 min on ice and sonicated 20 times for 1 sec at 30% input. NaCl concentration was increased to 250 mM thereafter by addition of 250 μl of lysis buffer. Finally, nuclear fractions were centrifuged at 13000 rpm for 20 min and the supernatant containing nuclear proteins was taken. Naturally, for centrosomal enrichment the cytoplasmic fractions were used. First, the fraction was filtered through a cell strainer of 40 μm pore size (Falcon, cat. 352340) to remove chromatin and nuclei. The remaining DNA was digested with 1 μg /ml DNaseI (Roche) for 30 min on ice. Thereafter, centrosomes were sedimented onto a 2 ml 60% sucrose solution by centrifugation at 7500 rpm for 30 min at 4°C in an Avanti J-30I centrifuge in thin-wall polypropylene ultracentrifuge tubes (38.5 ml, Beckman). After concentration, the supernatant was removed until approx. 0.5 cm over the interphase and the centrosome containing cushion was mixed by gentle vortexing and laid over a gradient of 70% (1 ml), 50% (0.6 ml) and 40% (0.6 ml) sucrose in thin-wall polypropylene ultracentrifuge tubes (38.5 ml, Beckman). Centrifugation was done at 24000 rpm for 80 min at 4°C. Fractions of ca. 400 μl were collected whether processed for WB

or stored frozen at -80°C.

Mass spectrometry, protein identification and label-free quantification

Mass spectrometric (MS) analysis of centrosome enriched fractions was performed at the Research Unit Protein Science (Helmholtz Zentrum München). I summarize here the procedure: 20 μl of each fraction were extracted by addition of 1 x Laemmli buffer and trypsin-digested by filter-aided sample preparations as described (Grosche et al., 2016). Eluted peptides were combined, acidified and directly used for analysis on a Q Exactive (QE) high field (HF) mass spectrometer (Thermo Fisher Scientific Inc.) online coupled to a RSLC HPLC system (Ultimate 3000, Thermo Fisher Scientific Inc.). MS data were acquired using a data-dependent top-10 method and recorded within a mass range from 300 to 1500 Da at a resolution of 60,000. Fragmentation was performed via higher energy collisional dissociation (HCD), on precursor peptides which were isolated with a 1.6 m/z window. Peptides were identified and quantified using the Progenesis QI software (Nonlinear, Waters) and the Mascot search algorithm (MatrixScience, London, UK; version 2.5.1) with the Ensembl mouse public database as described (Grosche et al., 2016). Normalized abundances of identified peptides were grouped to the minimum set of proteins fulfilling the rules of parsimony. Relative abundances (in percentages) of the single proteins in the eight gradient fractions were clustered with GProX (Rigboldt et al., 2011) to isolate proteins that co-elute with gamma-tubulin and Akna as observed by western blot, both for all quantified proteins and for proteins quantified with at least 2 unique peptides. The following settings were used in GProx: classification in 15 clusters without standardization or addition of a reference point, upper limit of 2 and lower limit of 0.5, fuzzification of 2, iterations 100 and minimal membership of 0.5.

Protein expression and purification

Protein expression and purification of recombinant Akna protein was performed at the corresponding facility of the Helmholtz Zentrum München. I summarize the procedure here: the pETM-11/AKNA construct was transformed into E. coli strain Rosetta2 (DE3) and cultured at 20°C in four 2-L flasks containing 500 ml ZYM 5052 auto-induction medium (Studier, 2005) with 100 μg/ml kanamycin and 33 μg/ml chloramphenicol. Cells were harvested by centrifugation after reaching saturation, resuspended in 70 ml lysis buffer

1 (50mM Tris-HCl, 300mM NaCl, 20mM imidazole, 10mM MgSO4, 10 μg/ml DNaseI, 1mM AEBSF.HCl, 0.2% (v/v) NP-40, 1 mg/ml lysozyme, 0.02% (v/v) 1-thioglycerol, pH 8.0), and lysed by sonication. The lysates were clarified by centrifugation (40,000 x g) and filtration (0.2 μM). The supernatant was applied to a 5 ml HiTrap Chelating HP column (GE Healthcare), equilibrated in buffer A (50mM Tris-HCl, 300mM NaCl, 20mM imidazole, 0.01% (v/v) 1- thioglycerol, pH 8.0) using an Äkta Purifier (GE Healthcare). The column was washed with buffer A, then with buffer A supplemented with 1M NaCl, and lastly with buffer A containing 50mM imidazole, until a stable baseline was reached (monitored at 280nm). Bound proteins were eluted with buffer B (50mM Tris-HCl, 300mM NaCl, 300mM imidazole, 0.01% (v/v) 1-thioglycerol, pH 8.0) and fractions containing proteins pooled and concentrated to less than 5 ml. This was subsequently applied to size exclusion chromatography using a HiLoad 16/600 Superdex 200 column (GE Healthcare), equilibrated in buffer C (50mM Tris-HCl, 300mM NaCl, and 0.01% (v/v) 1- thioglycerol, pH 8.0). The fractions containing full length AKNA were collected, pooled and stored at 4°C. Protein concentrations were determined by measuring the absorbance at 280nm using a specific absorbance for His6-tagged full length AKNA of 0.851 ml.mg-1.

RNA isolation and RT-qPCR

For cell lines and sorted cells, total RNA was extracted using the RNeasy Mini and Micro Kits (Qiagen) and RNA reversed transcribed into cDNA using the Maxima First Strand cDNA Synthesis Kit (Thermo Fischer) and Superscript III First-Strand Synthesis Super-Mix (Invitrogen), respectively. The real time RT-PCR assay was conducted using SYBR Green Dye Master Mix (Bio-Rad) or QuantiFast SYBR Green PCR Kit (Qiagen) according to manufacturer recomendations. Primer sets were validated using melting curve analysis and gel electrophoresis. Assays were performed in triplicate on a DNA Engine Opticon machine (Bio-Rad) or a QuantStudio 6 Flex Real-Time PCR System (Thermo Fischer). The relative expression of Akna mRNA was calculated using the comparative Ct method normalized to Gapdh.

For ferret RNA extraction, pups were anesthetized, decapitated, their brains dissected and blocked in ice-cold ACSF (140 mM NaCl, 5 mM KCl, 1 mM MgCl2, 24 mM D-glucose, 10 mM HEPES, 1 mM CaCl2, pH 7.2), and tissue blocks containing the occipital cortex were cut in 300 μm-thick slices at the vibratome. Living cortical slices were further

microdissected with microscalpels in ice-cold ACSF to isolate the VZ, from the caudal pole of the cerebral cortex. Total RNA was extracted using RNeasy Mini Kit (Qiagen) followed by treatment with RNase-Free DNase Set (Qiagen). Template cDNA was generated using Maxima First Strand cDNA Synthesis Kit for quantitative real-time PCR (qRT-PCR) (Thermo Fisher). Quantitative RT-PCR was performed using the Step One Plus sequence detection system and the SYBR Green method (Applied BiosystemsIn each experimental group we analyzed 4-7 samples, each consisting of a pool of 2-3 embryos/kits. Reactions were performed in triplicate per independent sample. Akna transcript levels were calculated using the comparative Ct method normalized using Actin.

Isolation of genomic DNA for genotyping

Tissue was incubated at 95°C in 100 μl 50 mM NaOH for 20 min, followed by incubation on ice for 5 min. NaOH was buffered with 30 μl 1M Tris (pH 7.6). 1 μl was used for a PCR reaction. Products were analysed in agarose gels.

Manipulation and culture of competent bacteria

Transformation of chemically competent Dh5alpha (New England Biolabs or home-made) and TOP10 (home-made) was done as following: cell were incubated with DNA for 20 min on ice, then heat-shocked for 30 sec at 42°C, cooled-down on ice for 5 min an finally allowed to recover at 37°C in LB medium for 1 hour with constant shaking. Cells were plated on agar plates supplemented with corresponding antibiotics and grown over night. Mini-, medi- and maxi-preps were prepared by picking single colonies and growing them overnight at 37°C in liquid LB supplemented with antibiotics. Next day, DNA was isolated using the corresponding Kit and according to manufacturer instructions. For colony-PCR, single colonies were resuspended in 20-50 μl LB medium and 1 μl was used as template.

Assessment of nucleic acid integrity and quantity

In general, DNA and RNA quantity and quality were checked with a Nanodrop spectrophotometer (PeqLab) or a Bio-Analyzer (Invitrogen).

PCR set-up

Conventional PCR protocol (20μl)

mix		conditions		cycles
10X buffer (Coral)	2μl	95°C	5 min	1
dNTPs (10 mM)	1μl	95°C	30 sec	35
for primer (10 μM)	1 μl	58°C	30 sec	35
rev primer (10 μM)	1 μl	72°C	1 min/kb	35
Tag-pol	0.2 μl	72°C	5 min	1
template	1 μl	16°C	-	
H20	13.8 μl			

Phusion Pol PCR protocol (50μl)

mix		conditions		cycles
10X buffer (HF/GC)	10μl	98°C	2 min	1
dNTPs (10 mM)	1μl	98°C	20 sec	35
for primer (10 μM)	2.5 μl	59°C	20 sec	35
rev primer (10 μM)	2.5 μl	72°C	1 min/kb	35
Phu-pol	0.5 μl	72°C	4 min	1
template	1 μl	16°C	-	
H20	32.5 μl			

RT - qPCR protocol (10μl)

mix		conditions		cycles
2xSybr Green	5μl	95°C	5 min	1
H20	2.8μl	95°C	10 sec	40
for primer (0.1-1 μM)	0.1 μl	60°C	30 sec	40
rev primer (0.1-1 μM)	0.1 μl	16°C		
template	2 μl			

4.1.2   Methods in cell biology

Antibody generation

Monoclonal antibodies were generated and established at the antibody facility of the Helmholtz Zentrum München. In brief, for the generation of monoclonal antibodies against human AKNA and Cas9, the following antigens were used: 50 μg purified his-tagged full-length murine AKNA protein, 40 μg of ovalbumin-coupled peptides spanning aa 428-439 (AKNA-A) and aa 983-993 (AKNA-B) of human AKNA and 60 μg purified His-tagged full-length Cas9 protein. Lou/c rats and C57BL/6 mice were immunized with antigen using standard procedures as described before (Feederle et al., 2016). Hybridoma supernatants were validated using enzyme-linked immunoassay (ELISA), western blot and immunofluorescent stainings. The hybridoma cells of AKNA- or Cas9-specific supernatants were cloned at least twice by limiting dilution. Experiments in this study were performed with hybridoma culture supernatant or purified antibodies of Akna 25F1 (mouse IgG1, IP, IF, STED and immunogold-EM), Akna 14D7 (rat IgG2a, WB and IF), AKNA-A 9G1 (rat IgG1/k, IF), AKNA-B 4F5 (rat IgG2a/k, IF), and Cas9 8G4 (rat IgG2a/l).

Fluorescence-activated cell sorting (FACS)

Cortices from E14 embryos were dissected removing the ganglionic eminence, the olfactory bulb, the hippocampal anlage and the meninges. Cortices from each litter were pooled and cells were enzymatically dissociated using 0.05% Trypsin for 15 min at 37°C in a water-bad, re-suspended in DMEM containing 10% FCS to block Trypsin and then washed with PBS. For isolation of cortical subpopulations the samples were incubated for 30 min on ice with an APC-conjugated Prominin-1 antibody (CD133, eBioscience) or PE-conjugated PSA-NCAM antibody (Miltenyi Biotec). Gating parameters were determined by side and forward scatter to eliminate debris (P1 gate) and aggregated cells (P2 gate). PE- and APC conjugated isotype control (eBioscience, Miltenyi Biotec) stained cells were used to set the positive gates for the stained populations (both set to include maximum 0.1% of non-fluorescent cells). Positive cells were isolated using the FACSAriaIII (BD Bioscience) system at 4-way purity mode. Cells were directly sorted into RLT (QIAGEN) or Neurosphere media for in vitro experiments. The sorted cells were first examined in separate experiments through plating and immunohistochemistry (fixation 2-4 hours after plating)

which confirmed their expected radial glial (Pax6 positive) and neuronal identity (Tubb3 positive) and the purity of the sorting procedure. For cell lines expressing GFP reporters, dissociation was done with 0.05% Trypsin for 5 min at 37°C. Trypsin was blocked with growing media containing bovine serum and cells washed once with 1X PBS. Untransfected cells were used to set negative and positive gates. Sorting was done as mentioned above. DNA content analysis was done with

Primary embryonic forebrain cultures and treatments

Tissue from E14 cortices or ganglionic eminences was dissociated as described above. Dissociated cells were seeded onto poly-D-lysine-coated plastic plates or glass coverslips in DMEM:F12/ GlutaMAX with 2% B27 supplement, 10mM HEPES and Penicillin / Streptomycin (100 units/ml) for a minimum of 2 hrs. Plasmid DNA (1 μg) and siRNA (25 nM, see below) transfection was done with Lipofectamine 3000 (Life technologies) or DharmaFect1 reagent (Dharmacon), respectively, according to manufacturer's instruction. Cell cultures were fixed in 4% PFA for 15 min or ice-cold methanol at -20°C and washed with PBS. Microtubule regrowth assays were done by treating cells with 3.3 μM Nocodazole (Sigma) for 4 hours at 37°C. Nocodazole washout was carried out 3 times with warm 1X HBSS and microtubules were allowed to regrow in warm medium (DMEM-GlutaMAX with 10% FCS) at 37°C for the desired time points. Cells where then fixed with 1X PHEM fixative (3.7% PFA/Sucrose, 1x PHEM buffer, pH 6.9, 0.25% glutaraldehyde 0.25%, 0.1% Triton X-100) for 15-20 min at room temperature and washed three times with 1X PBS. Glutaraldehyde was quenched with 50mM Ammonium chloride in 1X PBS for 10 min and cells were washed again three times with 1X PBS.

Primary adult SEZ cultures and treatments

Cultures were performed with cells from 8-10 weeks old C57BL/6 wild type mice. Animals wered killed by cervical dislocation. The head of each animal was separated from the body, the brain surgically removed and put in fresh ice-cold sterile HBSS-Hepes. The SEZ was dissected as described in Fischer et al., 2011 and cut into small pieces in 5 ml ice-cold HBSS-Hepes. After SEZ pieces settled down, the supernatant was removed and 5 ml of Dissociation Media were added. The tissue was incubated for 30 min at 37°C. The enzyme activity was stopped by addition of an equal volume of ice-cold Solution 3 and filtered with

a 70 μm filter/strainer (BD Transduction Laboratory) into a 50 ml Falcon Tube. Cells were spun 5 min at 4℃ and 1300 rpm, resuspended in Solution 2 and spun again 10 min at 4℃ and 2000 rpm. The cell pellet was resuspended in 2 ml of Solution 3, placed on top of 10 ml Solution 3, and centrifuged for 7 min at 4℃ and 1500 rpm for 7 minutes. This step is necessary to separate astrocytes from neural stem and progenitor cells through their different migration in Solution 3. Astrocytes would remain in the supernatant and neural stem and progenitor cells in the pellet at the bottom of the tube. Finally, cell pellets were re-suspended in neurosphere medium and plated on PDL-coated glass coverslips in 24-well plates at a density of approximately 200 cells per mm^2. MT regrowth assay was performed as above.

Cultures and treatments of cell lines

A20 cells (kind gift of Elisabeth Kremmer, Helmholtz Zentrum München) were maintained in RPMI 1640 Medium, GlutaMAX Supplement (Life Technologies) supplemented 10% FCS, 1X NEAA (Life Technologies), 100 μM sodium pyruvate (Sigma) and + 1% Penicillin/Streptomycin (Life Technologies). To generate A20 Akna-EGFP transgenic lines, 3x10^6 cells were nucleofected with 2 μg of BAC-plasmid (Amaxa nucleofector 2b devise, program U-015, kit VPA-1001). Cells were allowed to recover for 2 days in complete medium supplemented with 25 μg/ml vitamin C (to increase viability) and then put under Geneticin G418 selection (first 100 μg/ml, Life Technologies for one week; then 500 μg/ml). After approximately two weeks, GFP signal was checked by IF. Neuro2A (N2A) and NMuMG cells (gifts of Oskar Martinez, Helmholtz Zentrum München and Vijay Tiwary, previously at IMB Mainz, respectively) were maintained in DMEM:GlutaMAX (Life Technologies) supplemented with 10% FCS, 1% NEAA and 1% Pen/Strep. Mpf ferret cells (a gift of Victor Borrell, Instituto de Neurociencias, Sant Joan d'Alacant, Spain) were maintained in BME (Thermo Fischer) supplemented with 15% Lamb Serum, 1% NEAA and 1% Pen/Strep. Transfection of N2A and NMuMG cells was done with Lipofectamine2000 according to manufacturer's instruction. To generate piggy-bac transgenic lines, cells were transfected in wells of a 6 well plate with approx. 600 ng pCMV-hyPBase and approx. 2 μg of the corresponding piggy-bac vector. Positive colonies were selected by antibiotic resistant or by FACS. . To generate Odf2 lines, NMuMG cells stably expressing Cas9 were generated with piggy-bacs encoding Cas9-2A-puro (validated by WB using home-made Cas9 monoclonal antibodies, see below). A clonal line was subsequently transfected with

plasmids expressing gRNAs targeting exons 5 and 8 of Odf2. Deletion of Odf2 was validated by IF in clonal cell lines. For all siRNA-mediated knockdown experiments, cells were seeded at the same starting density and transfected every second day with ON-TARGET plus SMART pool siRNAs (50 nM) (i.e., a mixture of 4 siRNAs provided as a single reagent) (Dharmacon). For siRNA transfections, Lipofectamine RNAiMAX (Invitrogen, 13778-150) or DharmaFect1 reagent (Dharmacon) were used according to the manufacturer's instructions. For experiments involving TGFb1-induced EMT, TGFb1 treatment (2 ng/ml, rhTGF-beta-1 240-B, R&D systems) was performed at the same time the siRNA was added.

RNA *in situ* hybridization of mouse tissue

The pSC-A_Akna plasmid was used to generate labeled RNA probes. The plasmid was linearized by cutting with BamHI or SalI (NEB) to produce sense or anti-sense RNA-probes, respectively. The digested DNA was purified through phenol-chloroform-isoamyl-alcohol (SIGMA), precipitated with 4M NH_4Ac in 100% ethanol, washed in 70% ethanol and diluted in RNase-free H_2O. Alternatively, the digested DNA was column-purified with the PCR-purification Kit (Qiagen). Digoxigenin-labeled RNA probes were produced by in vitro transcription as described below. Sense and anti-sense probes were generated with T3 and T7 RNA polymerases, respectively. The reaction time was 2 h at 37℃. RNA probes were treated with DNaseI for 30-45 mins to eliminate plasmid DNA, precipitated with 4M LiCl in 100% ethanol, washed in 70% ethanol and diluted in RNase-free H_2O.

RNase-free H2O	12.5 μl - x μl DNA
10x transcription buffer	2 μl
DNA	1 μl
RNase-inhibitor	1 μl
Dig-RNA labeling mix	2 μl
T3 or T7 RNA pol	2.5 μl
Total volume	**20 μl**

In situ hybridization was performed on 20-40 μm thick cryostat sections or 70 μm vibratome sections immediately after perfusion of brains with 4% PFA. 500 ng digoxigenin-labeled RNA was heated up to 74℃ for 4 minutes in hybridization buffer to separate RNA strands

and then applied to each brain section and hybridized overnight at 65℃. The next day, sections were incubated twice for 30 minutes at 65℃ in washing solution followed by two washing steps in 1 x MABT for 30 minutes at room temperature. The sections were incubated afterwards in blocking solution for 1 hour at room temperature and then overnight at 4℃ in antibody solution. Antibodies were coupled to alkaline phosphatase (Fab Fragments, Roche, 1:2000). The next day, sections were washed 4 times in 1 x MABT buffer and twice in freshly prepared AP staining buffer. NBT and BCIP (Roche) (3.5 μl per ml AP staining buffer) were added to the AP buffer and put onto the sections until the desired staining intensity was reached. Reaction was stopped by washing the section in distilled water or PBS. Sections were processed for immunohistochemistry or mounted. Images were taken with a Leica Stereo Microscope and processed with Adobe Photoshop.

4.1.3 In vivo experimental methods

Generation of Akna KO mice

This mouse line was generated at the institute of developmental biology, Helmholtz Zentrum München.

The Akna KO3 mouse line was generated using CRISPR/Cas9-based gene editing by microinjection into one cell embryos. For this, two gene specific guide RNAs (see list below) flanking exon 3 (i.e. one sgRNA targeting intron 2 and another sgRNA targeting intron 3) were generated by cloning sequence specific, 20 nt long double stranded oligonucleotides into pX330 vector before the chimeric guide RNA scaffold. The sequence of the T7 promoter was also included before (i.e. 5-prime) of the genomic target sequence. The T7-sgRNA sequences were PCR amplified, column-purified and the product used as template for T7-RNA polymerase based in vitro transcription according to manufacturer instructions (MEGAshortscript Kit, AMBION). The RNA was then column purified and eluted in microinjection buffer (10 mM Tris, 0.1 mM EDTA, pH 7.2). sgRNAs were tested by T7-endonuclease assay according to manufacturer instruction (New England Biolabs). For that, N2A cells stably expressing Cas9 (kind gift of Oskar Martinez, Helmholtz Zentrum München) where transfected with 1 μg sgRNAs per well of a 48 well plate, according to manufacturer recommendations (Lipofectamine MessengerMAX Transfection Reagent). Two days later cells were processed for T7-endonuclease assay. Cas9 mRNA was made by

T7-RNA polymerase based in vitro transcription according to manufacturer instructions (mMESSAGE mMACHINE T7 Transcription Kit, AMBION) using a plasmid encoding HA-tagged NLS-containing human codon-optimized Cas9. The RNA was column purified and eluted in microinjection buffer (10 mM Tris, 0.1 mM EDTA, pH 7.2).

Prior to pronuclear injection, the duplex is diluted in microinjection buffer together with Cas9 mRNA to a working concentration of each of 50 ng/μl (sgRNA) and 50 ng/μl (Cas9 mRNA). One-cell embryos were obtained by mating of C57BL/6N males (Charles River, Sulzbach, Germany) with C57BL/6N females superovulated with 7.5 units PMSG (Pregnant Mare's Serum Gonadotropin) and 7.5 units HCG (Human Chorionic Gonadotropin). One-cell embryos were mirco-injected into the larger pronucleus. Subsequently, zygotes were transferred into pseudo-pregnant CD1 female mice to obtain live pups. All mice showed normal development and appeared healthy. Handling of the animals is performed in accordance to institutional guidelines and approved by the animal welfare committee of the government of upper Bavaria. The mice are housed in standard cages in a specific pathogen-free facility on a 12 h light/dark cycle with ad libitum access to food and water. Analysis of gene editing events has been performed on genomic DNA isolated from ear biopsies of founder mice and biopsies of the F1 progeny, using the conventional lysis buffer and PCR.

In utero electroporation

Animals were operated as approved by the Government of Upper Bavaria. Electroporations were carried out by Sven Falk, Pia Johansson and Elise Peyre as described in Falk et al., 2017 and Nguyen et al., 2006.

Time-lapse imaging

Time-lapse imaging was carried out by Sven Falk. The cerebral cortex of E13 embryos was in utero electroporated with pCAG-LoxP-mKO2-f, pCAG-Cre (Shitamukai et al., 2011) and the respective Akna constructs. Slices were prepared and imaged as described previously (Pilz et al., 2013; Shitamukai et al., 2011). Briefly, slices were cut at 300 μm thickness on a vibratome (Leica VT 1200S) in ice-cold DMEM/F12 GlutaMax (Invitrogen) oxygenated with 95% O2, embedded in cell matrix type I-A (Nitta Gelatin) on a

nylon filter (Millicell) and then cultured in DMEM/F12 GlutaMax (Invitrogen), 5% FCS (Gibco), 5% Horse Serum (Gibco), N2 supplement (Invitrogen), B27 supplement (Invitrogen) and PenStrep (Invitrogen). The slices were kept in an atmosphere with 40% O2, 5% CO2 at 37°C and pictures were taken every 20 min.

EB3-GFP comets analysis

In vivo time-lapse imaging was carried out by Elise Peyre. Brains were electroporated at E14 and harvested at E15 (1 day after IUE), embedded in agarose 4% - HBSS solution, sections of 300 μm were cut at the vibratome and mounded on Matrigel (Corning) coated MatTek dishes. Sections were then covered with Matrigel matrix (one half diluted), left 20min at 37°C and supplemented Neurobasal culture medium was then added. Time-lapse imaging was done on a Zeiss Super Resolution LSM880 AiryScan Elyra S1 (63X magnification). Image of a single plane at the level of the ventricular wall was acquired every 2s for 5min. Speed of comets was measured in ImageJ using the MTrack plugin and angles between the mean orientation of comet tracks and the apical surface were measured. For each analysis, at least 2 electroporation experiments were done by condition.

Morphology analysis of Dcx expressing cells

Morphology analsysis was carried out by Elise Peyre. Brain were electroporated at E14 and harvested at E16 (2 days after IUE), embedded in agarose 4% - HBSS solution, sections of 300 μm were cut at the vibratome and mounted on Millicell culture inserts and cultured with Neurobasal culture medium (supplemented with 1% B27 and 5% Fetal calf serum). Inserts were transferred after 6h in MatTek glass bottom dishes and time-lapse imaging was done on a Nikon A1 confocal microscope (20X magnification), image acquisition was done every 15 min during 10 hours.

4.1.4   Light and electron microscopy assays

Tissue processing

Mouse embryos or brains were fixed for 1-8 hrs (E9 and E14: 1-2 h; E16: 4 h; E18: 1 h or 6 h) in 4% Paraformaldehyde (PFA, in phosphate buffered saline, PBS) at 4°C. Brains were then cryoprotected in 30% sucrose (in PBS) overnight, embedded in tissue-tek, stored at –20°C and then sectioned in a Leica cryostat.

Immunofluorescence microscopy

Tissue sections (12-50 μm) or cells plated on poly-D-lysine coated glass coverslips were treated with 10% Normal goat serum or 1% BSA, 0.5% Triton-X (in PBS) for 30 min prior to staining. Primary antibodies were applied in blocking solution overnight at 4°C. Fluorescent secondary antibodies were applied in blocking solution for 1-2 hours at room temperature. DAPI was used to visualize nuclei. Sections were mounted in Aqua Poly-mount (Polysciences). TUNEL assay was performed as from manufacturer's instructions using ApopTag Red In Situ Apoptosis Detection Kit from Millipore. Images were taken using an Olympus FV1000 confocal laser-scanning microscope using 20X/ 0.85 N.A. and 63x/ 1.35 N.A. water or oil-immersion objective. Confocal micrographs were acquired with a step size of 250 nm to 1 μm. High-resolution light microscopy was performed on DeltaVision Core system (Applied Precision) using 100x/ 1.40 N.A. oil-immersion objective. Optical z-sections were acquired in 200 nm steps. Z-stacks were deconvolved by a built-in deconvolution program (Softworx) using "Conservative" parameters. Deconvolved z-stacks were corrected for a chromatic shift and used for Maximum Intensity Projection visualization (Fiji/ImageJ). STED images were taken with a Leica SP8X STED 3D DLS using a 100x/1.40 OIL STED White objective and images where deconvolved with Huygens Software. See Supplementary Table 1 for the list of primary and secondary antibodies.

Quantitative analysis of in utero electroporated cells

Single optical sections (confocal microscopy) of each brain slice were analyzed in an approximately 200 μm thick radial stripe. Using Fiji each stripe was divided in five equally sized bins, adjusted to the radial thickness of the cerebral cortex. Quantifications are given

as mean ±SEM. Different sections representing the full rostro-caudal distribution of the electroporated area were used for quantifications of each condition. For each condition (overexpression, rescues, knock-downs and corresponding controls) more than 4000 cells were quantified from 5-8 different embryos (from 2-4 different litters). These analyses were largely conducted by Sven Falk and Pia Johansson.

Immuno-electron microscopy and correlative light and electron microscopic investigation

These experiments were done by Michaela Wilsch-Bräuninger as described in Wilsch-Bräuninger et al., 2012; Paridaen et al., 2013; and Paridaen et al., 2015.

Statistical analyses

Per experimental conditions, quantifications of mouse brain sections were performed with at least four brains from 2-4 different litters and at least 2 coronal sections were used per brain (see above). Quantification of organoid-sections were done with more than 30 germinal zones from 3 independent experiments. Quantifications of primary cortical cells were done with brains from 4 different litters per experimental conditions. Quantification of cells in live imaging experiments are derived from 3 different experiments per experimental condition, using at least 3 embryonic brains. Data were statistically analyzed with Graph-Pad Prism or R software using Mann Whitney U test or Student's t-Test, as indicated throughout the manuscript.

4.2 Materials and reagents

4.2.1 Animals and mouse lines

C57BL/6J wild-type mice were bred in the animal facility of the Helmholtz Center Munich and the Biomedical Center Munich. The day of the vaginal plug was considered embryonic day (E) 0. All animal experiments were approved by the government of Upper Bavaria. Sas4fl/fl p53fl/fl conditional knockout mice (Insolera et al., 2014) were maintained in the animal facility of Memorial Sloan Kettering Cancer Center (MSKCC) and bred with Emx1-Cre (stock 005628; The Jackson Laboratory) to delete these genes in the cortex. All experimental procedures were performed in accordance with the regulations of the Helmholtz Center Munich and MSKCC IACUC.

4.2.2 Buffers and Solutions

10X electroforesis buffer - WB (1l):

Glycin	144.2 g
Tris (base)	30.2 g
SDS	10 g
H_2O_{dest}	to 1 ml

10X transfer buffer - WB (1l):

Glycin	144.2 g
Tris (base)	30.2 g
SDS	2 g
H_2O_{dest}	to 1 ml

AP staining buffer (50 ml):

50% Formamide (Roth)	25 ml
20x SSC (pH 4.5)	12.5 ml
Blocking reagent (Roche)	1 g
10% SDS	10 ml
tRNAs	250 μl
Heparin	50 μl
H_2O_{dest}	2.2 ml

Blocking solution - ISH (10 ml):

MABT 5x	2 ml
Bovine Serum	2 ml
10% Blocking reagent	2 ml
H_2O_{dest}	4 ml

Dissociation Media (10 ml):

Solution1	10 ml
Trypsin (Sigma)	13.3 mg
Hyaluronidase (Sigma)	7 mg

Hybridization buffer (50 ml):

1 M Tris (pH 9.5)	5 ml
10% Tween 20 (Roth)	0.5 ml
5 M NaCl (Roth)	1 ml
1 M $MgCl_2$ (Roth)	2.5 ml
H_2O_{dest}	41 ml

MABT 5x (2 l):

Maleic acid (500 mM)	116.08 ml
NaCl (750 mM)	87.7 g
10% Tween 20	20 ml
H_2O_{dest}	1980 ml

Adjust pH to 7.5

Neurosphere Medium (50 ml):

Penicillin/Streptomycin	500 μl
HEPES (1M, Gibco)	400 μl ml
B27 (Gibco)	1 ml
DMEM:F12/Glutamax (Gibco)	to 50 ml

4% Paraformaldehyd solution (1 l):

PFA	40 g
1x PBS	1 l

Adjust pH to 7.5

Phosphate Buffered Saline (PBS):

NaCl	137 mM
KCl	2.7 mM
Na_2HPO_4	80.9 mM
KH_2PO_4	1.5 mM

in H_2O_{dest}

Adjust pH to 7.5

RIPA buffer:

Tris-HCl (pH 7.4)	20 mM
NaCl	137 mM
Glycerol	10% (v/v)
SDS	0.1% (w/v)
Deoxycholate	0.5% (w/v)
Triton X-100	1% /(v/v)
EDTA	2 mM

in H_2O_{dest}

Solution1 (500 ml):

HBSS (Life Tech, 10x)	50 ml
D-Glucose (45%, Sigma)	9 g
HEPES (1M, Gibco)	7.5 g
H_2O_{dest}	433.5 ml

Solution2 (500 ml):

HBSS (Life Tech, 10x)	25 ml
Succrose (Sigma)	154 g
H_2O_{dest}	475 ml

Solution3 (500 ml):

BSA (Sigma)	20 g
HEPES (Life Tech, 1 M)	10 ml
EBSS (Life Tech, 1x)	490 ml

Washing solution (50 ml):

20x SSC (pH 4.5)	2.5 ml
10% Tween (Roth)	0.5 ml
Formamide (Roth)	25 ml
H_2O_{dest}	22 ml

4.2.3   Antibodies

Commercial primary antibodies: Akna (DSHB 1C7, mouse), Arl13b (ProteinTech 17711-1AP, rabbit), Actb (C4) (Santa Cruz sc-47778, mouse), CAMSAP2 (ProteinTech 17880-1-AP, rabbit), Cux1/CDP (M-222) (Santa Cruz sc-13024, rabbit), CyclinD1 (Fischer Scientific RM9104R7, rabbit), Dynein IC (Millipore, MAB1618), Dctn1 (H-300) (Santa Cruz sc-11363, rabbit), Dctn1/p150Glued (BD Transduction Laboratories 612709, mouse), Dctn2 (H-300) (Santa Cruz sc-135135, rabbit), Dctn4 (Abcam ab170107, rabbit), Dcx (Millipore AB2253, guinea pig), EB1 (H-70) (Santa Cruz sc-8356, rabbit), E-Cadherin (BD Bioscience 610181, mouse), E-Cadherin (DECMA-1) (Abcam ab11512, rat), FLAG â€“ M2 (Sigma F1804, mouse), Gapdh (Millipore MAB374, mouse), Gapdh (Santa Cruz sc-47724, mouse), GCP2 (Novus NBP2-21793, mouse), GCP2 (F-3) (Santa Cruz sc-377117, rabbit), GCP4 (D-5) (Santa Cruz sc-271876, rabbit), GFP (Aves Lab GFP-1020, chicken), GT335 (AdipoGen AG20B-0020, mouse), HA (Roche 3F10, mouse), Histone H3 (Abcam ab1791, rabbit), Ki67 (Leica/Novocastra NCL-Ki67p, rabbit), Ki67 (Abcam ab92742, rabbit), Ki67 (ThermoFischer 14-5698-82, rat), Lamin B (C-20) (Santa Cruz sc-6216, goat), NEDD1 (Santa Cruz, sc-100961), Nestin (Millipore MAB353, mouse), NeuN (Millipore MAB377, mouse), Odf2 (Abcam ab43840, rabbit), Odf2 (G-2) (Santa Cruz sc-393881, mouse), Ctnnd1/p120 (Abcam ab92514, rabbit), p-120 (Abcam ab81318, rabbit), Pax6 (Millipore AB2237, rabbit), Pax6 (DSHB AB 528427, mouse), Paxillin (BD Transduction Laboratories 610052, mouse), PCNA (DAKO M0879, mouse), Pcnt (Covance PRB-432C, rabbit), Phalloidin-Atto 647N (Sigma, 65906), p-Histone H3 (Ser10) (Millipore 06-570, rabbit), RFP (Rockland 600401379, rabbit), SOX4 (DSHB 3F12, mouse), Tbr1 (Abcam ab31940, rabbit), Tbr2 (Millipore AB15894, chicken), Tbr2 (Abcam ab23345, rabbit), Tbr2 (Abcam ab183991, rabbit), Tuba (Sigma T5168, mouse), Tubb3 (Sigma T8660, mouse), Tubg (Sigma T6557, mouse), Tubg (Sigma T5192, rabbit), Tubg (ProteinTech 15176-1-AP, rabbit), Tubulin acetylated (Sigma T7451, mouse), Tubulin tyrosinated (Sigma MAB1864-I, rat), Tubulin detyrosinated (Sigma AB3201, rabbit), ZO-1 (Invitrogen 617300, rabbit), ZO-1 (ThermoFischer 33-9100, mouse). For flow cytometry PSA-NCAM PE-coupled (Miltenyi 130093274, mouse) and CD133 APC-coupled (eBioscience 17-1331, rat) were used.

Commercial secondary antibodies: mouse IgG HRP (Ge Healthcare Life Sciences NA931-1ML, sheep), rat IgG HRP (Ge Healthcare Life Sciences NA935, goat), rabbit IgG HRP (Ge Healthcare Life Sciences NA934-1ML, donkey), mouse IgG HRP (Rockland 18-8817-30,

rat), rabbit IgG HRP (Rockland 18-8816-31, mouse), goat IgG HRP (Chemicon AP106p, rabbit), chicken A488 (ThermoFischer A11039, goat), chicken A546 (ThermoFischer A11040, goat), rat A488 (ThermoFischer A11006, goat), rat A546 (ThermoFischer A11081, goat), rat A647 (ThermoFischer A21247, goat), rabbit A488 (ThermoFischer A11008, goat), rabbit A546 (ThermoFischer A11010, goat), rabbit A568 (ThermoFischer A11011, goat), rabbit A633 (ThermoFischer A21070, goat), rabbit A647 (ThermoFischer A21244, goat), guinea pig A488 (ThermoFischer A11073, goat), guinea pig A546 (ThermoFischer A11074, goat), mouse IgG A488 (ThermoFischer A11029, goat), mouse IgG1 A488 (ThermoFischer A21121, goat), mouse IgG1 A546 (ThermoFischer A21123, goat), mouse IgG1 (A647 ThermoFischer A21240, goat), mouse IgG2a A488 (ThermoFischer A21131, goat), mouse IgG2a A546 (ThermoFischer A21133, goat), mouse IgG2b A488 (ThermoFischer A21141, goat), mouse IgG2b A546 (ThermoFischer A21143, goat), rabbit AS635P (Abberior 2-0012-007-2, goat), mouse IgG AS580 (Abberior 2-0002-005-1, goat). *A = Alexa Fluor; ** AS = Abberior Star

Isotypes: IgG1 isotype (Biolegend 401402, mouse), normal IgG (Santa Cruz sc-2027, rabbit), IgM isotype PE (Miltenyi 130093177, mouse), IgG1 isotype APC (eBioscience 17-4301, rat)

Home-made antibodies: Akna (25F1, mouse IgG1), Akna (14D7, rat IgG2a), AKNA-A (9G1, rat IgG1), AKNA-B (4F5, rat IgG2a), Camsap3 (kind gift of Masatoshi Takeichi, Meng et al., 2008, rabbit), Cas9 (8G1-1-1, rat IgG2a), Sox4 (kind gift of Elisabeth Sock, Hoser et al., 2008, guinea pig)

4.2.4   Oligonucleotides

RNAi

Akna shRNA 1: ATGTGCTTCTGCAGCTAATAA
Akna shRNA 2: ACAAGGAAGCAAGGTCTTATCCT
Akna miRNA1: TTCACACTCAAGCTCCGTACA
Akna miRNA2: AGCAAGAGAAGATTCCTTGGC

Akna miRNA3: TTGACTGGGAAACAACAGCGG

Akna miRNA4: CTAAGTGGATGCCAAAGACAT

Odf2 gRNA1: GGTCGGTTGTCTCAAATCTG

Odf2gRNA2: GCACCCTCCGAGATCTGTTGA

hsaAKNA miR1 (611): TTCCATGGCCTTCCAAGCTGA

hsaAKNA miR2 (1456): TTGCTCAGGCGTCTGAAATTC

p53 miR: AACAGATCGTCCATGCAGTGA

p53 miR: AAACACGAACCTCAAAGCTGT

mpfAKNA gRNA1: CTCCACCTCAGGACCTCCAA

mpfAKNA gRNA1: CCACAGCATCCACACAGGGA

mpfAKNA gRNA1: CAGCAGCTTGTCAGATCCCA

mpfAKNA gRNA1: CTTAGCCCTGCGAGCAGTGA

ON-TARGETplus Mouse Akna (100182) siRNA - SMARTpool (L-167159-00-0005)

CAGAAAUGGAGGUGACGUU

UGAGAACACUAUCGACCAA

CAGCUGAGAUUGUUCGGGA

GACCGAAGCUGACGAUGCA

ON-TARGETplus Non-targeting Pool (D-001810-10-05)

UGGUUUACAUGUCGACUAA

UGGUUUACAUGUUGUGUGA

UGGUUUACAUGUUUUCUGA

UGGUUUACAUGUUUUCCUA

ON-TARGETplus Human AKNA (80709) siRNA - SMARTpool (L-021423-00-0005)

CAGCACAGCAGGAACAUUA

AGACAAAGACGUCACCUAA

GAGAUAUACCGUCUGGGAA

GCAUCAGGAUUCCGAGUCA

RT-qPCR primers

mmuAkna-FP1 CCTTCAACTGGAGGACAGC
mmuAkna-RP1 AGCCTCTCTGTGGATTTACTGC
mmuAkna-FP2 ACCCCTCATCTTCAAGTCGC
mmuAkna-RP2 TAGCTCAGTGGCTTGTTCGG
mmuGapdh-FP1 ATTCAACGGCACAGTCAAGG
mmuGapdh-RP1 TGGATGCAGGGATGATGTTC
mmuGapdh-FP2 GTGTTCCTACCCCCAATGTGT
mmuGapdh-RP2 ATTGTCATACCAGGAAATGAGCTT
mmuSox4-FP CCTCGCTCTCCTCGTCCT
mmuSox4-RP TCGTCTTCGAACTCGTCGT
mpfAKNA-FP TGGAACAAAGACCTCATGGG
mpfAKNA-RP CATCTTCAGGAGACAGAGCTG
mpfACTB-FP TGACCGGATGCAGAAGGA
mpfACTB-RP CCGATCCACACCGAGTACT
miR-129-3p 5'AAGCCCUUACCCCAAAAAGUAU (QIAGEN, MS00024108)
miR-129-5p 5'CUUUUUGCGGUCUGGGCUUGC (QIAGEN,MS00006020)
Hs-RNU6-2-11 QIAGEN, MS00033740

Akna KO animal

Intron2 sgRNA no1 TAATACGACTCACTATAGGGGTTTGGAGGACCTTTGATAG
Intron3 sgRNA no2 TAATACGACTCACTATAGGGCAACAAGTGTCTAGGTAACA
Seq primer U6 GAGGGCCTATTTCCCATGATTC
IVT primerT7 for GTACAAAATACGTGACGTAGAAAG
IVT primer TRAC rev AAAAAAAGCACCGACTCGGTG
T7 Intron2 for GGGATTGGGGATGTTGGAGC
Intron3 rev2 GCCCACTAGACTGTTCTCCTTAC

4.2.5 Kits

Name	Company
Apoptag Red In Situ Apoptosis detection kit	Millipore
EndoFree Plasmid Maxi Kit	Qiagen
Gateway LR Clonase Enzyme	Life Technologies
GeneJET Gel Extraction Kit	Fischer Scientific
GeneJET PCR Purification Kit	Fischer Scientific
GeneJET Plasmid Miniprep Kit	Fischer Scientific
LongRange PCR Kit	Qiagen
MEGAclear Transcription Clean-Up Kit	Ambion
MEGAshortscript T7 Transcription Kit	Ambion
mMESSAGE mMACHINE T7 ULTRA Transcription Kit	Ambion
PureLink HiPure Plasmid Maxiprep Kit	Life Technologies
Phusion High-Fidelity DNA Polymerase	New England Biolabs
RNeasy Mini Kit	Qiagen
RNeasy Micro Kit	Qiagen
StrataClone PCR Cloning Kit	Agilent
StrataClone Blunt PCR Cloning Kit	Agilent
T4 DNA Ligase	Thermo Fischer Scientific
T4 DNA Polymerase	New England Biolabs
T7 Endonuclease I	New England Biolabs
Taq DNA Polymerase kit	Qiagen

4.2.6 Chemicals

Name	Company
Acetic Acid	Merck
Actinomycin D	Sigma
Acrylamide/Bis solution	Sigma
Agarose	Biozym
Ammonium persulfate (APS)	Thermo Fisher Scientific
Ampicillin	Roth
Aqua Poly / Mount	Polyscience Inc.
Corn oil	Sigma
Chloramphenicol	Sigma
Chloroform	Sigma
Cytochalasin D	Sigma
DAPI (4,6-dasmindino-2-phenylindol)	AppliChem
Difco LB-Agar	Hartenstein Labor.
DNA Ladder (Generuler 1kb/100bp)	Fermentas
DPBS	GIBCO
EDTA	Merck, Roth
Ethanol	Merck
Fast Green	Sigma
G418/Geneticin	GIBCO
Glycerol	Sigma
Glycine	Sigma
HEPES	Roth, GIBCO
Hydrochloric acid	Merck
IGEPAL NP40	Sigma
Isopropanol	Merck
Methanol	Merck
Nocodazole	Sigma
Normal goat serum (NGS)	Vector Lab.
Orange G	Sigma
Paraformaldehyde (PFA)	Merck
PCR buffer (10X Taq Buffer)	Qiagen

PCR dNTP Mix (25mM each)	Fermentas
PCR reagent: MgCl2 (25mM)	Qiagen
Potassium chloride	Sigma
Potassium phosphate monobasic	Sigma
Potassium perruthanate	Sigma
Phenol:Chloroform:Isoamyl alcohol	Thermo Fisher Scientific
Pierce ECL western blotting substrate	Thermo Fisher Scientific
PMSF	Thermo Fisher Scientific
COmplete, Protease inhibitor cocktail	Roche
Proteinase K	Roth
Puromycin	Thermo Fisher Scientific
Q solution	Qiagen
QIAzol	Invitrogen
RNase-free DNase	Qiagen
Sodium acetate	Sigma
Sodium chloride	Fisher Bioreagents
Sodium citrate	Merck
Sodium dodecyl sulphate (SDS)	Roth
Sodium phosphate monobasic	Sigma
Sodium phosphate dibasic	Sigma
Sodium hydroxide	Roth
Spectinomycin	Sigma
SYBR green	Qiagen
SYBR safe DNA gel stain	Thermo Fisher Scientific
Tamoxifen	Sigma
Taq DNA Polymerase	Qiagen
TEMED	Sigma
Tissue Tek	Hartenstein Labor.
Tris Base	Sigma
Tris-HCl	Sigma
Trizma acetate	Sigma
Triton-X-100	Roth
Tween-20	Sigma

Chapter 5

References

Adlakha, Y.K., and Saini, N. (2014). Brain microRNAs and insights into biological functions and therapeutic potential of brain enriched miRNA-128. Molecular cancer 13, 33.

Aillaud, C., Bosc, C., Peris, L., Bosson, A., Heemeryck, P., Van Dijk, J., Le Friec, J., Boulan, B., Vossier, F., Sanman, L.E., et al. (2017). Vasohibins/SVBP are tubulin carboxypeptidases (TCPs) that regulate neuron differentiation. Science 358, 1448-1453.

Akhmanova, A., and Hoogenraad, C.C. (2015). Microtubule minus-end-targeting proteins. Current biology : CB 25, R162-171.

Altman, J. (2011). The Discovery of Adult Mammalian Neurogenesis. In Neurogenesis in the Adult Brain I: Neurobiology, T. Seki, K. Sawamoto, J.M. Parent, and A. Alvarez-Buylla, eds. (Tokyo: Springer Japan), pp. 3-46.

Anthony, T.E., Mason, H.A., Gridley, T., Fishell, G., and Heintz, N. (2005). Brain lipid-binding protein is a direct target of Notch signaling in radial glial cells. Genes & development 19, 1028-1033.

Aprea, J., and Calegari, F. (2015). Long non-coding RNAs in corticogenesis: deciphering the non-coding code of the brain. The EMBO journal 34, 2865-2884.

102

Aprea, J., Prenninger, S., Dori, M., Ghosh, T., Monasor, L.S., Wessendorf, E., Zocher, S., Massalini, S., Alexopoulou, D., Lesche, M., et al. (2013). Transcriptome sequencing during mouse brain development identifies long non-coding RNAs functionally involved in neurogenic commitment. The EMBO journal 32, 3145-3160.

Arnold, S.J., Huang, G.J., Cheung, A.F., Era, T., Nishikawa, S., Bikoff, E.K., Molnar, Z., Robertson, E.J., and Groszer, M. (2008). The T-box transcription factor Eomes/Tbr2 regulates neurogenesis in the cortical subventricular zone. Genes & development 22, 2479-2484.

Asami, M., Pilz, G.A., Ninkovic, J., Godinho, L., Schroeder, T., Huttner, W.B., and Gotz, M. (2011). The role of Pax6 in regulating the orientation and mode of cell division of progenitors in the mouse cerebral cortex. Development 138, 5067-5078.

Askham, J.M., Vaughan, K.T., Goodson, H.V., and Morrison, E.E. (2002). Evidence that an interaction between EB1 and p150(Glued) is required for the formation and maintenance of a radial microtubule array anchored at the centrosome. Molecular biology of the cell 13, 3627-3645.

Barkovich, A.J., Guerrini, R., Kuzniecky, R.I., Jackson, G.D., and Dobyns, W.B. (2012). A developmental and genetic classification for malformations of cortical development: update 2012. Brain : a journal of neurology 135, 1348-1369.

Bazzi, H., and Anderson, K.V. (2014). Acentriolar mitosis activates a p53-dependent apoptosis pathway in the mouse embryo. Proceedings of the National Academy of Sciences of the United States of America 111, E1491-1500.

Beckervordersandforth, R., Tripathi, P., Ninkovic, J., Bayam, E., Lepier, A., Stempfhuber, B., Kirchhoff, F., Hirrlinger, J., Haslinger, A., Lie, D.C., et al. (2010). In vivo fate mapping and expression analysis reveals molecular hallmarks of prospectively isolated adult

neural stem cells. Cell stem cell 7, 744-758.

Berg, D.A., Bond, A.M., Ming, G.L., and Song, H. (2018). Radial glial cells in the adult dentate gyrus: what are they and where do they come from? F1000Research 7, 277.

Berghoff, E.G., Clark, M.F., Chen, S., Cajigas, I., Leib, D.E., and Kohtz, J.D. (2013). Evf2 (Dlx6as) lncRNA regulates ultraconserved enhancer methylation and the differential transcriptional control of adjacent genes. Development 140, 4407-4416.

Betizeau, M., Cortay, V., Patti, D., Pfister, S., Gautier, E., Bellemin-Menard, A., Afanassieff, M., Huissoud, C., Douglas, R.J., Kennedy, H., et al. (2013). Precursor diversity and complexity of lineage relationships in the outer subventricular zone of the primate. Neuron 80, 442-457.

Bijnsdorp, I.V., Hodzic, J., Lagerweij, T., Westerman, B., Krijgsman, O., Broeke, J., Verweij, F., Nilsson, R.J., Rozendaal, L., van Beusechem, V.W., et al. (2016). miR-129-3p controls centrosome number in metastatic prostate cancer cells by repressing CP110. Oncotarget 7, 16676-16687.

Boldrini, M., Fulmore, C.A., Tartt, A.N., Simeon, L.R., Pavlova, I., Poposka, V., Rosoklija, G.B., Stankov, A., Arango, V., Dwork, A.J., et al. (2018). Human Hippocampal Neurogenesis Persists throughout Aging. Cell stem cell 22, 589-599 e585.

Bornens, M. (2002). Centrosome composition and microtubule anchoring mechanisms. Current opinion in cell biology 14, 25-34.

Bornens, M. (2012). The centrosome in cells and organisms. Science 335, 422-426.

Borrego-Pinto, J., Somogyi, K., Karreman, M.A., Konig, J., Muller-Reichert, T., Bettencourt-Dias, M., Gonczy, P., Schwab, Y., and Lenart, P. (2016). Distinct mechanisms eliminate mother and daughter centrioles in meiosis of starfish oocytes. The Journal of cell biology

104

212, 815-827.

Brill, M.S., Ninkovic, J., Winpenny, E., Hodge, R.D., Ozen, I., Yang, R., Lepier, A., Gascon, S., Erdelyi, F., Szabo, G., et al. (2009). Adult generation of glutamatergic olfactory bulb interneurons. Nature neuroscience 12, 1524-1533.

Brill, M.S., Snapyan, M., Wohlfrom, H., Ninkovic, J., Jawerka, M., Mastick, G.S., Ashery-Padan, R., Saghatelyan, A., Berninger, B., and Gotz, M. (2008). A dlx2- and pax6-dependent transcriptional code for periglomerular neuron specification in the adult olfactory bulb. The Journal of neuroscience : the official journal of the Society for Neuroscience 28, 6439-6452.

Britz, O., Mattar, P., Nguyen, L., Langevin, L.M., Zimmer, C., Alam, S., Guillemot, F., and Schuurmans, C. (2006). A role for proneural genes in the maturation of cortical progenitor cells. Cerebral cortex 16 Suppl 1, i138-151.

Burkhardt, J.K., Echeverri, C.J., Nilsson, T., and Vallee, R.B. (1997). Overexpression of the dynamitin (p50) subunit of the dynactin complex disrupts dynein-dependent maintenance of membrane organelle distribution. The Journal of cell biology 139, 469-484.

Burute, M., Prioux, M., Blin, G., Truchet, S., Letort, G., Tseng, Q., Bessy, T., Lowell, S., Young, J., Filhol, O., et al. (2017). Polarity Reversal by Centrosome Repositioning Primes Cell Scattering during Epithelial-to-Mesenchymal Transition. Developmental cell 40, 168-184.

Bury, L., Coelho, P.A., Simeone, A., Ferries, S., Eyers, C.E., Eyers, P.A., Zernicka-Goetz, M., and Glover, D.M. (2017). Plk4 and Aurora A cooperate in the initiation of acentriolar spindle assembly in mammalian oocytes. The Journal of cell biology 216, 3571-3590.

Cajigas, I., Leib, D.E., Cochrane, J., Luo, H., Swyter, K.R., Chen, S., Clark, B.S., Thompson, J., Yates, J.R., 3rd, Kingston, R.E., et al. (2015). Evf2 lncRNA/BRG1/DLX1 in-

teractions reveal RNA-dependent inhibition of chromatin remodeling. Development 142, 2641-2652.

Calzolari, F., Michel, J., Baumgart, E.V., Theis, F., Gotz, M., and Ninkovic, J. (2015). Fast clonal expansion and limited neural stem cell self-renewal in the adult subependymal zone. Nature neuroscience 18, 490-492.

Camp, J.G., Badsha, F., Florio, M., Kanton, S., Gerber, T., Wilsch-Brauninger, M., Lewitus, E., Sykes, A., Hevers, W., Lancaster, M., et al. (2015). Human cerebral organoids recapitulate gene expression programs of fetal neocortex development. Proceedings of the National Academy of Sciences of the United States of America 112, 15672-15677.

Cao, J., Shen, Y., Zhu, L., Xu, Y., Zhou, Y., Wu, Z., Li, Y., Yan, X., and Zhu, X. (2012). miR-129-3p controls cilia assembly by regulating CP110 and actin dynamics. Nature cell biology 14, 697-706.

Cappello, S., Attardo, A., Wu, X., Iwasato, T., Itohara, S., Wilsch-Brauninger, M., Eilken, H.M., Rieger, M.A., Schroeder, T.T., Huttner, W.B., et al. (2006). The Rho-GTPase cdc42 regulates neural progenitor fate at the apical surface. Nature neuroscience 9, 1099-1107.

Cappello, S., Bohringer, C.R., Bergami, M., Conzelmann, K.K., Ghanem, A., Tomassy, G.S., Arlotta, P., Mainardi, M., Allegra, M., Caleo, M., et al. (2012). A radial glia-specific role of RhoA in double cortex formation. Neuron 73, 911-924.

Cappello, S., Gray, M.J., Badouel, C., Lange, S., Einsiedler, M., Srour, M., Chitayat, D., Hamdan, F.F., Jenkins, Z.A., Morgan, T., et al. (2013). Mutations in genes encoding the cadherin receptor-ligand pair DCHS1 and FAT4 disrupt cerebral cortical development. Nature genetics 45, 1300-1308.

Carvalho-Santos, Z., Azimzadeh, J., Pereira-Leal, J.B., and Bettencourt-Dias, M. (2011). Evolution: Tracing the origins of centrioles, cilia, and flagella. The Journal of cell biology

106

194, 165-175.

Casenghi, M., Meraldi, P., Weinhart, U., Duncan, P.I., KöÃ¶rner, R., and Nigg, E.A. (2003). Polo-like Kinase 1 Regulates Nlp, a Centrosome Protein Involved in Microtubule Nucleation. Developmental cell 5, 113-125.

Cech, T.R., and Steitz, J.A. (2014). The noncoding RNA revolution-trashing old rules to forge new ones. Cell 157, 77-94.

Chen, C., Lee, G.A., Pourmorady, A., Sock, E., and Donoghue, M.J. (2015). Orchestration of Neuronal Differentiation and Progenitor Pool Expansion in the Developing Cortex by SoxC Genes. The Journal of neuroscience : the official journal of the Society for Neuroscience 35, 10629-10642.

Chen, T., Wu, Q., Zhang, Y., Lu, T., Yue, W., and Zhang, D. (2016). Tcf4 Controls Neuronal Migration of the Cerebral Cortex through Regulation of Bmp7. Frontiers in molecular neuroscience 9, 94.

Chen, X., Ruan, A., Wang, X., Han, W., Wang, R., Lou, N., Ruan, H., Qiu, B., Yang, H., and Zhang, X. (2014). miR-129-3p, as a diagnostic and prognostic biomarker for renal cell carcinoma, attenuates cell migration and invasion via downregulating multiple metastasis-related genes. Journal of cancer research and clinical oncology 140, 1295-1304.

Cheng, L.C., Pastrana, E., Tavazoie, M., and Doetsch, F. (2009). miR-124 regulates adult neurogenesis in the subventricular zone stem cell niche. Nature neuroscience 12, 399-408.

Chenn, A., and McConnell, S.K. (1995). Cleavage orientation and the asymmetric inheritance of Notch1 immunoreactivity in mammalian neurogenesis. Cell 82, 631-641.

Codega, P., Silva-Vargas, V., Paul, A., Maldonado-Soto, A.R., Deleo, A.M., Pastrana, E., and Doetsch, F. (2014). Prospective identification and purification of quiescent adult neu-

ral stem cells from their in vivo niche. Neuron 82, 545-559.

Coelho, P.A., Bury, L., Sharif, B., Riparbelli, M.G., Fu, J., Callaini, G., Glover, D.M., and Zernicka-Goetz, M. (2013). Spindle formation in the mouse embryo requires Plk4 in the absence of centrioles. Developmental cell 27, 586-597.

Cooper, J.A. (2014). Molecules and mechanisms that regulate multipolar migration in the intermediate zone. Frontiers in cellular neuroscience 8, 386.

Costa, M.R., Wen, G., Lepier, A., Schroeder, T., and Gotz, M. (2008). Par-complex proteins promote proliferative progenitor divisions in the developing mouse cerebral cortex. Development 135, 11-22.

Culurgioni, S., Mari, S., Bonetti, P., Gallini, S., Bonetto, G., Brennich, M., Round, A., Nicassio, F., and Mapelli, M. (2018). Insc:LGN tetramers promote asymmetric divisions of mammary stem cells. Nature communications 9, 1025.

Cunha-Ferreira, I., Chazeau, A., Buijs, R.R., Stucchi, R., Will, L., Pan, X., Adolfs, Y., van der Meer, C., Wolthuis, J.C., Kahn, O.I., et al. (2018). The HAUS Complex Is a Key Regulator of Non-centrosomal Microtubule Organization during Neuronal Development. Cell reports 24, 791-800.

Dammermann, A., and Merdes, A. (2002). Assembly of centrosomal proteins and microtubule organization depends on PCM-1. The Journal of cell biology 159, 255-266.

Das, R.M., and Storey, K.G. (2014). Apical abscission alters cell polarity and dismantles the primary cilium during neurogenesis. Science 343, 200-204.

de Chevigny, A., Core, N., Follert, P., Wild, S., Bosio, A., Yoshikawa, K., Cremer, H., and Beclin, C. (2012). Dynamic expression of the pro-dopaminergic transcription factors Pax6 and Dlx2 during postnatal olfactory bulb neurogenesis. Frontiers in cellular neuroscience

108

6, 6.

de Juan Romero, C., and Borrell, V. (2017). Genetic maps and patterns of cerebral cortex folding. Current opinion in cell biology 49, 31-37.

de Juan Romero, C., Bruder, C., Tomasello, U., Sanz-Anquela, J.M., and Borrell, V. (2015). Discrete domains of gene expression in germinal layers distinguish the development of gyrencephaly. The EMBO journal 34, 1859-1874.

Dehay, C., Kennedy, H., and Kosik, K.S. (2015). The outer subventricular zone and primate-specific cortical complexification. Neuron 85, 683-694.

Delgehyr, N., Sillibourne, J., and Bornens, M. (2005). Microtubule nucleation and anchoring at the centrosome are independent processes linked by ninein function. Journal of cell science 118, 1565-1575.

Dong, C., Xu, H., Zhang, R., Tanaka, N., Takeichi, M., and Meng, W. (2017). CAMSAP3 accumulates in the pericentrosomal area and accompanies microtubule release from the centrosome via katanin. Journal of cell science 130, 1709-1715.

Dormoy, V., Tormanen, K., and Sutterlin, C. (2013). Par6gamma is at the mother centriole and controls centrosomal protein composition through a Par6alpha-dependent pathway. Journal of cell science 126, 860-870.

Duparc, R.H., Boutemmine, D., Champagne, M.P., Tetreault, N., and Bernier, G. (2006). Pax6 is required for delta-catenin/neurojugin expression during retinal, cerebellar and cortical development in mice. Developmental biology 300, 647-655.

Ebert, M.S., Neilson, J.R., and Sharp, P.A. (2007). MicroRNA sponges: competitive inhibitors of small RNAs in mammalian cells. Nat Methods 4, 721-726.

Englund, C., Fink, A., Lau, C., Pham, D., Daza, R.A., Bulfone, A., Kowalczyk, T., and Hevner, R.F. (2005). Pax6, Tbr2, and Tbr1 are expressed sequentially by radial glia, intermediate progenitor cells, and postmitotic neurons in developing neocortex. The Journal of neuroscience : the official journal of the Society for Neuroscience 25, 247-251.

Ernst, A., Alkass, K., Bernard, S., Salehpour, M., Perl, S., Tisdale, J., Possnert, G., Druid, H., and Frisen, J. (2014). Neurogenesis in the striatum of the adult human brain. Cell 156, 1072-1083.

Falk, S., Bugeon, S., Ninkovic, J., Pilz, G.A., Postiglione, M.P., Cremer, H., Knoblich, J.A., and Gotz, M. (2017). Time-Specific Effects of Spindle Positioning on Embryonic Progenitor Pool Composition and Adult Neural Stem Cell Seeding. Neuron 93, 777-791 e773.

Falk, S., Wurdak, H., Ittner, L.M., Ille, F., Sumara, G., Schmid, M.T., Draganova, K., Lang, K.S., Paratore, C., Leveen, P., et al. (2008). Brain area-specific effect of TGF-beta signaling on Wnt-dependent neural stem cell expansion. Cell stem cell 2, 472-483.

Farioli-Vecchioli, S., Ceccarelli, M., Saraulli, D., Micheli, L., Cannas, S., D'Alessandro, F., Scardigli, R., Leonardi, L., Cina, I., Costanzi, M., et al. (2014). Tis21 is required for adult neurogenesis in the subventricular zone and for olfactory behavior regulating cyclins, BMP4, Hes1/5 and Ids. Frontiers in cellular neuroscience 8, 98.

Farioli-Vecchioli, S., Micheli, L., Saraulli, D., Ceccarelli, M., Cannas, S., Scardigli, R., Leonardi, L., Cina, I., Costanzi, M., Ciotti, M.T., et al. (2012). Btg1 is Required to Maintain the Pool of Stem and Progenitor Cells of the Dentate Gyrus and Subventricular Zone. Frontiers in neuroscience 6, 124.

Farioli-Vecchioli, S., Tanori, M., Micheli, L., Mancuso, M., Leonardi, L., Saran, A., Ciotti, M.T., Ferretti, E., Gulino, A., Pazzaglia, S., et al. (2007). Inhibition of medulloblastoma tumorigenesis by the antiproliferative and pro-differentiative gene PC3. FASEB journal : official publication of the Federation of American Societies for Experimental Biology 21,

110

2215-2225.

Farkas, L.M., Haffner, C., Giger, T., Khaitovich, P., Nowick, K., Birchmeier, C., Paabo, S., and Huttner, W.B. (2008). Insulinoma-associated 1 has a panneurogenic role and promotes the generation and expansion of basal progenitors in the developing mouse neocortex. Neuron 60, 40-55.

Feederle, R., Gerber, J.K., Middleton, A., Northrup, E., Kist, R., Kremmer, E., and Peters, H. (2016). Generation of Pax1/PAX1-Specific Monoclonal Antibodies. Monoclon Antib Immunodiagn Immunother.

Fei, J.F., Haffner, C., and Huttner, W.B. (2014). 3' UTR-dependent, miR-92-mediated restriction of Tis21 expression maintains asymmetric neural stem cell division to ensure proper neocortex size. Cell reports 7, 398-411.

Feliciano, D.M., Bordey, A., and Bonfanti, L. (2015). Noncanonical Sites of Adult Neurogenesis in the Mammalian Brain. Cold Spring Harbor perspectives in biology 7, a018846.

Fernandez, V., Llinares-Benadero, C., and Borrell, V. (2016). Cerebral cortex expansion and folding: what have we learned? The EMBO journal 35, 1021-1044.

Fietz, S.A., Kelava, I., Vogt, J., Wilsch-Brauninger, M., Stenzel, D., Fish, J.L., Corbeil, D., Riehn, A., Distler, W., Nitsch, R., et al. (2010). OSVZ progenitors of human and ferret neocortex are epithelial-like and expand by integrin signaling. Nature neuroscience 13, 690-699.

Fietz, S.A., Lachmann, R., Brandl, H., Kircher, M., Samusik, N., Schroder, R., Lakshmanaperumal, N., Henry, I., Vogt, J., Riehn, A., et al. (2012). Transcriptomes of germinal zones of human and mouse fetal neocortex suggest a role of extracellular matrix in progenitor self-renewal. Proceedings of the National Academy of Sciences of the United States of America 109, 11836-11841.

Filarsky, M., Zillner, K., Araya, I., Villar-Garea, A., Merkl, R., Langst, G., and Nemeth, A. (2015). The extended AT-hook is a novel RNA binding motif. RNA Biol 12, 864-876.

Fischer, J., Beckervordersandforth, R., Tripathi, P., Steiner-Mezzadri, A., Ninkovic, J., and Gotz, M. (2011). Prospective isolation of adult neural stem cells from the mouse subependymal zone. Nature protocols 6, 1981-1989.

Fliegauf, M., Benzing, T., and Omran, H. (2007). When cilia go bad: cilia defects and ciliopathies. Nature reviews Molecular cell biology 8, 880-893.

Florio, M., Albert, M., Taverna, E., Namba, T., Brandl, H., Lewitus, E., Haffner, C., Sykes, A., Wong, F.K., Peters, J., et al. (2015). Human-specific gene ARHGAP11B promotes basal progenitor amplification and neocortex expansion. Science 347, 1465-1470.

Florio, M., Namba, T., Paabo, S., Hiller, M., and Huttner, W.B. (2016). A single splice site mutation in human-specific ARHGAP11B causes basal progenitor amplification. Science advances 2, e1601941.

Fode, C., Gradwohl, G., Morin, X., Dierich, A., LeMeur, M., Goridis, C., and Guillemot, F. (1998). The bHLH protein NEUROGENIN 2 is a determination factor for epibranchial placode-derived sensory neurons. Neuron 20, 483-494.

Fuentealba, L.C., Rompani, S.B., Parraguez, J.I., Obernier, K., Romero, R., Cepko, C.L., and Alvarez-Buylla, A. (2015). Embryonic Origin of Postnatal Neural Stem Cells. Cell 161, 1644-1655.

Gal, J.S., Morozov, Y.M., Ayoub, A.E., Chatterjee, M., Rakic, P., and Haydar, T.F. (2006). Molecular and morphological heterogeneity of neural precursors in the mouse neocortical proliferative zones. The Journal of neuroscience : the official journal of the Society for Neuroscience 26, 1045-1056.

112

Garcia-Moreno, F., Vasistha, N.A., Trevia, N., Bourne, J.A., and Molnar, Z. (2012).

Compartmentalization of cerebral cortical germinal zones in a lissencephalic primate and gyrencephalic rodent. Cerebral cortex 22, 482-492.

Gauthier-Fisher, A., Lin, D.C., Greeve, M., Kaplan, D.R., Rottapel, R., and Miller, F.D. (2009). Lfc and Tctex-1 regulate the genesis of neurons from cortical precursor cells. Nature neuroscience 12, 735-744.

Gingold, H., Tehler, D., Christoffersen, N.R., Nielsen, M.M., Asmar, F., Kooistra, S.M., Christophersen, N.S., Christensen, L.L., Borre, M., Sorensen, K.D., et al. (2014). A dual program for translation regulation in cellular proliferation and differentiation. Cell 158, 1281-1292.

Götz, M. (2012). Radial glia cells. In Neuroglia, H. Kettenmann, and B.R. Ransom, eds. (Oxford University Press).

Gotz, M., and Huttner, W.B. (2005). The cell biology of neurogenesis. Nature reviews Molecular cell biology 6, 777-788.

Gotz, M., Nakafuku, M., and Petrik, D. (2016). Neurogenesis in the Developing and Adult Brain-Similarities and Key Differences. Cold Spring Harbor perspectives in biology 8.

Gotz, M., Stoykova, A., and Gruss, P. (1998). Pax6 controls radial glia differentiation in the cerebral cortex. Neuron 21, 1031-1044.

Gradwohl, G., Fode, C., and Guillemot, F. (1996). Restricted expression of a novel murine atonal-related bHLH protein in undifferentiated neural precursors. Developmental biology 180, 227-241.

Graser, S., Stierhof, Y.D., Lavoie, S.B., Gassner, O.S., Lamla, S., Le Clech, M., and Nigg, E.A. (2007). Cep164, a novel centriole appendage protein required for primary cilium formation. The Journal of cell biology 179, 321-330.

Grosche, A., Hauser, A., Lepper, M.F., Mayo, R., von Toerne, C., Merl-Pham, J., and Hauck, S.M. (2016). The Proteome of Native Adult Muller Glial Cells From Murine Retina. Molecular & cellular proteomics : MCP 15, 462-480.

Guarguaglini, G., Duncan, P.I., Stierhof, Y.D., Holmstrom, T., Duensing, S., and Nigg, E.A. (2005). The forkhead-associated domain protein Cep170 interacts with Polo-like kinase 1 and serves as a marker for mature centrioles. Molecular biology of the cell 16, 1095-1107.

Guo, Z., Zhang, L., Wu, Z., Chen, Y., Wang, F., and Chen, G. (2014). In vivo direct reprogramming of reactive glial cells into functional neurons after brain injury and in an Alzheimer's disease model. Cell stem cell 14, 188-202.

Hack, M.A., Saghatelyan, A., de Chevigny, A., Pfeifer, A., Ashery-Padan, R., Lledo, P.M., and Gotz, M. (2005). Neuronal fate determinants of adult olfactory bulb neurogenesis. Nature neuroscience 8, 865-872.

Hansen, D.V., Lui, J.H., Parker, P.R., and Kriegstein, A.R. (2010). Neurogenic radial glia in the outer subventricular zone of human neocortex. Nature 464, 554-561.

Haubensak, W., Attardo, A., Denk, W., and Huttner, W.B. (2004). Neurons arise in the basal neuroepithelium of the early mammalian telencephalon: a major site of neurogenesis. Proceedings of the National Academy of Sciences of the United States of America 101, 3196-3201.

Heck, J.N., Ponik, S.M., Garcia-Mendoza, M.G., Pehlke, C.A., Inman, D.R., Eliceiri, K.W.,

114

and Keely, P.J. (2012). Microtubules regulate GEF-H1 in response to extracellular matrix stiffness. Molecular biology of the cell 23, 2583-2592.

Heide, M., Long, K.R., and Huttner, W.B. (2017). Novel gene function and regulation in neocortex expansion. Current opinion in cell biology 49, 22-30.

Heins, N., Malatesta, P., Cecconi, F., Nakafuku, M., Tucker, K.L., Hack, M.A., Chapouton, P., Barde, Y.A., and Gotz, M. (2002). Glial cells generate neurons: the role of the transcription factor Pax6. Nature neuroscience 5, 308-315.

Hendershott, M.C., and Vale, R.D. (2014). Regulation of microtubule minus-end dynamics by CAMSAPs and Patronin. Proceedings of the National Academy of Sciences of the United States of America 111, 5860-5865.

Hevner, R.F., Hodge, R.D., Daza, R.A., and Englund, C. (2006). Transcription factors in glutamatergic neurogenesis: conserved programs in neocortex, cerebellum, and adult hippocampus. Neuroscience research 55, 223-233.

Hintermair, C., Voss, K., Forne, I., Heidemann, M., Flatley, A., Kremmer, E., Imhof, A., and Eick, D. (2016). Specific threonine-4 phosphorylation and function of RNA polymerase II CTD during M phase progression. Scientific reports 6, 27401.

Hodges, M.E., Scheumann, N., Wickstead, B., Langdale, J.A., and Gull, K. (2010). Reconstructing the evolutionary history of the centriole from protein components. Journal of cell science 123, 1407-1413.

Holm, P.C., Mader, M.T., Haubst, N., Wizenmann, A., Sigvardsson, M., and Gotz, M. (2007). Loss- and gain-of-function analyses reveal targets of Pax6 in the developing mouse telencephalon. Molecular and cellular neurosciences 34, 99-119.

Hoser, M., Potzner, M.R., Koch, J.M., Bosl, M.R., Wegner, M., and Sock, E. (2008). Sox12

deletion in the mouse reveals nonreciprocal redundancy with the related Sox4 and Sox11 transcription factors. Molecular and cellular biology 28, 4675-4687.

Huang, N., Xia, Y., Zhang, D., Wang, S., Bao, Y., He, R., Teng, J., and Chen, J. (2017). Hierarchical assembly of centriole subdistal appendages via centrosome binding proteins CCDC120 and CCDC68. Nature communications 8, 15057.

Huang, Y.W., Liu, J.C., Deatherage, D.E., Luo, J., Mutch, D.G., Goodfellow, P.J., Miller, D.S., and Huang, T.H. (2009). Epigenetic repression of microRNA-129-2 leads to overexpression of SOX4 oncogene in endometrial cancer. Cancer research 69, 9038-9046.

Hung, H.F., Hehnly, H., and Doxsey, S. (2016). The Mother Centriole Appendage Protein Cenexin Modulates Lumen Formation through Spindle Orientation. Current biology : CB 26, 793-801.

Hurtado, L., Caballero, C., Gavilan, M.P., Cardenas, J., Bornens, M., and Rios, R.M. (2011). Disconnecting the Golgi ribbon from the centrosome prevents directional cell migration and ciliogenesis. The Journal of cell biology 193, 917-933.

Iacopetti, P., Michelini, M., Stuckmann, I., Oback, B., Aaku-Saraste, E., and Huttner, W.B. (1999). Expression of the antiproliferative gene TIS21 at the onset of neurogenesis identifies single neuroepithelial cells that switch from proliferative to neuron-generating division. Proceedings of the National Academy of Sciences of the United States of America 96, 4639-4644.

Ibi, M., Zou, P., Inoko, A., Shiromizu, T., Matsuyama, M., Hayashi, Y., Enomoto, M., Mori, D., Hirotsune, S., Kiyono, T., et al. (2011). Trichoplein controls microtubule anchoring at the centrosome by binding to Odf2 and ninein. Journal of cell science 124, 857-864.

Icha, J., Kunath, C., Rocha-Martins, M., and Norden, C. (2016). Independent modes of ganglion cell translocation ensure correct lamination of the zebrafish retina. The Journal

116

of cell biology 215, 259-275.

In, T.S.H., Trotman-Grant, A., Fahl, S., Chen, E.L.Y., Zarin, P., Moore, A.J., Wiest, D.L., Zuniga-Pflucker, J.C., and Anderson, M.K. (2017). HEB is required for the specification of fetal IL-17-producing gammadelta T cells. Nature communications 8, 2004.

Insolera, R., Bazzi, H., Shao, W., Anderson, K.V., and Shi, S.H. (2014). Cortical neurogenesis in the absence of centrioles. Nature neuroscience 17, 1528-1535.

Ishikawa, H., Kubo, A., Tsukita, S., and Tsukita, S. (2005). Odf2-deficient mother centrioles lack distal/subdistal appendages and the ability to generate primary cilia. Nature cell biology 7, 517-524.

Itoh, Y., Moriyama, Y., Hasegawa, T., Endo, T.A., Toyoda, T., and Gotoh, Y. (2013). Scratch regulates neuronal migration onset via an epithelial-mesenchymal transition-like mechanism. Nature neuroscience 16, 416-425.

Jiang, K., Hua, S., Mohan, R., Grigoriev, I., Yau, K.W., Liu, Q., Katrukha, E.A., Altelaar, A.F., Heck, A.J., Hoogenraad, C.C., et al. (2014). Microtubule minus-end stabilization by polymerization-driven CAMSAP deposition. Developmental cell 28, 295-309.

Jiang, K., Toedt, G., Montenegro Gouveia, S., Davey, N.E., Hua, S., van der Vaart, B., Grigoriev, I., Larsen, J., Pedersen, L.B., Bezstarosti, K., et al. (2012). A Proteome-wide screen for mammalian SxIP motif-containing microtubule plus-end tracking proteins. Current biology : CB 22, 1800-1807.

Johansson, P.A., Irmler, M., Acampora, D., Beckers, J., Simeone, A., and Gotz, M. (2013). The transcription factor Otx2 regulates choroid plexus development and function. Development 140, 1055-1066.

Johnson, M.B., Wang, P.P., Atabay, K.D., Murphy, E.A., Doan, R.N., Hecht, J.L., and

Walsh, C.A. (2015). Single-cell analysis reveals transcriptional heterogeneity of neural progenitors in human cortex. Nature neuroscience 18, 637-646.

Jossin, Y., and Cooper, J.A. (2011). Reelin, Rap1 and N-cadherin orient the migration of multipolar neurons in the developing neocortex. Nature neuroscience 14, 697-703.

Kasioulis, I., Das, R.M., and Storey, K.G. (2017). Inter-dependent apical microtubule and actin dynamics orchestrate centrosome retention and neuronal delamination. eLife 6.

Kawaguchi, D., Yoshimatsu, T., Hozumi, K., and Gotoh, Y. (2008). Selection of differentiating cells by different levels of delta-like 1 among neural precursor cells in the developing mouse telencephalon. Development 135, 3849-3858.

Klyachko, V.A., and Stevens, C.F. (2003). Connectivity optimization and the positioning of cortical areas. Proceedings of the National Academy of Sciences of the United States of America 100, 7937-7941.

Knoblich, J.A. (2008). Mechanisms of asymmetric stem cell division. Cell 132, 583-597.

Kodani, A., Salome Sirerol-Piquer, M., Seol, A., Garcia-Verdugo, J.M., and Reiter, J.F. (2013). Kif3a interacts with Dynactin subunit p150 Glued to organize centriole subdistal appendages. The EMBO journal 32, 597-607.

Kodani, A., Tonthat, V., Wu, B., and Sutterlin, C. (2010). Par6 alpha interacts with the dynactin subunit p150 Glued and is a critical regulator of centrosomal protein recruitment. Molecular biology of the cell 21, 3376-3385.

Kokoeva, M.V., Yin, H., and Flier, J.S. (2005). Neurogenesis in the hypothalamus of adult mice: potential role in energy balance. Science 310, 679-683.

118

Konno, D., Shioi, G., Shitamukai, A., Mori, A., Kiyonari, H., Miyata, T., and Matsuzaki, F. (2008). Neuroepithelial progenitors undergo LGN-dependent planar divisions to maintain self-renewability during mammalian neurogenesis. Nature cell biology 10, 93-101.

Kosodo, Y., Roper, K., Haubensak, W., Marzesco, A.M., Corbeil, D., and Huttner, W.B. (2004). Asymmetric distribution of the apical plasma membrane during neurogenic divisions of mammalian neuroepithelial cells. The EMBO journal 23, 2314-2324.

Kowalczyk, T., Pontious, A., Englund, C., Daza, R.A., Bedogni, F., Hodge, R., Attardo, A., Bell, C., Huttner, W.B., and Hevner, R.F. (2009). Intermediate neuronal progenitors (basal progenitors) produce pyramidal-projection neurons for all layers of cerebral cortex. Cerebral cortex 19, 2439-2450.

Krendel, M., Zenke, F.T., and Bokoch, G.M. (2002). Nucleotide exchange factor GEF-H1 mediates cross-talk between microtubules and the actin cytoskeleton. Nature cell biology 4, 294-301.

Kriegstein, A., and Alvarez-Buylla, A. (2009). The glial nature of embryonic and adult neural stem cells. Annual review of neuroscience 32, 149-184.

Kuwahara, A., Hirabayashi, Y., Knoepfler, P.S., Taketo, M.M., Sakai, J., Kodama, T., and Gotoh, Y. (2010). Wnt signaling and its downstream target N-myc regulate basal progenitors in the developing neocortex. Development 137, 1035-1044.

Lang, M.F., and Shi, Y. (2012). Dynamic Roles of microRNAs in Neurogenesis. Frontiers in neuroscience 6, 71.

Li, Y., Brauer, P.M., Singh, J., Xhiku, S., Yoganathan, K., Zuniga-Pflucker, J.C., and Anderson, M.K. (2017). Targeted Disruption of TCF12 Reveals HEB as Essential in Human Mesodermal Specification and Hematopoiesis. Stem cell reports 9, 779-795.

Lim, D.A., Huang, Y.C., Swigut, T., Mirick, A.L., Garcia-Verdugo, J.M., Wysocka, J., Ernst, P., and Alvarez-Buylla, A. (2009). Chromatin remodelling factor Mll1 is essential for neurogenesis from postnatal neural stem cells. Nature 458, 529-533.

Lim, D.A., Suarez-Farinas, M., Naef, F., Hacker, C.R., Menn, B., Takebayashi, H., Magnasco, M., Patil, N., and Alvarez-Buylla, A. (2006). In vivo transcriptional profile analysis reveals RNA splicing and chromatin remodeling as prominent processes for adult neurogenesis. Molecular and cellular neurosciences 31, 131-148.

Lin, W.J., Gary, J.D., Yang, M.C., Clarke, S., and Herschman, H.R. (1996). The mammalian immediate-early TIS21 protein and the leukemia-associated BTG1 protein interact with a protein-arginine N-methyltransferase. The Journal of biological chemistry 271, 15034-15044.

Llorens-Bobadilla, E., Zhao, S., Baser, A., Saiz-Castro, G., Zwadlo, K., and Martin-Villalba, A. (2015). Single-Cell Transcriptomics Reveals a Population of Dormant Neural Stem Cells that Become Activated upon Brain Injury. Cell stem cell 17, 329-340.

Luders, J., Patel, U.K., and Stearns, T. (2006). GCP-WD is a gamma-tubulin targeting factor required for centrosomal and chromatin-mediated microtubule nucleation. Nature cell biology 8, 137-147.

Ludwig, N., Leidinger, P., Becker, K., Backes, C., Fehlmann, T., Pallasch, C., Rheinheimer, S., Meder, B., Stahler, C., Meese, E., et al. (2016). Distribution of miRNA expression across human tissues. Nucleic acids research 44, 3865-3877.

M. Moudjou, M.B. (1994). Isolation of Centrosomes from Cultured Animal Cells. In Cell biology: A laboratory handbook, J. Celis, ed. (San Diego: Academic Press), pp. 595-604.

Ma, W., Ortiz-Quintero, B., Rangel, R., McKeller, M.R., Herrera-Rodriguez, S., Castillo, E.F., Schluns, K.S., Hall, M., Zhang, H., Suh, W.K., et al. (2011). Coordinate activation

120

of inflammatory gene networks, alveolar destruction and neonatal death in AKNA deficient mice. Cell research 21, 1564-1577.

Malatesta, P., Hartfuss, E., and Gotz, M. (2000). Isolation of radial glial cells by fluorescent-activated cell sorting reveals a neuronal lineage. Development 127, 5253-5263.

Mao, L., Yang, P., Hou, S., Li, F., and Kijlstra, A. (2011). Label-free proteomics reveals decreased expression of CD18 and AKNA in peripheral CD4+ T cells from patients with Vogt-Koyanagi-Harada syndrome. PloS one 6, e14616.

Mardin, B.R., Agircan, F.G., Lange, C., and Schiebel, E. (2011). Plk1 controls the Nek2A-PP1gamma antagonism in centrosome disjunction. Current biology : CB 21, 1145-1151.

Martinez-Martinez, M.A., De Juan Romero, C., Fernandez, V., Cardenas, A., Gotz, M., and Borrell, V. (2016). A restricted period for formation of outer subventricular zone defined by Cdh1 and Trnp1 levels. Nature communications 7, 11812.

Masserdotti, G., Gillotin, S., Sutor, B., Drechsel, D., Irmler, M., Jorgensen, H.F., Sass, S., Theis, F.J., Beckers, J., Berninger, B., et al. (2015). Transcriptional Mechanisms of Proneural Factors and REST in Regulating Neuronal Reprogramming of Astrocytes. Cell stem cell 17, 74-88.

Mazo, G., Soplop, N., Wang, W.J., Uryu, K., and Tsou, M.B. (2016). Spatial Control of Primary Ciliogenesis by Subdistal Appendages Alters Sensation-Associated Properties of Cilia. Developmental cell 39, 424-437.

Meitinger, F., Anzola, J.V., Kaulich, M., Richardson, A., Stender, J.D., Benner, C., Glass, C.K., Dowdy, S.F., Desai, A., Shiau, A.K., et al. (2016). 53BP1 and USP28 mediate p53 activation and G1 arrest after centrosome loss or extended mitotic duration. The Journal of cell biology 214, 155-166.

Meng, W., Mushika, Y., Ichii, T., and Takeichi, M. (2008). Anchorage of microtubule minus ends to adherens junctions regulates epithelial cell-cell contacts. Cell 135, 948-959.

Meng, W., and Takeichi, M. (2009). Adherens junction: molecular architecture and regulation. Cold Spring Harbor perspectives in biology 1, a002899.

Merkle, F.T., Mirzadeh, Z., and Alvarez-Buylla, A. (2007). Mosaic organization of neural stem cells in the adult brain. Science 317, 381-384.

Merkle, F.T., Tramontin, A.D., Garcia-Verdugo, J.M., and Alvarez-Buylla, A. (2004). Radial glia give rise to adult neural stem cells in the subventricular zone. Proceedings of the National Academy of Sciences of the United States of America 101, 17528-17532.

Mesman, S., and Smidt, M.P. (2017). Tcf12 Is Involved in Early Cell-Fate Determination and Subset Specification of Midbrain Dopamine Neurons. Frontiers in molecular neuroscience 10, 353.

Mihalas, A.B., Elsen, G.E., Bedogni, F., Daza, R.A.M., Ramos-Laguna, K.A., Arnold, S.J., and Hevner, R.F. (2016). Intermediate Progenitor Cohorts Differentially Generate Cortical Layers and Require Tbr2 for Timely Acquisition of Neuronal Subtype Identity. Cell reports 16, 92-105.

Mikule, K., Delaval, B., Kaldis, P., Jurcyzk, A., Hergert, P., and Doxsey, S. (2007). Loss of centrosome integrity induces p38-p53-p21-dependent G1-S arrest. Nature cell biology 9, 160-170.

Militti, C., Maenner, S., Becker, P.B., and Gebauer, F. (2014). UNR facilitates the interaction of MLE with the lncRNA roX2 during Drosophila dosage compensation. Nature communications 5, 4762.

Ming, G.L., and Song, H. (2011). Adult neurogenesis in the mammalian brain: significant

122

answers and significant questions. Neuron 70, 687-702.

Miyamoto, T., Hosoba, K., Ochiai, H., Royba, E., Izumi, H., Sakuma, T., Yamamoto, T., Dynlacht, B.D., and Matsuura, S. (2015). The Microtubule-Depolymerizing Activity of a Mitotic Kinesin Protein KIF2A Drives Primary Cilia Disassembly Coupled with Cell Proliferation. Cell reports.

Miyata, T., Kawaguchi, A., Saito, K., Kawano, M., Muto, T., and Ogawa, M. (2004). Asymmetric production of surface-dividing and non-surface-dividing cortical progenitor cells. Development 131, 3133-3145.

Mizutani, K., Yoon, K., Dang, L., Tokunaga, A., and Gaiano, N. (2007). Differential Notch signalling distinguishes neural stem cells from intermediate progenitors. Nature 449, 351-355.

Mogensen, M.M., Malik, A., Piel, M., Bouckson-Castaing, V., and Bornens, M. (2000). Microtubule minus-end anchorage at centrosomal and non-centrosomal sites: the role of ninein. Journal of cell science 113 (Pt 17), 3013-3023.

Moliterno, A.R., and Resar, L.M. (2011). AKNA: another AT-hook transcription factor "hooking-up" with inflammation. Cell research 21, 1528-1530.

Moudjou, M., and Bornens, M. (1994). Isolation of centrosomes from cultured animal cells. In Cell biology: A laboratory handbook J. Celis, ed. (San Diego: Academic Press), pp. 595-604.

Mu, L., Berti, L., Masserdotti, G., Covic, M., Michaelidis, T.M., Doberauer, K., Merz, K., Rehfeld, F., Haslinger, A., Wegner, M., et al. (2012). SoxC transcription factors are required for neuronal differentiation in adult hippocampal neurogenesis. The Journal of neuroscience : the official journal of the Society for Neuroscience 32, 3067-3080.

Nagae, S., Meng, W., and Takeichi, M. (2013). Non-centrosomal microtubules regulate F-actin organization through the suppression of GEF-H1 activity. Genes to cells : devoted to molecular & cellular mechanisms 18, 387-396.

Nguyen, L., Besson, A., Heng, J.I., Schuurmans, C., Teboul, L., Parras, C., Philpott, A., Roberts, J.M., and Guillemot, F. (2006). p27kip1 independently promotes neuronal differentiation and migration in the cerebral cortex. Genes & development 20, 1511-1524.

Nigg, E.A., and Stearns, T. (2011). The centrosome cycle: Centriole biogenesis, duplication and inherent asymmetries. Nature cell biology 13, 1154-1160.

Ninkovic, J., Pinto, L., Petricca, S., Lepier, A., Sun, J., Rieger, M.A., Schroeder, T., Cvekl, A., Favor, J., and Gotz, M. (2010). The transcription factor Pax6 regulates survival of dopaminergic olfactory bulb neurons via crystallin alphaA. Neuron 68, 682-694.

Ninkovic, J., Steiner-Mezzadri, A., Jawerka, M., Akinci, U., Masserdotti, G., Petricca, S., Fischer, J., von Holst, A., Beckers, J., Lie, C.D., et al. (2013). The BAF complex interacts with Pax6 in adult neural progenitors to establish a neurogenic cross-regulatory transcriptional network. Cell stem cell 13, 403-418.

Nishimura, T., and Takeichi, M. (2009). Remodeling of the adherens junctions during morphogenesis. Current topics in developmental biology 89, 33-54.

Noordstra, I., Liu, Q., Nijenhuis, W., Hua, S., Jiang, K., Baars, M., Remmelzwaal, S., Martin, M., Kapitein, L.C., and Akhmanova, A. (2016). Control of apico-basal epithelial polarity by the microtubule minus-end-binding protein CAMSAP3 and spectraplakin ACF7. Journal of cell science 129, 4278-4288.

Ohama, Y., and Hayashi, K. (2009). Relocalization of a microtubule-anchoring protein, ninein, from the centrosome to dendrites during differentiation of mouse neurons. Histochemistry and cell biology 132, 515-524.

124

Ohtsuka, T., Shimojo, H., Matsunaga, M., Watanabe, N., Kometani, K., Minato, N., and Kageyama, R. (2011). Gene expression profiling of neural stem cells and identification of regulators of neural differentiation during cortical development. Stem Cells 29, 1817-1828.

Palazzo, A.F., and Lee, E.S. (2015). Non-coding RNA: what is functional and what is junk? Frontiers in genetics 6, 2.

Paredes, M.F., Sorrells, S.F., Garcia-Verdugo, J.M., and Alvarez-Buylla, A. (2016). Brain size and limits to adult neurogenesis. The Journal of comparative neurology 524, 646-664.

Paridaen, J.T., Huttner, W.B., and Wilsch-Brauninger, M. (2015). Analysis of primary cilia in the developing mouse brain. Methods in cell biology 127, 93-129.

Paridaen, J.T., Wilsch-Brauninger, M., and Huttner, W.B. (2013). Asymmetric inheritance of centrosome-associated primary cilium membrane directs ciliogenesis after cell division. Cell 155, 333-344.

Park, M.G., Jang, H., Lee, S.H., and Lee, C.J. (2017). Flow Shear Stress Enhances the Proliferative Potential of Cultured Radial Glial Cells Possibly Via an Activation of Mechanosensitive Calcium Channel. Experimental neurobiology 26, 71-81.

Passeri, D., Marcucci, A., Rizzo, G., Billi, M., Panigada, M., Leonardi, L., Tirone, F., and Grignani, F. (2006). Btg2 enhances retinoic acid-induced differentiation by modulating histone H4 methylation and acetylation. Molecular and cellular biology 26, 5023-5032.

Pataskar, A., Jung, J., Smialowski, P., Noack, F., Calegari, F., Straub, T., and Tiwari, V.K. (2016). NeuroD1 reprograms chromatin and transcription factor landscapes to induce the neuronal program. The EMBO journal 35, 24-45.

Paton, J.A., and Nottebohm, F.N. (1984). Neurons generated in the adult brain are recruited into functional circuits. Science 225, 1046-1048.

Perales, G., Burguete-Garcia, A.I., Dimas, J., Bahena-Roman, M., Bermudez-Morales, V.H., Moreno, J., and Madrid-Marina, V. (2010). A polymorphism in the AT-hook motif of the transcriptional regulator AKNA is a risk factor for cervical cancer. Biomarkers : biochemical indicators of exposure, response, and susceptibility to chemicals 15, 470-474.

Peyre, E., Jaouen, F., Saadaoui, M., Haren, L., Merdes, A., Durbec, P., and Morin, X. (2011). A lateral belt of cortical LGN and NuMA guides mitotic spindle movements and planar division in neuroepithelial cells. The Journal of cell biology 193, 141-154.

Pilz, G.A., Shitamukai, A., Reillo, I., Pacary, E., Schwausch, J., Stahl, R., Ninkovic, J., Snippert, H.J., Clevers, H., Godinho, L., et al. (2013). Amplification of progenitors in the mammalian telencephalon includes a new radial glial cell type. Nature communications 4, 2125.

Pinto, L., Drechsel, D., Schmid, M.T., Ninkovic, J., Irmler, M., Brill, M.S., Restani, L., Gianfranceschi, L., Cerri, C., Weber, S.N., et al. (2009). AP2gamma regulates basal progenitor fate in a region- and layer-specific manner in the developing cortex. Nature neuroscience 12, 1229-1237.

Pinto, L., Mader, M.T., Irmler, M., Gentilini, M., Santoni, F., Drechsel, D., Blum, R., Stahl, R., Bulfone, A., Malatesta, P., et al. (2008). Prospective isolation of functionally distinct radial glial subtypes–lineage and transcriptome analysis. Molecular and cellular neurosciences 38, 15-42.

Pollen, A.A., Nowakowski, T.J., Chen, J., Retallack, H., Sandoval-Espinosa, C., Nicholas, C.R., Shuga, J., Liu, S.J., Oldham, M.C., Diaz, A., et al. (2015). Molecular identity of human outer radial glia during cortical development. Cell 163, 55-67.

126

Pongrakhananon, V., Saito, H., Hiver, S., Abe, T., Shioi, G., Meng, W., and Takeichi, M. (2018). CAMSAP3 maintains neuronal polarity through regulation of microtubule stability. Proceedings of the National Academy of Sciences of the United States of America.

Pons-Espinal, M., de Luca, E., Marzi, M.J., Beckervordersandforth, R., Armirotti, A., Nicassio, F., Fabel, K., Kempermann, G., and De Pietri Tonelli, D. (2017). Synergic Functions of miRNAs Determine Neuronal Fate of Adult Neural Stem Cells. Stem cell reports 8, 1046-1061.

Postiglione, M.P., Juschke, C., Xie, Y., Haas, G.A., Charalambous, C., and Knoblich, J.A. (2011). Mouse inscuteable induces apical-basal spindle orientation to facilitate intermediate progenitor generation in the developing neocortex. Neuron 72, 269-284.

Rai, A.K., Chen, J.X., Selbach, M., and Pelkmans, L. (2018). Kinase-controlled phase transition of membraneless organelles in mitosis. Nature 559, 211-216.

Rajman, M., and Schratt, G. (2017). MicroRNAs in neural development: from master regulators to fine-tuners. Development 144, 2310-2322.

Ramesh, V., Bayam, E., Cernilogar, F.M., Bonapace, I.M., Schulze, M., Riemenschneider, M.J., Schotta, G., and Gotz, M. (2016). Loss of Uhrf1 in neural stem cells leads to activation of retroviral elements and delayed neurodegeneration. Genes & development 30, 2199-2212.

Ramos, A.D., Andersen, R.E., Liu, S.J., Nowakowski, T.J., Hong, S.J., Gertz, C., Salinas, R.D., Zarabi, H., Kriegstein, A.R., and Lim, D.A. (2015). The long noncoding RNA Pnky regulates neuronal differentiation of embryonic and postnatal neural stem cells. Cell stem cell 16, 439-447.

Ramos, A.D., Diaz, A., Nellore, A., Delgado, R.N., Park, K.Y., Gonzales-Roybal, G., Oldham, M.C., Song, J.S., and Lim, D.A. (2013). Integration of genome-wide approaches

identifies lncRNAs of adult neural stem cells and their progeny in vivo. Cell stem cell 12, 616-628.

Ravindran, E., Hu, H., Yuzwa, S.A., Hernandez-Miranda, L.R., Kraemer, N., Ninnemann, O., Musante, L., Boltshauser, E., Schindler, D., Hubner, A., et al. (2017). Homozygous ARHGEF2 mutation causes intellectual disability and midbrain-hindbrain malformation. PLoS genetics 13, e1006746.

Reillo, I., and Borrell, V. (2012). Germinal zones in the developing cerebral cortex of ferret: ontogeny, cell cycle kinetics, and diversity of progenitors. Cerebral cortex 22, 2039-2054.

Reillo, I., de Juan Romero, C., Garcia-Cabezas, M.A., and Borrell, V. (2011). A role for intermediate radial glia in the tangential expansion of the mammalian cerebral cortex. Cerebral cortex 21, 1674-1694.

Reynolds, A.B. (2007). p120-catenin: Past and present. Biochimica et biophysica acta 1773, 2-7.

Rigbolt, K.T., Vanselow, J.T., and Blagoev, B. (2011). GProX, a user-friendly platform for bioinformatics analysis and visualization of quantitative proteomics data. Molecular & cellular proteomics : MCP 10, O110 007450.

Rinn, J.L., and Chang, H.Y. (2012). Genome regulation by long noncoding RNAs. Annual review of biochemistry 81, 145-166.

Rios, R.M. (2014). The centrosome-Golgi apparatus nexus. Philosophical transactions of the Royal Society of London Series B, Biological sciences 369.

Robins, S.C., Stewart, I., McNay, D.E., Taylor, V., Giachino, C., Goetz, M., Ninkovic, J., Briancon, N., Maratos-Flier, E., Flier, J.S., et al. (2013). alpha-Tanycytes of the adult hypothalamic third ventricle include distinct populations of FGF-responsive neural pro-

128

genitors. Nature communications 4, 2049.

Rousso, D.L., Pearson, C.A., Gaber, Z.B., Miquelajauregui, A., Li, S., Portera-Cailliau, C., Morrisey, E.E., and Novitch, B.G. (2012). Foxp-mediated suppression of N-cadherin regulates neuroepithelial character and progenitor maintenance in the CNS. Neuron 74, 314-330.

Sahara, S., and O'Leary, D.D. (2009). Fgf10 regulates transition period of cortical stem cell differentiation to radial glia controlling generation of neurons and basal progenitors. Neuron 63, 48-62.

Sahu, S.K., Garding, A., Tiwari, N., Thakurela, S., Toedling, J., Gebhard, S., Ortega, F., Schmarowski, N., Berninger, B., Nitsch, R., et al. (2015). JNK-dependent gene regulatory circuitry governs mesenchymal fate. The EMBO journal 34, 2162-2181.

Sakakibara, A., Sato, T., Ando, R., Noguchi, N., Masaoka, M., and Miyata, T. (2014). Dynamics of centrosome translocation and microtubule organization in neocortical neurons during distinct modes of polarization. Cerebral cortex 24, 1301-1310.

Sako-Kubota, K., Tanaka, N., Nagae, S., Meng, W., and Takeichi, M. (2014). Minus end-directed motor KIFC3 suppresses E-cadherin degradation by recruiting USP47 to adherens junctions. Molecular biology of the cell 25, 3851-3860.

Sanchez, A.D., and Feldman, J.L. (2017). Microtubule-organizing centers: from the centrosome to non-centrosomal sites. Current opinion in cell biology 44, 93-101.

Schmid, M.T., Weinandy, F., Wilsch-Brauninger, M., Huttner, W.B., Cappello, S., and Gotz, M. (2014). The role of alpha-E-catenin in cerebral cortex development: radial glia specific effect on neuronal migration. Frontiers in cellular neuroscience 8, 215.

Schmidt-Edelkraut, U., Daniel, G., Hoffmann, A., and Spengler, D. (2014). Zac1 regulates

cell cycle arrest in neuronal progenitors via Tcf4. Molecular and cellular biology 34, 1020-1030.

Sessa, A., Mao, C.A., Hadjantonakis, A.K., Klein, W.H., and Broccoli, V. (2008). Tbr2 directs conversion of radial glia into basal precursors and guides neuronal amplification by indirect neurogenesis in the developing neocortex. Neuron 60, 56-69.

Shibata, M., Nakao, H., Kiyonari, H., Abe, T., and Aizawa, S. (2011). MicroRNA-9 regulates neurogenesis in mouse telencephalon by targeting multiple transcription factors. The Journal of neuroscience : the official journal of the Society for Neuroscience 31, 3407-3422.

Shinohara, H., Sakayori, N., Takahashi, M., and Osumi, N. (2013). Ninein is essential for the maintenance of the cortical progenitor character by anchoring the centrosome to microtubules. Biology open 2, 739-749.

Shitamukai, A., Konno, D., and Matsuzaki, F. (2011). Oblique radial glial divisions in the developing mouse neocortex induce self-renewing progenitors outside the germinal zone that resemble primate outer subventricular zone progenitors. The Journal of neuroscience : the official journal of the Society for Neuroscience 31, 3683-3695.

Siddiqa, A., Sims-Mourtada, J.C., Guzman-Rojas, L., Rangel, R., Guret, C., Madrid-Marina, V., Sun, Y., and Martinez-Valdez, H. (2001). Regulation of CD40 and CD40 ligand by the AT-hook transcription factor AKNA. Nature 410, 383-387.

Singh, S., Howell, D., Trivedi, N., Kessler, K., Ong, T., Rosmaninho, P., Raposo, A.A., Robinson, G., Roussel, M.F., Castro, D.S., et al. (2016). Zeb1 controls neuron differentiation and germinal zone exit by a mesenchymal-epithelial-like transition. eLife 5.

Sirko, S., Behrendt, G., Johansson, P.A., Tripathi, P., Costa, M., Bek, S., Heinrich, C., Tiedt, S., Colak, D., Dichgans, M., et al. (2013). Reactive glia in the injured brain acquire stem cell properties in response to sonic hedgehog. [corrected]. Cell stem cell 12, 426-439.

130

Smart, I.H., Dehay, C., Giroud, P., Berland, M., and Kennedy, H. (2002). Unique morphological features of the proliferative zones and postmitotic compartments of the neural epithelium giving rise to striate and extrastriate cortex in the monkey. Cerebral cortex 12, 37-53.

Song, Y., and Brady, S.T. (2015). Post-translational modifications of tubulin: pathways to functional diversity of microtubules. Trends in cell biology 25, 125-136.

Sorokin, S. (1962). Centrioles and the formation of rudimentary cilia by fibroblasts and smooth muscle cells. The Journal of cell biology 15, 363-377.

Sorrells, S.F., Paredes, M.F., Cebrian-Silla, A., Sandoval, K., Qi, D., Kelley, K.W., James, D., Mayer, S., Chang, J., Auguste, K.I., et al. (2018). Human hippocampal neurogenesis drops sharply in children to undetectable levels in adults. Nature 555, 377-381.

Soung, N.K., Kang, Y.H., Kim, K., Kamijo, K., Yoon, H., Seong, Y.S., Kuo, Y.L., Miki, T., Kim, S.R., Kuriyama, R., et al. (2006). Requirement of hCenexin for proper mitotic functions of polo-like kinase 1 at the centrosomes. Molecular and cellular biology 26, 8316-8335.

Stahl, R., Walcher, T., De Juan Romero, C., Pilz, G.A., Cappello, S., Irmler, M., Sanz-Aquela, J.M., Beckers, J., Blum, R., Borrell, V., et al. (2013). Trnp1 regulates expansion and folding of the mammalian cerebral cortex by control of radial glial fate. Cell 153, 535-549.

Stancik, E.K., Navarro-Quiroga, I., Sellke, R., and Haydar, T.F. (2010). Heterogeneity in ventricular zone neural precursors contributes to neuronal fate diversity in the postnatal neocortex. The Journal of neuroscience : the official journal of the Society for Neuroscience 30, 7028-7036.

Stiess, M., Maghelli, N., Kapitein, L.C., Gomis-Ruth, S., Wilsch-Brauninger, M., Hoogen-

raad, C.C., Tolic-Norrelykke, I.M., and Bradke, F. (2010). Axon extension occurs independently of centrosomal microtubule nucleation. Science 327, 704-707.

Stinchcombe, J.C., and Griffiths, G.M. (2014). Communication, the centrosome and the immunological synapse. Philosophical transactions of the Royal Society of London Series B, Biological sciences 369.

Stinchcombe, J.C., Randzavola, L.O., Angus, K.L., Mantell, J.M., Verkade, P., and Griffiths, G.M. (2015). Mother Centriole Distal Appendages Mediate Centrosome Docking at the Immunological Synapse and Reveal Mechanistic Parallels with Ciliogenesis. Current biology : CB 25, 3239-3244.

Stoykova, A., Gotz, M., Gruss, P., and Price, J. (1997). Pax6-dependent regulation of adhesive patterning, R-cadherin expression and boundary formation in developing forebrain. Development 124, 3765-3777.

Studier, F.W. (2005). Protein production by auto-induction in high density shaking cultures. Protein expression and purification 41, 207-234.

Stupfler, B., Birck, C., Seraphin, B., and Mauxion, F. (2016). BTG2 bridges PABPC1 RNA-binding domains and CAF1 deadenylase to control cell proliferation. Nature communications 7, 10811.

Suram, S., Silveira, L.J., Mahaffey, S., Brown, G.D., Bonventre, J.V., Williams, D.L., Gow, N.A., Bratton, D.L., Murphy, R.C., and Leslie, C.C. (2013). Cytosolic phospholipase A(2)alpha and eicosanoids regulate expression of genes in macrophages involved in host defense and inflammation. PloS one 8, e69002.

Tanaka, N., Meng, W., Nagae, S., and Takeichi, M. (2012). Nezha/CAMSAP3 and CAMSAP2 cooperate in epithelial-specific organization of noncentrosomal microtubules. Proceedings of the National Academy of Sciences of the United States of America 109, 20029-

132

20034.

Tanaka, T., Serneo, F.F., Higgins, C., Gambello, M.J., Wynshaw-Boris, A., and Gleeson, J.G. (2004). Lis1 and doublecortin function with dynein to mediate coupling of the nucleus to the centrosome in neuronal migration. The Journal of cell biology 165, 709-721.

Tanos, B.E., Yang, H.J., Soni, R., Wang, W.J., Macaluso, F.P., Asara, J.M., and Tsou, M.F. (2013). Centriole distal appendages promote membrane docking, leading to cilia initiation. Genes & development 27, 163-168.

Tavano, S., Taverna, E., Kalebic, N., Haffner, C., Namba, T., Dahl, A., Wilsch-Brauninger, M., Paridaen, J., and Huttner, W.B. (2018). Insm1 Induces Neural Progenitor Delamination in Developing Neocortex via Downregulation of the Adherens Junction Belt-Specific Protein Plekha7. Neuron 97, 1299-1314 e1298. Taverna, E., Gotz, M., and Huttner, W.B. (2014). The cell biology of neurogenesis: toward an understanding of the development and evolution of the neocortex. Annual review of cell and developmental biology 30, 465-502.

Taverna, E., Mora-Bermudez, F., Strzyz, P.J., Florio, M., Icha, J., Haffner, C., Norden, C., Wilsch-Brauninger, M., and Huttner, W.B. (2016). Non-canonical features of the Golgi apparatus in bipolar epithelial neural stem cells. Scientific reports 6, 21206.

Thawani, A., Kadzik, R.S., and Petry, S. (2018). XMAP215 is a microtubule nucleation factor that functions synergistically with the gamma-tubulin ring complex. Nature cell biology 20, 575-585.

Tiwari, N., Tiwari, V.K., Waldmeier, L., Balwierz, P.J., Arnold, P., Pachkov, M., Meyer-Schaller, N., Schubeler, D., van Nimwegen, E., and Christofori, G. (2013). Sox4 is a master regulator of epithelial-mesenchymal transition by controlling Ezh2 expression and epigenetic reprogramming. Cancer Cell 23, 768-783.

Toya, M., Kobayashi, S., Kawasaki, M., Shioi, G., Kaneko, M., Ishiuchi, T., Misaki, K.,

Meng, W., and Takeichi, M. (2016). CAMSAP3 orients the apical-to-basal polarity of microtubule arrays in epithelial cells. Proceedings of the National Academy of Sciences of the United States of America 113, 332-337.

Toya, M., and Takeichi, M. (2016). Organization of Non-centrosomal Microtubules in Epithelial Cells. Cell structure and function 41, 127-135.

Tsai, J.W., Lian, W.N., Kemal, S., Kriegstein, A.R., and Vallee, R.B. (2010). Kinesin 3 and cytoplasmic dynein mediate interkinetic nuclear migration in neural stem cells. Nature neuroscience 13, 1463-1471.

Tylkowski, M.A., Yang, K., Hoyer-Fender, S., and Stoykova, A. (2015). Pax6 controls centriole maturation in cortical progenitors through Odf2. Cellular and molecular life sciences : CMLS 72, 1795-1809.

Uittenbogaard, M., and Chiaramello, A. (2002). Expression of the bHLH transcription factor Tcf12 (ME1) gene is linked to the expansion of precursor cell populations during neurogenesis. Brain research Gene expression patterns 1, 115-121.

Uzbekov, R., and Alieva, I. (2018). Who are you, subdistal appendages of centriole? Open biology 8. Van Bortle, K., Phanstiel, D.H., and Snyder, M.P. (2017). Topological organization and dynamic regulation of human tRNA genes during macrophage differentiation. Genome biology 18, 180.

Vasioukhin, V., and Fuchs, E. (2001). Actin dynamics and cell-cell adhesion in epithelia. Current opinion in cell biology 13, 76-84.

Walcher, T., Xie, Q., Sun, J., Irmler, M., Beckers, J., Ozturk, T., Niessing, D., Stoykova, A., Cvekl, A., Ninkovic, J., et al. (2013). Functional dissection of the paired domain of Pax6 reveals molecular mechanisms of coordinating neurogenesis and proliferation. Development 140, 1123-1136.

134

Wienholds, E., Kloosterman, W.P., Miska, E., Alvarez-Saavedra, E., Berezikov, E., de Bruijn, E., Horvitz, H.R., Kauppinen, S., and Plasterk, R.H. (2005). MicroRNA expression in zebrafish embryonic development. Science 309, 310-311.

Wilsch-Brauninger, M., Peters, J., Paridaen, J.T., and Huttner, W.B. (2012). Basolateral rather than apical primary cilia on neuroepithelial cells committed to delamination. Development 139, 95-105.

Witte, H., Neukirchen, D., and Bradke, F. (2008). Microtubule stabilization specifies initial neuronal polarization. The Journal of cell biology 180, 619-632.

Wu, J., and Akhmanova, A. (2017). Microtubule-Organizing Centers. Annual review of cell and developmental biology 33, 51-75.

Wu, J., Qian, J., Li, C., Kwok, L., Cheng, F., Liu, P., Perdomo, C., Kotton, D., Vaziri, C., Anderlind, C., et al. (2010). miR-129 regulates cell proliferation by downregulating Cdk6 expression. Cell cycle 9, 1809-1818.

Yan, X., Habedanck, R., and Nigg, E.A. (2006). A complex of two centrosomal proteins, CAP350 and FOP, cooperates with EB1 in microtubule anchoring. Molecular biology of the cell 17, 634-644.

Yang, C., Wu, J., de Heus, C., Grigoriev, I., Liv, N., Yao, Y., Smal, I., Meijering, E., Klumperman, J., Qi, R.Z., et al. (2017). EB1 and EB3 regulate microtubule minus end organization and Golgi morphology. The Journal of cell biology 216, 3179-3198.

Yang, T.T., Chong, W.M., Wang, W.J., Mazo, G., Tanos, B., Chen, Z., Tran, T.M.N., Chen, Y.D., Weng, R.R., Huang, C.E., et al. (2018). Super-resolution architecture of mammalian centriole distal appendages reveals distinct blade and matrix functional components. Nature communications 9, 2023.

Yonezawa, S., Shigematsu, M., Hirata, K., and Hayashi, K. (2015). Loss of gamma-tubulin, GCP-WD/NEDD1 and CDK5RAP2 from the Centrosome of Neurons in Developing Mouse Cerebral and Cerebellar Cortex. Acta Histochem Cytochem 48, 145-152.

Young, K.M., Fogarty, M., Kessaris, N., and Richardson, W.D. (2007). Subventricular zone stem cells are heterogeneous with respect to their embryonic origins and neurogenic fates in the adult olfactory bulb. The Journal of neuroscience : the official journal of the Society for Neuroscience 27, 8286-8296.

Zander, M.A., Burns, S.E., Yang, G., Kaplan, D.R., and Miller, F.D. (2014). Snail coordinately regulates downstream pathways to control multiple aspects of mammalian neural precursor development. The Journal of neuroscience : the official journal of the Society for Neuroscience 34, 5164-5175.

Zhang, X., Chen, M.H., Wu, X., Kodani, A., Fan, J., Doan, R., Ozawa, M., Ma, J., Yoshida, N., Reiter, J.F., et al. (2016). Cell-Type-Specific Alternative Splicing Governs Cell Fate in the Developing Cerebral Cortex. Cell 166, 1147-1162 e1115.

136

Chapter 6

Abbreviations

In the following, the most relevant abbreviations used in this manuscript are listed in alphabetical order.

%	percent
°C	Degree Celsius
Actb	Anctin beta
ac-Tub	acetylated Tubulin
aNSC	adult Neural Stem Cell
AP	Alkaline Phosphatase
AP	Apical Progenitor
Arl13b	ADP-ribosylation factor-like protein 13B
Ascl1	Achaete-scute homolog 1
(d)ATP	(deoxy) Adenosine Triphosphate
BAC	Bacterial Artificial Chromosome
BCA	Bicinchoninic Acid
BCIP	5-bromo-4-chloro-3'-indolylphosphate
bHLH	basic Helix-Loop-Helix
BP	Basal Progenitor
bp	base pair
BrdU	5-bromo-2'-deoxyuridine

BSA	Bovine Serum Albumin
CAG	Cytomegalovirus early enhancer/chicken beta-actin promoter
Camsap	Calmodulin regulated spectrin associated protein
CD	Cluster of Differentiation
cDNA	complementary DNA
CDH	Cadherin
CNS	Central Nervous System
CP	Cortical Plate
co	control
CTX	(cerebral) cortex
Cux1	Cut-like homeobox 1
d	day(s)
DA(s)	Distal Appendage(s)
DAPI	4',6-diamidino-2-phenylindole
DC	Daughter Centriole
Dcx	Doublecortin, X-linked lissencephaly
Dctn	Dynactin
detyr-Tub	detyrosinated Tubulin
DG	Dentate Gyrus
Dlx	Distal-less
DTT	Dithiothreitol
DMEM	Dulbecco's Modified Eagle's Medium
DNA	Deoxyribonucleic Acid
dNTP	Deoxynucleoside TriPhosphate
DTT	Dithiothreitol
E	Embryonic day
EB1	End Binding protein 1 (also known as Mapre1)
EB3	End Binding protein 3
e.g.	exempli gratia (for example)
EDTA	Ethylene-Diamine-tetra-Acetic-Acid
EGF	Epidermal Growth Factor
EM	Electron Microscopy
Emx1	Empty spiracles homeobox 1
FACS	Fluorescence-activated Cell Sorting

FCS	Fetal Calf Serum
FGF	Fibroblast growth factor
FSC-A	Forward scatterâ€"area
FSC-W	Forward scatter- width
G	Gram
GABA	gamma-Amino Butyric Acid
GAPDH	Glyceraldehyde 3-phosphate dehydrogenase
(Tub)Gcp	(Tubulin) gamma complex associated protein
GFAP	Glial fibrillary acidic protein
GE	Ganglionic Eminence
(E)GFP	(Enhanced) Green Fluorescent Protein
GOF	Gain Of Function
h(s)	hours
HBSS	Hank's balanced salt solution
HCl	Hydrochloric acid
HEPES	4-(2-Hydroxyethyl)-1-piperazineethanesulfonic acid
het	heterozygous (also described at +/-)
hiPS cell	human induced Pluripotency Stemm cell
HRP	Horseradish Peroxidase
IF	Immunofluorescence
IP	Immunoprecipitation
IZ	Intermediate Zone
Kb	Kilobase
KD	Knock-down
kDa	kiloDalton
Kg	Kilogram(s)
(c)KO	(conditional) Knock-Out
L	Litre
LB	lysogeny broth
LGE	Lateral Ganglionic Eminence
Lmnb1	Lamin b1
LOF	Loss Of Function
LV	Lateral Ventricle
μg	microgramm(s)

μl	microliter(s)
μM	micromolar
MABT	Maleic Acid Buffer/Tween
MC	Mother Centriole
MGE	Medial Ganglionic Eminence
Min	Minute
mM	Millimolar
mRNA	messenger Ribonucleic Acid
miRNA/miR	micro Ribonucleic Acid (also
MT(s)	micotubule(s)
N2A	Neuro2a
NaCl	sodium chloride
NBT	Nitro-blue tetrazolium
neg	negative
NeuN	Neuronal Nuclei (also known as Rbfox3)
Neurog	Neurogenin
ng	nanogram
Ngn	Neurogenin
NGS	Normal Goat Serum
ns	not significant
OA	Ocadaic Acid
OB	Olfactory Bulb
Odf2	Outer Dense Fiber
OE	Over Expression
OPC(s)	Oligodentrocyte progenitor cells
oSVZ	outer Subventricular Zone
P	Postnatal day
Pax6	Paired box gene 6
PBS	Phosphate Buffered Saline
PC	Primary Cilium
PCR	Polymerase Chain Reaction
Pcnt	Pericentrin
PDFGFR2	Platelet Derived Growth Factor Receptor 2
PDL	Poly-D-Lysin

PE	Proximal ENd
Pen/Strep (P/S)	Penicillin/Streptomycin
PFA	Paraformaldehyde
pHH3	phospho Histone H3
Prom1	Prominin 1 (also known as CD133)
PSA-NCAM	Polysialylated-neural cell adhesion molecule
PVDF	Polyvinylidene Fluoride
pol	polymerase
RFP	Red Fluorescent Protein
RGC(s)	Radial Glia Cell(s)
RMS	Rostral Migratory Stream
rpm	revolutions per minute
RT	Room Temperature
RT-qPCR	Real Time Quantitative Polymerase Chain Reaction
S100b	S100 calcium-binding protein beta
SDA(s)	Subdistal Appendage(s)
SDS	Sodium dodecyl sulfate
sec	seconds
SEM	Standard Error of Mean
SEZ	Subependymal Zone
shRNA/sh	small hairpin Ribonucleic Acid
siRNA/si	small interfering Ribonucleic Acid
Sox4	SRY (sex determining region Y)-box 4
SSC	Saline-Sodium Citrate
SVZ	Subventricular Zone
TAP	Transient Amplifying Progenitor
Tbr1	T-box brain gene 1
Tbr2	T-box brain gene 2 (also known as Eomesodermin)
TCF12	Transcription Factor 12
TAE	Tris Acetate EDTA
TGFbeta 1	Transforming Growth Factor - beta 1
TF	Transcription Factor
tRNA	transfer Ribonucleic Acid
(d)TTP	(deoxy) Thymidine Triphosphate

Tuba	Tubulin alpha
Tubb3	Tubulin beta 3
Tubg	Tubulin gamma
TUNEL	Terminal deoxynucleotidyl transferase (TdT) dUTP Nick-End Labeling
tyr-Tub	tyrosinated Tubulin
U	Enzyme unit
UTR	Untranslated Region
VZ	Venticular Zone
w/v	weight/volume
wt	wild type
ZO1	Zonula Occludens 1

Chapter 7

Apendix

7.1 Curriculum vitae

Education

1995–2005	Primary and high school, German School Barranquilla, Colombia
Nov. 2005	High School Degree (Honor Valedictorian), German School, Barranquilla, Colombia
2006–2007	Certificate of General Qualification for University Entrance (Hochschulzugangsberechtigung), University of Cologne, Germany
2007–2011	Study of Biology, Ludwig-Maximilians University Munich, Germany
Sep. 2011	B.Sc. Degree in Biology, Ludwig-Maximilians University Munich, Germany
Oct. 2012–	PhD studies, Institute of Stem Cell Research, Helmholtz Zentrum München and Ludwig-Maximilians University Munich, Germany

Experience and Courses

06.2010–08.2010	Internship, Group Hematopoiesis (Juan Carlos Zúñiga-Pflücker), Sunnybrook Health Science Centre, MCB

09.2011–01.2012	Internship, Laboratory for Stem Cell Biology (Shin-ichi Nishikawa), RIKEN CDB Kobe, Japan
03.2012–10.2012	Internship, Group Mesenchymal Stem Cells (Katarina Le Blanc) and Group Notch-Signaling (Urban Lendhal), Karolinska Insitutet Stockholm (HERM & CMB), Sweden
15–21.09.2012	Hydra VIII - European Summer School on Stem Cells & Regenerative Medicine, Hydra, Greece
11–23.04.2016	Genetic Engineering of Mammalian Stem Cells, Wellcome Genome Campus, Hinxton, Cambridge, UK
7–26.06.2017	CSH Course Mouse Development, Stem Cells & Cancer, Cold Spring Harbor Laboratory, New York, U.S.A

Language Skills

Spanish	native speaker
German	near native (C2)
English	highly proficient in spoken and written English (C1)

Affiliations

German Society for Biochemistry and Molecular Biology (GBM)

Japanese Society of Developmental Biologists (JSDB)

International Society for Stem Cell Research (ISSCR)

German Society for Stem Cells Research (DSZ)

German Society for Cell Biology (DGZ)

German Stem Cell Network (GSCN)

Awards

100 Colombianos (2014-2015) –100 successful Colombians abroad

German Stem Cell Network travel grant –Keystone Symposium, U.S.A.

RIKEN CDB travel fellowship –RIKEN CDB Symposium 2017, Japan

HHMI travel grant –CSH Mouse Course, U.S.A

Boehringer Ingelheim Fonds travel grant –CSH Mouse Course, U.S.A

ISSCR Travel award –ISSCR Annual Meeting 2018, Australia

ISSCR Merit award –ISSCR Annual Meeting 2018, Australia

7.2   List of publications

Bratkovic, T., Modic, M., **Camargo Ortega, G**., Drukker, M., and Rogelj, B. (2018). Neuronal differentiation induces SNORD115 expression and is accompanied by post-transcriptional changes of serotonin receptor 2c mRNA. Scientific reports 8, 5101.

Lanner, F., Lee, K.L., **Ortega, G.C.**, Sohl, M., Li, X., Jin, S., Hansson, E.M., Claesson-Welsh, L., Poellinger, L., Lendahl, U., et al. (2013). Hypoxia-induced arterial differentiation requires adrenomedullin and notch signaling. Stem cells and development 22, 1360-1369.

Martini, S., Bernoth, K., Main, H., **Ortega, G.D.**, Lendahl, U., Just, U., and Schwanbeck, R. (2013). A critical role for Sox9 in notch-induced astrogliogenesis and stem cell maintenance. Stem Cells 31, 741-751.

7.3   List of contributions

The author discovered the centrosome localization and cell specific heterogeneity of Akna, planned, designed and performed all biochemical and in vitro experiments addressing Akna function at the centrosome.

The following persons contributed with materials and experimental assays, or provided help with analysis and interpretation of data:

Sven Falk (BMC, Munich), Pia Johansson (previously at Helmholtz Zentrum München), Laurent Nguyen (University of Liège, Belgium), Elise Peyre (University of Liège, Belgium) and Loic Broix (University of Liège, Belgium) performed all experiments addressing Akna function in vivo in the mouse. Kaviya Chinnappa (previously at Helmholtz Zentrum München) and Anna Gavranovic (previously at Helmholtz Zentrum München) contributed to the in vivo analysis. Sven Falk, Elise Peyre and Loic Broic performed all live imaging experiments. Michaela Wilsch-Bräuninger (MPI-CBG, Dresden) and Wieland B. Huttner (MPI-CBG, Dresden) contributed the immuno-EM experiments and analysis. Arie Geerlof (Helmholtz Zentrum München) and Regina Feederle (Helmholtz Zentrum München) generated the Akna antibodies and the author tested them. Juliane Merl-Pham (Helmholtz Zentrum München) and Stefanie Hauck (Helmholtz Zentrum München) contributed the proteome expertise and analysis. Stanislav Vinopal (DZNE, Bonn) and Frank Bradke (DZNE, Bonn) provided high resolution light microscopy images and expertise in centrosome function. Wei Shao (Memorial Sloan Kettering Cancer Center, USA) and Song-Hai Shi (Memorial Sloan Kettering Cancer Center, USA) contributed with the generation and sample processing of Sas4fl/fl p53fl/fl Emx1-Cre conditional knockout mice. Sanjeeb Kumar Sahu (previously at IMB, Mainz), Vijay Tiwary (previously at IMB, Mainz), and the author performed experiments in NMuMG cells and analyzed the role of Akna during EMT. Simone Reber (IRI for Life Sciences, Berlin), William Hirst (Humboldt-University, Berlin) contributed with expertise in centrosome and MT functions and together with the author performed MT-cosedimentation assays with Akna. Silvia Cappello (MPI-P, Munich) provided GAD65-EGFP knock-in mice. Tugay Karakaya (Helmholtz Zentrum München), Thomas Staininger (Helmholtz Zentrum München) and Jeannine Widmann (Helmholtz Zentrum München) were students under my supervision and contributed to *in*

vitro analyses of Akna.

Germán Camargo Ortega

Dr. Magdalena Götz

7.4 Affidavit

Eidesstattliche Versicherung/Affidavit Hiermit versichere ich an Eides statt, dass ich die vorliegende Dissertation **Novel mechanims of neurogenesis: the role of the new centrosomal protein Akna** selbstständig angefertigt habe, mich außer der angegebenen keiner weiteren Hilfsmittel bedient und alle Erkenntnisse, die aus dem Schrifttum ganz oder annähernd übernommen sind, als solche kenntlich gemacht und nach ihrer Herkunft unter Bezeichnung der Fundstelle einzeln nachgewiesen habe.

I hereby confirm that the dissertation **Novel mechanims of neurogenesis: the role of the new centrosomal protein Akna** is the result of my own work and that I have only used sources or materials listed and specified in the dissertation.

München, date January 18, 2019

Germán Camargo Ortega